UNIVERSITY OF HAWAII
LIBRARY
Nov 15 '61

Geochimica et Cosmochimica Acta

JOURNAL OF THE GEOCHEMICAL SOCIETY

Executive Editors

J. A. S. ADAMS, *Houston, Texas* C. W. CORRENS, *Göttingen* L. R. WAGER, *Oxford.*

Editors

L. H. AHRENS, *Capetown.* S. R. NOCKOLDS, *Cambridge.* H. C. UREY, *La Jolla, Calif.*
JOHN VERHOOGEN, *Berkeley, Calif.* E. A. VINCENT, *Oxford*
A. P. VINOGRADOV, *Moscow.*

CONTENTS VOLUME 25, No. 2 SEPTEMBER 1961

W. BLUMER and G. S. OMENN: Fossil porphyrins: uncomplexed chlorins in a triassic sediment 81

L. H. AHRENS and R. A. EDGE: The K/Cs ratio in some basic rocks . 91

VAGN BUCHWALD: The iron meteorite "Thule", North Greenland . . 95

JOHN J. W. ROGERS and PAUL C. RAGLAND: Variation of thorium and uranium in selected granitic rocks 99

S. K. EL WAKEEL and J. P. RILEY: Chemical and mineralogical studies of deep-sea sediments 110

H. BAADSGAARD, J. LIPSON and R. E. FOLINSBEE: The leakage of radiogenic argon from sanidine 147

Geochemical Note:

JOHN A. O'KEEFE and PAUL D. LOWMAN, Jr.: New investigations of the Igast "meteorite" 158

PERGAMON PRESS OXFORD • LONDON • NEW YORK • PARIS

GEOCHIMICA ET COSMOCHIMICA ACTA

EXECUTIVE EDITORS

Prof. J. A. S. Adams, *Department of Geology, Rice University, Houston* 1, *Texas, U.S.A.*
Prof. C. W. Correns, *Sedimentpetrographisches Institut der Universität, Lotzestr.* 13, *Göttingen, Germany*
Prof. L. R. Wager, F.R.S., *Department of Geology and Mineralogy, The University Museum, Oxford, England*

EDITORS

Prof. L. H. Ahrens, *Department of Chemistry, University of Capetown, Rondebosch, Cape Province, South Africa*
Dr. S. R. Nockolds, *Department of Mineralogy and Petrology, The University, Cambridge, England*
Prof. H. C. Urey, For. Mem. R. S., *University of California, La Jolla, California, U.S.A.*
Dr. John Verhoogen, *Department of Geology, University of California, Berkeley, California, U.S.A.*
Dr. E. A. Vincent, *Department of Geology and Mineralogy, The University Museum, Oxford*
Prof. A. P. Vinogradov, *Vernadsky Institute, Moscow, U.S.S.R.*

EDITORIAL ADVISORY BOARD

EUROPE

T. F. W. Barth, *Oslo*
L. Capdecomme, *Toulouse*
E. J. Conway, *Dublin*
P. Eskola, *Helsinki*
P. Gallitelli, *Modena*
A. Hadding, *Lund*
O. Hahn, *Göttingen*
H. W. Harvey, *Plymouth*
F. Heide, *Jena*
A. Holmes, *Edinburgh*
Earl Ingerson, *Austin*
W. Q. Kennedy, *Leeds*
Ph. H. Kuenen, *Gröningen*
S. Landergren, *Stockholm*
F. Mashatschki, *Vienna*
A. Muir, *Harpenden*
J. Orcel, *Paris*
E. Raguin, *Paris*
E. Reinhard, *Basle*
Th. G. Sahama, *Helsinki*
C. E. Tilley, *Cambridge*
T. Vogt, *Trondheim*

AMERICAN CONTINENT

A. F. Buddington, *Princeton*
D. Guimarães, *Belo Horizonte*
G. E. Hutchinson, *New Haven*
B. H. Mason, *New York*
F. Whipple, *Cambridge*
R. Wildt, *New Haven*
H. S. Yoder, *Washington*

FAR EAST

T. Watanabe, *Tokyo*

AUSTRALIA

D. J. Swaine, *Sydney*

Publishing Offices: Pergamon Press Ltd., Headington Hill Hall, Oxford

Four issues per volume, three volumes per year

Subscription *per annum* (including postage) (A) £21 (U.S.A. $60.00); (B) For individual subscribers who write directly to the publisher certifying that the Journal is for their private use, £7.7s. (U.S.A. $21.50). Members of the Geochemical Society, or non-members who occasionally publish papers in the Journal, £3. 11s. 6d. (U.S.A. $10.00) *per annum.*

Back numbers, £10 (U.S.A. $28.00) per volume

Single issues, £2. 10s. (U.S.A. $7.00) each

Copyright © 1961 Pergamon Press Ltd.

PERGAMON PRESS LTD.

HEADINGTON HILL HALL, OXFORD 122 EAST 55TH STREET, NEW YORK 22, N.Y.

PRINTED IN NORTHERN IRELAND AT THE UNIVERSITIES PRESS, BELFAST

A Technical Writing Service for Industry

Do you need the services of professional technical writers, highly competent illustrators and compilers of modern, effective technical literature? A technical writing service is available to industrial companies and research organizations to prepare, illustrate, print and disseminate instruction manuals, parts lists, user handbooks, sales brochures, internal reports, etc.

The Technical Writing Division is staffed with experienced and highly qualified technical writers, engineers and illustrators and at their disposal are all the very extensive resources and connections of the Pergamon Press.

For further information please write to:

The Manager,
Pergamon Press Technical Writing Division,
566 Cable Street,
London, E.1

POTASSIUM – ARGON AGE DETERMINATIONS

GEOCHRON now offers complete determinations of geological age by potassium-argon isotope analysis.

Our Technical Director welcomes the opportunity to correspond with scientists concerning particular problems, or applications of interest to them.

For general details, send for our pamphlet, *Potassium-Argon Isotope Analysis*

GEOCHRON LABORATORIES, Inc.
Department O
24 Blackstone Street
Cambridge 39
Massachusetts
U.S.A.

PERGAMON PRESS

specialized journals for *specialized advertising!*

Advertise in GEOCHIMICA ET COSMOCHIMICA ACTA—

Space is available to all manufacturers of suitable products—the range which will appeal to readers of this journal is extensive and includes spectrometers, seismographs, seismic amplifiers and detectors, hydrometers, humidity instruments, monometers, galvanometers, radiation detectors and pyrometers, colorimeters, fluorometers, petrographic and other microscopes, flame photometers, surveying instruments, voltmeters, lenses and optical elements, mine ventilation instruments, X-ray microanalysers, pumps, pipe-lines, gas detection and measurement apparatus, microphotometers, X-ray films, plates and equipment, samplers of airborne dust and bacteria, telecommunications equipment, gyroscopic instruments, petroleum testing equipment, thermometers of all types, chemicals, oil boring equipment, electronic equipment . . . this list could easily be trebled!

We shall be happy to provide impartial advice as to the suitability of products not listed.

THIS IS ONE OF MORE THAN 70 INTERNATIONAL SCIENTIFIC JOURNALS. SPECIAL REDUCED "COMBINED RATES" ARE OFFERED TO MANUFACTURERS ADVERTISING IN MORE THAN ONE JOURNAL.

For details WRITE OR PHONE to

R. D. MILLER
Advertisement Manager

PERGAMON PRESS LIMITED
Pergamon House,
4 Fitzroy Square,
London W.1
Phone: EUSton 4455

PERGAMON PRESS INC.
122 East 55th Street,
New York 22, N.Y.,
U.S.A.
Phone: Plaza 3-9651

Geochimica et Cosmochimica Acta, 1961, Vol. 25, pp. 81 to 90. Pergamon Press Ltd. Printed in Northern Ireland

Fossil porphyrins: uncomplexed chlorins in a triassic sediment*

M. Blumer and G. S. Omenn
Woods Hole Oceanographic Institution, Woods Hole, Massachusetts, U.S.A.

(*Received* 9 *March* 1961)

Abstract—The Triassic oil shale of Serpiano (Switzerland) contains, besides the well-known tetrapyrrole pigments of the porphyrin class, some small amounts of chlorins. These pigments have now been isolated and identified as desoxomesoetiopyropheophorbide *a* and etiochlorin III, with their structure confirmed both by dehydrogenation to the corresponding porphyrins and by synthesis. These ancient chlorins are not direct descendants of chlorophyll; rather, they are secondary, synthetic chlorins, formed by hydrogenation of meso- and desoxophyllerythroetioporphyrin under extreme reducing conditions, probably in a late diagenetic stage in the sediment.

Introduction

The discovery of porphyrins in geological materials (Dhéré and Hradil, 1934; Treibs, 1934) marked a most decisive step in the development of the present thought on the transformation of organic matter in the sediments and on the genesis of petroleum, oil shales and coal. Treibs, in his pioneering investigations (summarized by Treibs, 1936), identified several fossil chlorophyll and haemin derivatives, some common to petroleum, oil shales and bituminous coals (mesoporphyrin (MP), desoxophyllerythrin (DP) and their etioporphyrins (MEP, DPEP)), and others restricted to coal (deutero- and deuteroetio-porphyrin). Occasionally, these pigments are found in their free state; usually, however, they are complexed with metals such as vanadium and nickel. Treibs also reported spectroscopic evidence for the frequent occurrence of small quantities of related pigments, including some green chlorophyll derivatives, in sediments of a wide age range. These green pigments, recognized by their characteristic absorption band at 640 mμ, were later found throughout the entire stratigraphic sequence of the Triassic oil shales of Serpiano, Switzerland (Blumer, 1950b). Because of their high pigment content, these shales have now been chosen for an attempt to isolate the ancient green pigments.†

Isolation

Uncomplexed tetrapyrrole pigments, due to their basic nature, are extracted from solvents such as ether into aqueous acids; this property is frequently utilized for the isolation of porphyrins and the resolution of pigments differing in their basicity. However, when applied to extracts from bituminous materials, solvent partitioning often fails to achieve the expected separation. This is caused by the presence of certain ether-soluble materials which alter the partition coefficients in favour of the organic phase. This difficulty can be overcome by using a poorer solvent (e.g. *iso*propyl ether (Blumer, 1950b)) or by first precipitating these compounds with a paraffin hydrocarbon. In either case, although some of the desired pigment is lost in the insoluble fraction, recovery by repeated extraction or precipitation is often possible.

* Contribution no. 1155 of the Woods Hole Oceanographic Institution.
† A brief report of this investigation appeared earlier (Blumer and Omenn, 1961).

For the isolation of the green pigment, the benzene–methanol extract of the oil shale is evaporated, redissolved in chloroform, and precipitated with an excess of *iso*octane; the asphaltenes are reprecipitated if spectroscopic examination indicates the necessity. The soluble fraction is transferred into ether and extracted with 2·5 and 5–6 N HCl. The first acid extract contains most of the free DPEP and MEP, while the less basic green pigments accumulate in the second extract. Some vanadium complex also enters the acid phase and must be removed by further partitioning of the pigments between ether and HCl (see experimental part).

Repetitive chromatography over alumina serves for the final purification of the pigments. A moderately active adsorbent (Brockmann II) is best suited for the initial separation of the pigment from hydrocarbons and coloured, high molecular weight materials. Rechromatography on alumina of lower activity (Brockmann III) then resolves the pigment mixture, eluting the green pigments ahead of the more strongly retained DPEP/MEP-fraction.

Structural evidence from spectroscopy and chromatography

The pigment exhibits a typical chlorin spectrum (STERN and WENDERLEIN, 1936) (Fig. 1a), characterizing it as a tetrapyrrole compound of the chlorophyll *a* series with one hydrogenated pyrrole ring. The high chromatographic mobility of the pigment on alumina and on paper (r_f-value of 0·75 on Whatman no. 3 paper, CCl_4-*iso*octane, 7:3, v/v) indicates the absence of polar groups such as —COOH, —COOR, —OH, —CO and —COH. The presence of a minor band (Ia) at 613 mμ, together with the partial resolution of the band V into two bands at 486 and 494 mμ is typical of mesochlorins (STERN and PRUCKNER, 1937), chlorophyll derivatives in which the 2-vinyl group has been hydrogenated to an ethyl group. Few chlorins have their main band (I) at a wavelength so low as 640 mμ; this again agrees with the assumption that the fossil pigment has a mesochlorin structure and lacks polar substitution.

Thus, the range of probable pigment structures is reduced to those of a small group of mesoetiochlorins, including etiochlorin, mesopyrro and mesophylloetiochlorin, as well as the unknown chlorin analogue of DPEP. Mesopyrroetiochlorin, with band I at a slightly higher wavelength (645 mμ), is not likely to be the major pigment component. Also, in contrast to the fossil chlorin, its band Ia has an extinction equal to that of band II; this is also the case for etiochlorin III. The spectrum of the fossil pigment resembles much more closely that of mesophyllochlorin or mesophylloetiochlorin (PRUCKNER, 1940).* The unknown chlorin analogue of DPEP differs from mesophylloetiochlorin only in the presence of an additional CH_2-group (in the isocyclic ring between the 8- and 6-carbon atoms); its spectrum, therefore, must be very similar.

Dehydrogenation of chlorins to porphyrins

Several reactions may be used for the conversion of chlorins into the more easily identified porphyrins. FISCHER's technique (FISCHER and STERN, 1940), using boiling formic acid and iron powder, was unsuccessful, when applied to the fossil

* PRUCKNER's paper contains two spectral plots for mesophyllochlorin in dioxane, showing the 490 mμ band resolved in one and unresolved in the other.

pigment; however, the dehydrogenation was found to take place rapidly with chloranil in refluxing xylene. The strongly basic dehydrogenation products are

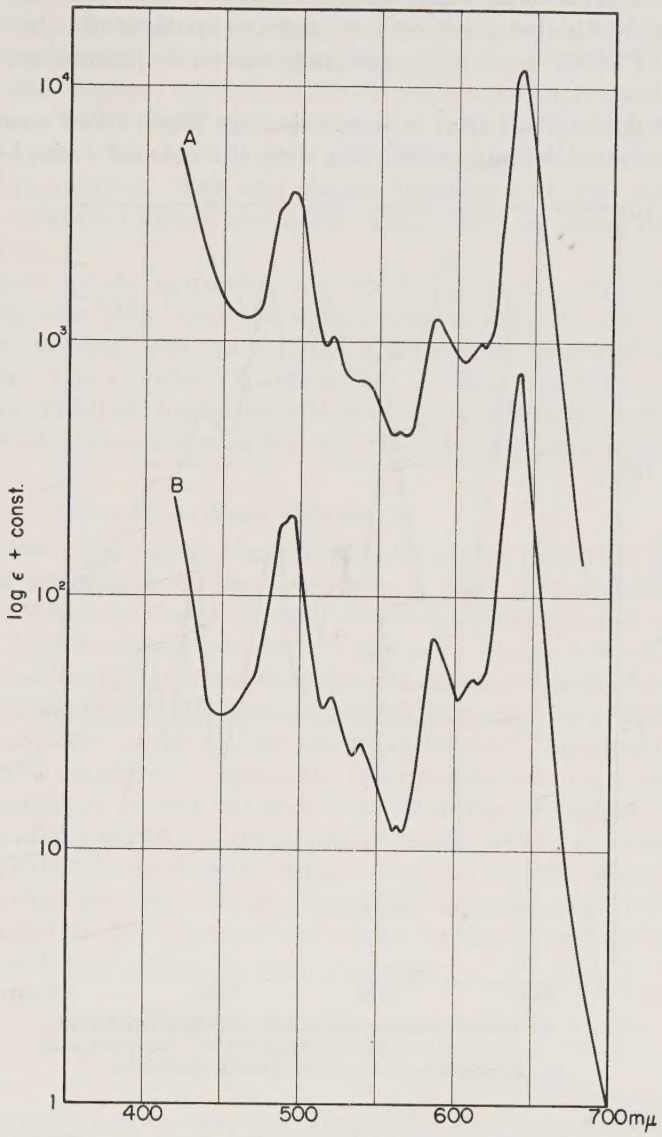

Fig. 1. (a) Natural desoxomesoetiopyropheophorbide *a*.
(b) Synthetic desoxomesoetiopyropheophorbide *a*.

easily separated from excess chloranil and any remaining chlorin. The products have a typical porphyrin spectrum (Fig. 2b), intermediate between those of DPEP and of MEP and identical with the spectrum of the DPEP/MEP-fraction of the same sediment. Chromatography over alumina (Brockmann III) partially resolves the dehydrogenated pigments. The fractions show a gradual change from the

etiospectrum of MEP to the phyllo spectrum of DPEP, accompanied by a corresponding increase in the ratio of band II to band III and a shift in the position of band III from 524 to 530 mμ. Paper chromatography confirms these spectroscopic findings: the early eluates produce two distinct spots at the location of MEP (r_f = 0·64) and of DPEP (r_f = 0·48) with only the latter present in the succeeding fractions.

It should be pointed out that mesochlorins are much more strongly reducing and more easily converted into porphyrins than the natural 2-vinyl-chlorins. The

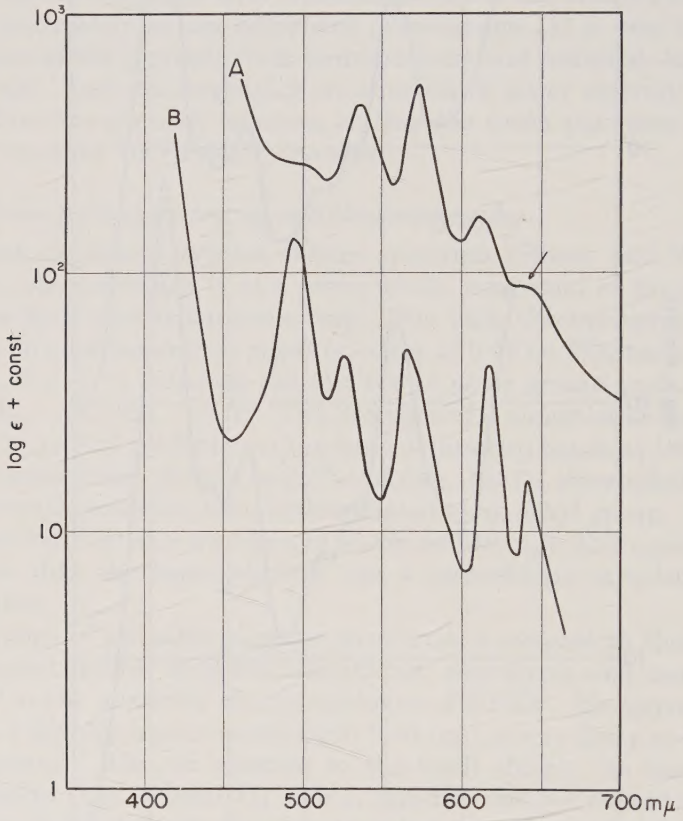

Fig. 2. (a) Benzene–methanol extract of Serpiano oil shale. (b) Porphyrins obtained by dehydrogenation; the small peak at 641 mμ is due to a trace of residual chlorin.

fossil chlorins, for instance, are dehydrogenated even by some rather strongly reducing media; thus, it was found that vanadyl sulfate in boiling acetic acid–pyridine (3 : 1, v/v) oxidized the chlorins to porphyrins at a rate far exceeding that of complex formation. Also, the pigments are quite unstable and are destroyed rapidly, even when stored in darkness and under refrigeration.

Synthesis of dihydro-DPEP (*desoxomesoetiopyropheophorbide* a)

The dehydrogenation experiments characterize the fossil pigment as a mixture

of a small amount of dihydro-MEP (etiochlorin III) with dihydro-DPEP (desoxo-mesoetiopyropheophorbide *a**). The presence of mesophylloetiochlorin is clearly excluded, since band I of phylloetioporphyrin (627 mμ) is not found in the dehydrogenated pigments. In order to substantiate this structural identification, dihydro-DPEP was synthesized. For that purpose, a mixture of DPEP and MEP was isolated from the Serpiano oil shale and resolved by chromatography. The fraction with the highest DPEP/MEP-ratio (extinction ratio of band II/band III = 1·47) was converted into the zinc complex and hydrogenated in boiling ethanol with Raney nickel as catalyst. The zinc chlorin complex was split with acid, and the chlorin was separated from unreacted porphyrins by acid fractionation and chromatography.

The spectrum of the synthetic dihydro-DPEP agrees very well with that of the natural pigment (Fig. 1b); the higher relative extinction of the latter in the regions of the 460 and 560 mμ minima indicates the presence of some residual contamination. The r_f value (Whatman no. 3, CCl_4–*iso*octane, 7 : 3, v/v) of the natural chlorin is slightly higher than that of the synthetic pigment (0·75 vs. 0·68), because of a higher proportion of the more rapidly moving etiochlorin III.

The geochemical history of the fossil chlorins

When Treibs first noted the presence of green pigments in some ancient sediments, he assumed that they stood in a close genetic relationship to the chlorophylls. With the isolation and structural identification of two of these pigments, his hypothesis can now be re-examined. In the case of etiochlorin III, a haemin derivative, it is obvious that the chlorin structure is of secondary origin. The porphyrin structure of MEP was converted, in a strongly reducing sedimentary environment, into the corresponding chlorin structure. The situation in the case of dihydro-DPEP is ambiguous; again, the chlorin structure might be of a secondary nature, or it might have been retained ever since the deposition of the sediment. A comparison of the parallel and competing redox pathways between chlorophyll and dihydro-DPEP shows that the former alternative is the more probable one.

One of the first geochemical reactions in this sequence—apart from the removal of magnesium and the hydrolysis of the esters—is the conversion of the vinyl into ethyl groups with formation of a meso pigment:

$$\text{vinylchlorin} + H_2 \rightarrow \text{mesochlorin} \qquad (1)$$

$$\text{vinylporphyrin} + H_2 \rightarrow \text{mesoporphyrin} \qquad (2)$$

In the chlorophyll series, reaction (1) probably competes with the isomerization of the vinylchlorins:

$$\text{vinylchlorin} \rightarrow \text{mesoporphyrin} \qquad (3)$$

It has long been known that vinyl groups in side chains of the tetrapyrrole system stabilize the reduced (chlorin) state of the pigments. This is revealed by

* Formally, the pigment belongs to the chlorophyll *a* series; however, this must not be taken to imply necessarily a genetic relationship. Under the strongly reducing conditions in the subsurface, chlorophyll *b* and bacteriochlorophyll may also be converted to the same pigment.

the much greater ease of dehydrogenation of the mesochlorins by air and other oxidants.

The carbonyl group (of the isocyclic ring and of the formyl and acetyl groups) is also rather easily attacked by the reducing enviroment of the sediments; here, the influence of the reduction state of the side chain on the redox potential of the tetrapyrrole system is less pronounced.

$$R—CO—R + 2H_2 \rightarrow R—CH_2—R + H_2O \quad (4)$$

$$R—COH + 2H_2 \rightarrow R—CH_3 + H_2O \quad (5)$$

$$R—CO—CH_3 + 2H_2 \rightarrow R—CH_2—CH_3 + H_2O \quad (6)$$

Reactions (1) to (6) proceed easily in the direction indicated. The rates of the reverse reactions are infinitely small; high redox potentials in the environment will much more readily lead to the complete destruction of the tetrapyrrole ring system than bring about the specific reverse reaction. Therefore, we can consider these reactions as entirely irreversible, even for geological time spans of 10^8–10^9 years. In contrast, the redox reactions, which involve the conjugated tetrapyrrole system, proceed rapidly enough in either direction to be considered *geochemically* reversible:

$$\text{vinylporphyrin} + H_2 \rightleftharpoons \text{vinylchlorin} \quad (7)$$

$$\text{mesoporphyrin} + H_2 \rightleftharpoons \text{mesochlorin} \quad (8)$$

The equilibria (7) and (8) are most important at intermediate and low redox potentials; an additional one of the four pyrrole rings can enter into the equilibrium at very low potentials, though it is still questionable whether the sedimentary environment ever reaches the low reduction state necessary:

$$\text{mesochlorin} + H_2 \rightleftharpoons \text{tetrahydromesoporphyrin} \quad (9)$$

The standard potentials of these "semi-reversible" redox systems are not easily measured, but we know—as already mentioned—that the redox potential of the meso pigments is considerably lower than that of the vinyl pigments. This is expressed in the semiquantitative diagram of Fig. 3, with which we can now trace the geochemical fate of a pigment of the type of chlorophyll *a*. Hydrolytic processes, such as the exchange of H^+ for Mg^{2+} and the saponification of the esters with the consecutive decarboxylation in 10-position, rapidly transform chlorophyll *a* into pyropheophorbide *a*, which is subsequently reduced. Most organic-rich sediments, immediately upon deposition or shortly thereafter, acquire a negative redox potential which is gradually lowered with increasing age of the sediment (ZoBell, 1946). Under these conditions, the reduction of the vinyl and of the carbonyl groups can take place. As irreversible reactions they will immediately proceed to completion; the ratio of starting-to-end product is independent of the potential of the environment. This explains why vinyl and carbonyl pigments have never been found in sediments of appreciable age. In contrast, reactions between chlorins and porphyrins lead to an equilibrium, and the potential of the environment determines the ratio of the two forms.

Thus, any mesochlorins, formed by the reduction of vinylchlorins during early diagenesis and at relatively high potential, will be largely reoxidized to mesoporphyrins, the overall effect being that of an isomerization. The mesochlorins reappear in appreciable quantities only much later, when the potential of the environment drops far below the values required for the reduction of vinyl and carbonyl groups.

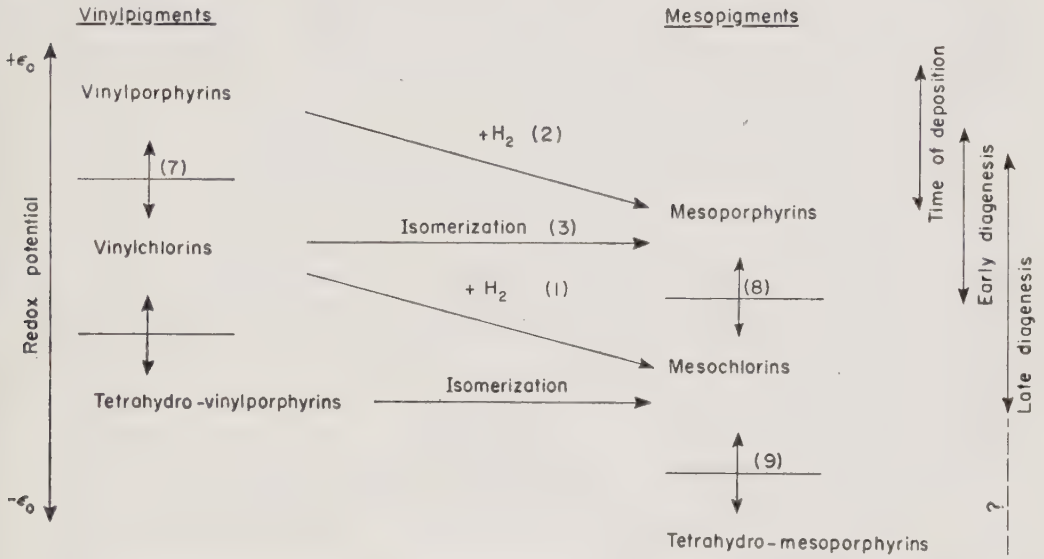

Fig. 3. Some redox processes of tetrapyrrole pigments. Under geochemical conditions, reactions occurring in a vertical direction are reversible, those in a horizontal direction are irreversible.

An earlier paper indicated (Blumer, 1950a) that the redox potential of the vanadium (III)–vanadium (IV) system nearly coincides with the lower potential limit reached by water-wet sediments. The presence in a sediment of fossil chlorins—capable of reducing V (IV)—therefore indicates extremely strong reducing conditions.

We can conclude that both the fossil etiochlorin III and the desoxomesoetiopyropheophorbide *a* are *secondary* chlorins, formed by the reduction of mesoetioporphyrins, in the extremely reducing environment of the oil shale of Serpiano, probably during a late diagenetic stage.

The sediments of Serpiano have been raised above the ground water table for a very considerable length of time. The fact that the chlorins survived this long exposure of the sediment to an oxidizing environment indicates that they are well protected—either by the low permeability of the oil shale or by the presence of protective agents which are preferentially oxidized. Any effect of the exposure since sampling is negligible compared to that of the exposure *in situ*.

Experimental

The oil shale used for this investigation was collected in the most recently worked section of the abandoned mine at Serpiano, Switzerland, during the autumn

of 1959. All samples originated at horizon S XVIII of the "Grenzbitumen" (Anisien-Ladinien, Triassic). They were stored air-dry until summer, 1960, when they were crushed and ground in a ball mill just prior to extraction.

The lability of the fossil chlorins requires considerable care and rapid work. Our initial experiments, which led to the isolation and tentative identification of the pigments, were spread out over a 6-week period; during that time most of the chlorin was lost by air-oxidation in spite of careful handling in near darkness. The important steps of the purification procedure and the characterization were therefore repeated within just 6 days; all fractions were stored at −20°C in order to retard air oxidation.

Continuous spectrophotometric control, using a Cary model 14 spectrophotometer, was maintained during the entire experimental sequence.

Isolation of the pigments

The extraction and isolation of the pigments was carried out in several batches, using a total of 1·6 kg of the oil shale. The following data are representative for a single 10-g sample of the sediment. After exhaustive extraction with benzene–methanol (1:1, v/v), using a Soxhlet extractor, the spectrum (Fig. 2a) indicated the presence in the extract of 37 mg (or 0·37 per cent by weight of sediment) of porphyrin vanadium complex and 250 μg (or 25 p.p.m.) of chlorin. Both values are approximate because of the need for a large background correction; also, the extinction coefficient may be somewhat inaccurate (Treibs' value for DPEP-V was used in the first case and the extinction coefficient for mesophyllochlorin at 640 mμ (Pruckner, 1940) in the second).

The dried extract was redissolved in 3 ml of chloroform and the asphaltenes were precipitated by adding 27 ml hot *iso*octane. The precipitate was filtered and washed with a mixture of chloroform and *iso*octane. The filtrate, containing 14 mg of vanadium complex and most of the chlorin, was evaporated, redissolved in warm diethyl ether, and extracted twice with 5 ml of 2·4 N HCl, three times with 5 ml of 4·9 N HCl and once with 5 ml of 6·1 N HCl. The 2·4 N extracts were diluted with water, neutralized with sodium acetate, and the pigments extracted with ether. This fraction contained only a little green pigment in addition to 1·8 mg of free DPEP and MEP. The 4·9 and 6·1 N extracts were diluted to 1·0 N acidity and the chlorins (210 μg) were recovered by ether extraction. They were further purified by re-extracting the ether solution first with 1·2 and then with 4·9 N HCl. The first extract (mainly DPEP/MEP) and the residual ether (containing DPEP-V) were discarded and the chlorins were recovered from the 4·9 N extract by dilution and extraction.

For final purification, the pigment, dissolved in benzene–*iso*octane (1:1), was adsorbed on an alumina (Brockmann II) column packed in *iso*octane. The elution was carried out with *iso*octane of increasing benzene content. The first eluates (up to 50–60 per cent benzene) contained non-pigment impurities. Relatively pure chlorin was recovered from the 70–80 per cent benzene eluates, while the succeeding fractions again were contaminated (with an unknown pigment, absorbing at 630 mμ and with much DPEP/MEP). Rechromatography of these last fractions yielded some additional chlorin. All equivalent fractions were combined and again

chromatographed, this time over a less active adsorbent (alumina, Brockmann III), using *cyclo*pentane as solvent for the pigments. Impurities were now eluted in the 5–10 per cent benzene fractions. The pure chlorin in the 15 per cent benzene fraction was followed by some contaminated material from which more chlorin was recovered upon rechromatography.

Dehydrogenation

The dehydrogenation of the fossil chlorin by chloranil takes place rapidly and with good yield only if the pigment has been highly purified. Impurities from the oil shale, if not completely removed, use up much chloranil; this retards the reaction and leads to excessive decomposition of the pigment.

In a successful dehydrogenation experiment, 23 μg of the natural pigment in 0·5 ml ether was added to 10 ml xylene and 5 mg chloranil. The solution was refluxed under intermittent spectrophotometric control. The 640 mμ chlorin peak decreased to 18 per cent of its initial extinction within 15 min. The reaction was then terminated and the product, dissolved in 50 ml, ether, was extracted twice with 10-ml fractions of 2·4 and 4·9 N HCl. The porphyrins in the 2·4 N HCl fraction and the unreacted chlorins in both fractions amounted to 10 μg and 2·4 μg, respectively.

The porphyrin fraction was adsorbed from its *cyclo*pentane solution on a 5-ml alumina (Brockmann III) column in *iso*octane and developed with mixtures of *iso*octane and benzene. Some chlorin was eluted in the early fractions. Mesoetioporphyrin with its typical etio spectrum, appeared in the fraction containing 50 per cent benzene and was followed immediately by DPEP. Four porphyrin fractions were collected and aliquots spotted on Whatman no. 3 paper. Development with CCl_4–*iso*octane (7:3, v/v) produced the results shown in Table 1.

Table 1. Paperchromatography of the dehydrogenated pigments

	r_f values					
	Chromatogram no. 1		Chromatogram no. 2		Average value	
Eluate no. 1	0·48	0·63	0·47	0·64	0·48	0·64
Eluate no. 2	0·49	0·65 (weak)	0·47		0·48	0·65
Eluate no. 3	0·46		0·47		0·47	
Eluate no. 4	0·46		0·47		0·47	

Literature value (Blumer, 1956): DPEP: $r_f = 0{\cdot}46$ MEP: $r_f = 0{\cdot}63$.

Synthesis of desoxomesoetiopyropheophorbide a

A DPEP concentrate was prepared from fossil DPEP-V/MEP-V by breaking the complex with HBr-acetic acid followed by solvent partitioning and chromatography. The fraction with the most pronounced phyllo spectrum (ratio of band II/band III = 1·47) was quantitatively converted into its zinc complex by boiling it briefly with zinc acetate in glacial acetic acid. It was then hydrogenated by refluxing for 3 hr in ethanol with Raney nickel as catalyst. The complexes in the filtrate and pyridine washings of the catalyst were split with 3·7 N HCl. The free

pigments, after transfer into ether, were separated by acid extraction, and the weakly basic chlorin was further purified by chromatography. Elution occurred under the same conditions and in the same fractions as described above for the natural pigment. Spectrum and paper chromatographic r_f values provide further support for the identity of the natural and synthetic pigments.

Acknowledgements—This investigation has been supported by a research contract with the United States Office of Naval Research (Contract NONR-2196 (00)) and the grant of a Woods Hole Oceanographic Institution summer student fellowship to one of us (G. O.).

References

Blumer M. (1950a) Die Existenzgrenzen anorganischer Ionen bei der Bildung von Sedimentgesteinen. *Helv. Chim. Acta* **33,** 1568–81.

Blumer M. (1950b) Porphyrinfarbstoffe und Porphyrin-Metallkomplexe in schweizerischen Bitumina. *Helv. Chim. Acta* **33,** 1627–37.

Blumer M. (1956) Separation of porphyrins by paper chromatography. *Analyt. Chem.* **28,** 1640–44.

Blumer M. and Omenn G. S. (1961) Fossil chlorins in a triassic sediment. *Nature, Lond.* **189,** In press.

Dhéré C. and Hradil G. (1934) Spectroscopic investigation of the fluorescence of oil shales. *Schweiz. min.-petr. Mittlg.* **14,** 279–95.

Fischer H. and Stern A. (1940) *Die Chemie des Pyrrols* Vol. II. Akad. Verlag., Leipzig.

Pruckner F. (1940) Lichtabsorption und Konstitution der Chlorophyll derivate—II. *Z. phys. Chem.* A **187,** 257–75.

Stern A. and Wenderlein H. (1936) Ueber die Lichtabsorption der Porphyrine—V. *Z. phys. Chem.* A **176,** 81–124.

Stern A. and Pruckner F. (1937) Lichtabsorption und Konstitution einiger Derivate der Chlorophylle. *Z. phys. Chem.* A **180,** 321–58.

Treibs A. (1934) Ueber das Vorkommen von Chlorophyllderivaten in einem Oelschiefer der oberen Trias. *Liebigs Ann.* **509,** 103–14.

Treibs A. (1936) Chlorophyll- und Haeminderivate in organischen Mineral-stoffen. *Angew. Chem.* **49,** 682–86.

Zobell C. E. (1946) Studies on redox potential of marine sediments. *Bull. Amer. Ass. Petr Geol.* **30,** 477–513.

Geochimica et Cosmochimica Acta, 1961, Vol. 25, pp. 91 to 94. Pergamon Press Ltd. Printed in Northern Ireland

The K/Cs ratio in some basic rocks

L. H. Ahrens and R. A. Edge
Department of Geochemistry, University of Cape Town

(*Received* 16 *March* 1961)

The equivalence, or near equivalence, of the alkali metal ratio K/Rb in common igneous rocks and chondrites, as first indicated by Ahrens *et al.* (1952), is now reasonably well established. The possibility that a similar terrestrial–chondrite equivalence (or near equivalence) may hold also for the ratio of potassium to caesium has been mentioned by Ahrens *et al.* (1960). They used an ion exchange enrichment–spectrochemical method to estimate the K/Cs ratio in six chondrites and seven basic rocks, including reference standard diabase W–1. This analytical procedure has been applied to a further ten specimens of basic rocks and we wish here to present these data (Table 1) and consider them together with earlier results in the light of the above possibility. The present note is concerned primarily with basic rocks and chondrites and only data which have been provided by the same technique (ion exchange–spectrochemical) will be considered aside from those on three basalt composites (Gast, 1960) which have been obtained by an isotope dilution procedure and which make a particularly useful comparison. Seven of the specimens listed in Table 1 are from the mildly differentiated Insizwa Lopolith (Matatiele district, Cape Province, South Africa) the average composition of which is similar to that of average Karoo dolerite (Poldervaart, 1945). For K/Cs data on rocks from the strongly differentiated Skaergaard Complex and Bushveld Igneous Complex, see Cabell and Smales (1957) and Liebenberg (1959), respectively.

It may be recalled (Edge,1960; Ahrens *et al.*, 1960) that in the ion exchange–spectrochemical procedure, an alkali metal rich concentrate is obtained in which the line intensity ratio I Cs 8511/I K 6911 is measured spectroscopically as a function of the concentration ratio. Reference rock W–1 is used as a standard as follows: as the K and Cs contents of W–1 have been estimated (Fairbairn *et al.*, 1951; Stevens *et al.*, 1960; and Cabell and Smales, 1957) the K/Cs ratio is known (4900). At this concentration ratio the line intensity ratio has been estimated at 0·32 and the K/Cs ratio in the unknowns may therefore be obtained from the relationship:

$$\frac{\mathrm{K}}{\mathrm{Cs}} = \frac{0{\cdot}32 \times 4900}{\text{line intensity ratio}}$$

With the exception of the average basalts (last entries in Table 1a) rock specimens in Table 1 are calibrated in terms of reference rock W–1 and the K/Cs ratios are therefore directly comparable; the same applies to the chondrites listed in Table 1(b). As the measurement of the K/Cs ratios involves the internal standard principle of spectrochemical analysis (see for example Chapter 8 of Ahrens and Taylor, 1961) and as the requirements for a good internal standard are satisfactorily fulfilled,

Table 1. Estimated line intensity ratios and K/Cs ratios in (a) some basic rocks and (b) some chondritic meteorites

Description	(a) I Cs 8521 / I K 6911		K/Cs	%K	Cs (p.p.m.)
Chill phase, Insizwa lopolith* (no. 1)	0·34 0·35	0·35	4500	0·48	0·86
Olivine hyperite (no. 2)	0·23	0·23	6800	0·36	0·43
Picrite (no. 3)	0·21 0·23	0·22	7100	0·32	0·35
Quartz hyperite (no. 7)	0·21 0·25	0·23	6800	0·46	0·55
Hypersthene gabbro (no. 10)	0·27 0·25	0·26	6000	0·35	0·49
Olivine hypersthene gabbro (no. 13)	0·13 0·15	0·14	11,200	0·23	0·17
Olivine hypersthene gabbro (no. 16)	0·21 0·22	0·22	7100	0·27	0·30
Norite, Bon Accord quarry Bushveld Igneous Complex (no. 5087)	0·20 0·22	0·21	7500		
Basalt, Messum, South West Africa†	0·18 0·20	0·21	7850		
Dolerite (diabase), Elephant's Head, Transkei‡	0·13 0·11	0·12	13,100		
Reference rock diabase W–1, Centerville, Virginia	0·35 0·29	0·32	4900	0·53	1·08
Basalt (T–83)§	0·26 0·24	0·25	6300	1·22	1·89
Basalt (T–100)	0·18 0·22	0·20	7850	1·44	1·80
Basalt (T–101)	0·20 0·22	0·21	7500	1·08	1·40
Olivine basalt (T–112)	0·19 0·19	0·19	8300	0·75	0·89
Dolerite (T–111)	0·19	0·19	8300	1·30	0·53
Gabbro (T–86)	0·28 0·28	0·28	5600	0·26	0·46
Three basalt composites of Gast (1960) I			8100	0·89	1·1
II			9400	0·94	1·0
III			8400	1·01	1·2
	(b)				
Limerick (O.U.M. 2)		0·19	8300		0·11
Modoc (A.M.N.H. 2454)		0·19	8300		0·11
Long Island (A.M.N.H. 2399)	0·25 0·20	0·23	6800		0·16
Bluff (A.M.N.H. 1043)		0·21	7500		0·14
Mangwendi		0·18	8700		0·10
Dhurmsala		0·17	9200		0·10
		0·20	8100		

* Samples no. 1 to 16 from Insizwa lopolith.
† For description, see Mathias (1957).
‡ For description, see Poldervaart (1945).
§ Specimen with T—numbers are from Akaroa, Banks Peninsula, New Zealand; for details, see Ahrens *et al.* (1960).

precision should be high and duplicate measurements in Table 1 are usually in close agreement. Provided potassium has been estimated in a separate analytical operation, Cs may be determined from the K/Cs ratios; some such Cs determinations are included in Table 1.

Unlike the very large dispersion of the K/Cs ratio in granites and allied rocks (AHRENS, 1954; DELEON and AHRENS 1957; HORSTMAN, 1957, and EDGE and AHRENS, 1961, for example) dispersion is comparatively small in the basic rocks so far investigated and most K/Cs ratios cluster about the average of 7500; the limits involve a factor of 3. It may be noted that the overall average is closely similar to that obtained by GAST (1960) for the three basalt composites; on the other hand, GAST (1960) reported high K/Cs ratios in two single specimens of olivine basalt.

These averages may be compared with those of the chondrites (after AHRENS *et al.*, 1960) which are almost identical. Although it is not the purpose here to consider in detail the K/Cs ratio in granites and other rocks we may note that the magnitude of the ratio in such rocks is often very similar to that reported here for basic rocks and chondrites; thus for example, GAST (1960) gives values of 9100 and 11,000 for two granite composites. Though many more data are required before firm conclusions can be made, the available evidence indicates that the terrestrial K/Cs ratio is at least similar and may be equal to that obtaining in chondrites; if equal, terrestrial K–Rb–Cs ≡ chondrite K–Rb–Cs or at least very nearly so. The significance of such possible equivalence, or near equivalence, will be considered in detail elsewhere.

Acknowledgements—Thanks are due to Dr. M. MATHIAS, Department of Geology, University of Capetown and Professor D. L. SCHOLTZ, Department of Geology, University of Stellenbosch, for kindly supplying specimens.

REFERENCES

AHRENS L. H., PINSON W. H. and KEARNS M. M. (1952) Association of rubidium and potassium in common igneous rocks and meteorites. *Geochim. et Cosmochim. Acta* **2,** 229–242.

AHRENS L. H. (1954) The lognormal distribution of the elements. *Geochim. et Cosmochim. Acta* **5,** 49–73.

AHRENS L. H., EDGE R. A. and TAYLOR S. R. (1960) The uniformity of concentration of lithophile elements in chondrites—with particular reference to Cs. *Geochim. et Cosmochim. Acta* **20,** 260–272.

AHRENS L. H. and TAYLOR S. R. (1961) *Spectrochemical Analysis* (2nd Ed.). Addison-Wesley, Reading, Mass.

CABELL M. J. and SMALES A. A. (1957) The determination of rubidium and caesium in rocks, minerals and meteorites by neutron-activation analysis. *Analyst* **82,** 390–406.

DELEON G. and AHRENS L. H. (1957) The distribution of Li, Rb, Cs and Pb in some Yugoslav granites. *Geochim. et Cosmochim. Acta* **12,** 94–96.

EDGE R. A. (1960) Ph.D. Thesis, Department of Chemistry, University of Cape Town.

EDGE R. A. and AHRENS L. H. (1961) The Sc, Y, La, Nd, Ce, Sn, Mo and Ga contents and K/Rb and K/Cs ratios of some southern African granites and related rocks. In press.

FAIRBAIRN H. W., SCHLECHT W. G., STEVENS R. E., DENNEN W. H., AHRENS L. H. and CHAYES F. A. (1951) A co-operative investigation of precision and accuracy in chemical, spectrochemical and modal analysis of silicate rocks. *Bull. U.S. Geol. Surv.* No. 980.

GAST P. W. (1960) Limitations on the composition of the upper mantle. *J. Geophys. Res.* **65,** 1287–1297.

HORSTMAN E. L. (1957) The distribution of lithium, rubidium and caesium in igneous and sedimentary rocks. *Geochim. et Cosmochim. Acta* **12,** 1–28.

Liebenberg C. J. (1959) Ph.D. Thesis, University of Pretoria.

Mathias Morna (1957) The geochemistry of the Messum Igneous Complex, South West Africa. *Geochim. et Cosmochim. Acta* **12,** 29–46.

Poldervaart A. (1945) The petrology of the Elephant's Head dike and the New Amalfi sheet (Matatile). *Trans. Roy. Soc. S. Afr.* **30,** 85–120.

Stevens R. E., Fleischer M., Niles W. W., Chodos A. A., Filby R. H., Leininger R. K., Ahrens L. H. and Flanagan F. J. (1960) Second report on a co-operative investigation of the composition of two silicate rocks. *Bull. U.S. Geol. Surv.* 1113.

Geochimica et Cosmochimica Acta, 1961, Vol. 25, pp. 95 to 98. Pergamon Press Ltd. Printed in Northern Ireland

The iron meteorite "Thule", North Greenland

Vagn Buchwald
Laboratory of Metallurgy, Technical University of Denmark,
Øster Voldgade 10, Trappe K, Copenhagen K., Denmark

(*Received* 21 *February* 1961)

Abstract—The paper describes a 48·6 kg siderite, which was found in 1955 on a nunatak near Thule, North Greenland. The Thule meteorite can be classified as a medium octahedrite with 8·13% Ni and other normal constituents. The micro-hardness of the phases are given. The examination of the well-preserved crust yielded data, which gave a value for heat ablation during the passage through the atmosphere of about 1·6 mm/sec.

During the summer of 1955, an iron meteorite was discovered by James E. Conel near Thule Air Base at Wolstenholme Fjord in North Greenland. It was found on a nunatak, which protruded through Moltkes Bræ (the Sermerssuaq Glacier); its position was 76° 32′N, 67° 33′W. The meteorite was brought to Copenhagen by the former Danish Liaison officer, Dr. J. Troelsen, and given to the Mineralogical Museum by the Ministry for Greenland.

The meteorite, which has been called Thule, weighed 48·6 kg and had the rather curious form of a lying bird (Fig. 1). It was unbroken and very tough with good coherence.

The surface was evenly covered with iron oxides, but microscopical slices showed later that this corrosion crust from the terrestrial environment was only 0·1 mm thick. There were many "thumb marks" of the usual type; often, 8–10 marks of 20–30 mm diameter were grouped together to form a larger, shallow depression of 70–80 mm diameter (Fig. 2). In some places small, deep cavities about 30 mm diameter and 30 mm deep were seen. All these features were definitely not caused by corrosion, as the thin heat-affected zone was preserved.

The meteorites most obvious traits are the neck (25 × 110 mm) and head (about 50 × 100 × 100 mm). They are sculptured from the atmospheric flight, and had the journey lasted a few more seconds, the head would no doubt have been separated from the main mass.

It is very difficult to say when the fall occurred. As the corrosive action is slow in the area, one is inclined to estimate that the fall took place a few hundred years ago.

The Thule meteorite is a medium octahedrite with the normal constituents kamacite, taenite, plessite, troilite and schreibersite. Cohenite and daubreelite have not been seen. The octahedral pattern is well developed (Fig. 3) with broad kamacite bands (0·8–1·5 mm) and narrow taenite bands (0·08–0·15 mm). Interchanging with the taenite and with about the same dimensions, there is schreibersite, which is distributed at random. The kamacite shows abundant Neumann bands.

Three hardness impressions (Vickers 100 kg) gave 215, 240 and 242, which is a

true scattering, owing to the heterogeneity of the meteorite. The meteorite has the following composition:

Fe	90·7	Mn	0	P	0·15
Ni	8·13	C	0·09	S	0·043
Co	0·25	N	0·0044		
Cu	0·03	Si	0·02		

This is normal for medium octahedrites. The nitrogen content is comparable to that of a normal Siemens–Martin steel.

After wet-grinding on emery papers 220, 320, 400 and 600, the specimens were polished with alumina (Dujardin Tonerde no. 2); finally, a thin deformed surface layer was dissolved by electropolishing, according to the Knuth–Winterfeldt method (1952) (Disa-Electropol). This provides a good surface for measuring microhardness, without fear of interference from deformed layers created during the preparation of the surface.

In the following table, microhardness values are given (Vickers, 30 g) for the different phases:

Kamacite, broad bands, 175 $\pm$ 7 kg/mm^2.
Kamacite, in plessite, 172 $\pm$ 5.
Taenite, veinlets and border zones, 340 $\pm$ 15.
Taenite, light martensite structure, 355 $\pm$ 15.
Taenite, yellow-brown martensite, 300 $\pm$ 20.
Taenite, dark-etching nucleus, 240 $\pm$ 40.
Taenite, 3–15 μ veinlets in plessite, 290 $\pm$ 30.
Schreibersite (often split open by the impress.) 760 $\pm$ 40.
Troilite, variation owing to anisotropy 260 $\pm$ 50.

The hardness of the taenite varies very much; this must be due to the nickel content, which is known to vary, from about 40 per cent (hardest) to about 6 per cent as recently shown with the microprobe analyser by Agrell and Long (1960). The microhardness variation in the different phases in the interior of the meteorite is shown in Fig. 4.

A slice of the posterior of the meteorite (Fig. 1) revealed an egg-shaped troilite inclusion (32 $\times$ 47 mm). This consisted of numerous individuals, which formed a polygonal mosaic. A partial analysis gave 0.115 per cent Ni —0·127 per cent Co —0·135 per cent Cu, and it was nonmagnetic. The troilite contains sparks of a yellowish sulphide, "S_2", and in the border zones there are irregular patches of a yellowish-green sulphide, "S_7", and veinlets and flames of a chalcopyrite like sulphide, "S_4". The relation between these sulphides will be described by Pauly (1961).

The border zone is heat-affected, owing to the frictional heating in the atmosphere. The zone varies between 1·5 and 2·5 mm in thickness, judging from the macro-etching (Fig. 5). The kamacite is granulated and the Neumann bands have disappeared (Fig. 6), but the microhardness is not altered very much, 186 $\pm$ 7. No definite hardness gradation in the border zone could be established.

In the heat-affected zone, also the schreibersite is altered. Fig. 7 shows an inclusion, which happens to lie normal to the invading heat front, 0·9 mm from the

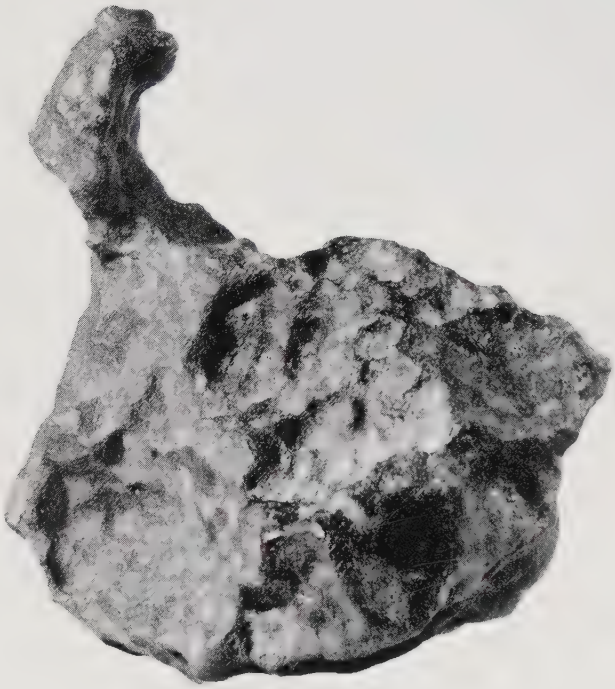

Fig. 1. The Thule iron meteorite, 48·6 kg (Chr. Halkier fot.).

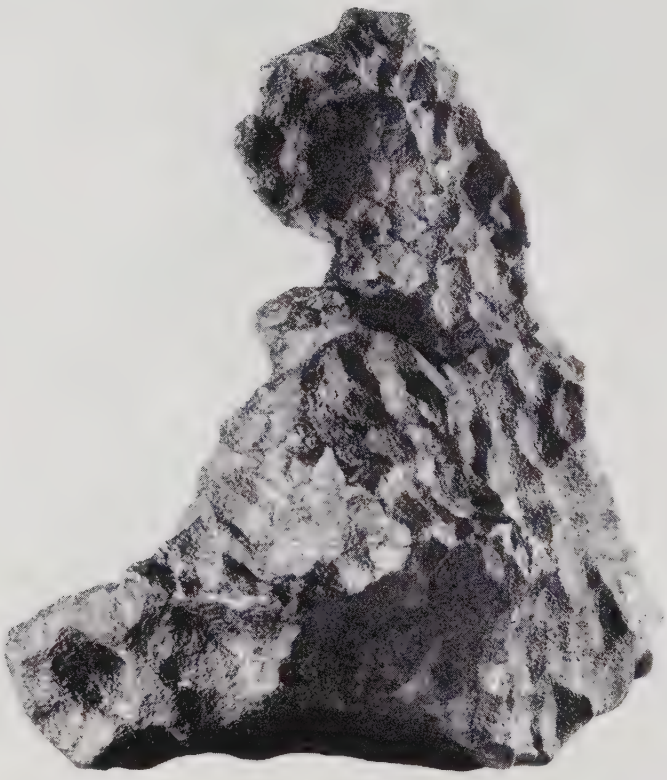

Fig. 2. The Thule iron meteorite seen from the side (Chr. Halkier fot.).

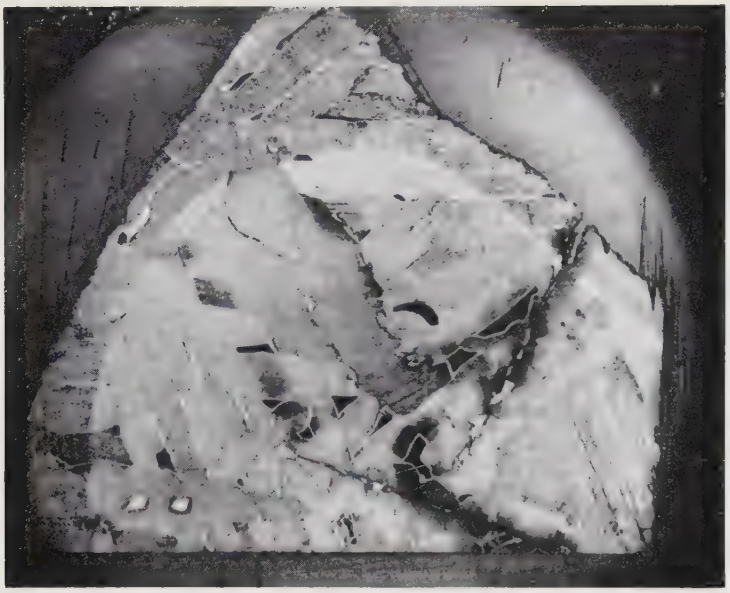

Fig. 3. Slice of Thule meteorite showing the octahedral pattern, and the distribution of the taenite-bordered plessite fields. The heat-affected zone from the passage of the atmosphere is readily seen. $\times 3{\cdot}7$

Fig. 5. Octahedral structure and heat-affected border. $\times 6$

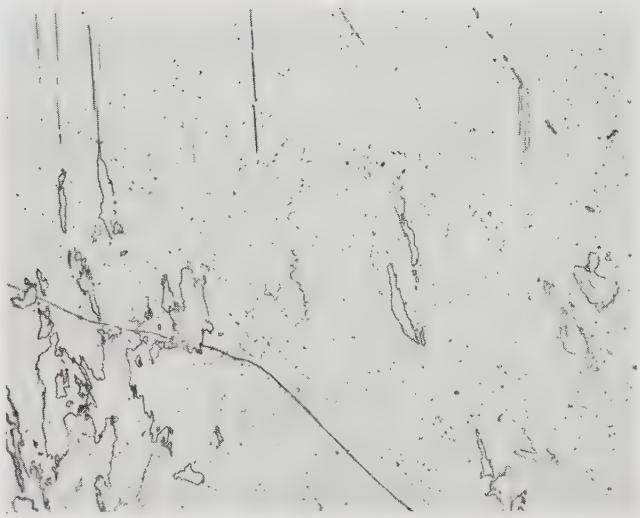

Fig. 6. The interior with Neuman bands (above) and the heat-affected surface zone with granulated kamacite and a grain border (below). ×135.

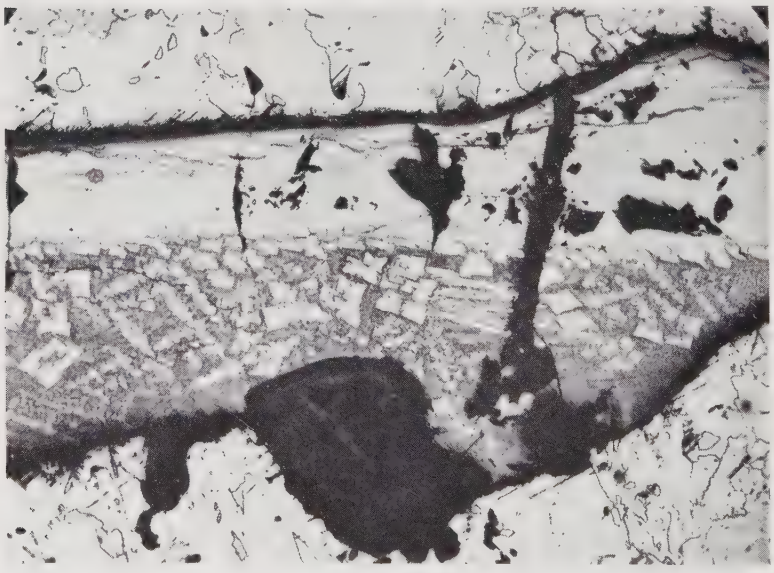

Fig. 7. Section through the heat-affected zone, the surface is below the picture. A schreibersite inclusion is partly melted; rhombohedral fragments of schreibersite swim in a background matrix of eutectic structure of Fe-P and kamacite. The black parts are invading oxide from terrestrial corrosion. ×135.

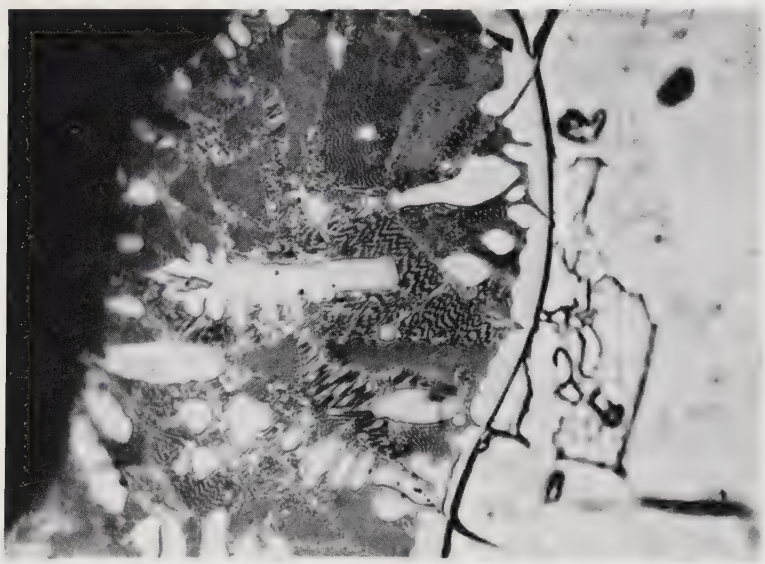

Fig. 8. Dendrites of kamacite and eutectic structure from a melted schreibersite inclusion 0·5 mm from the surface. ×800.

surface, so that it reflects different states of melting. Fig. 8 shows the structure of another schreibersite inclusion nearer the surface.

This inclusion has been totally molten and, although the time was very short, has partially dissolved the surrounding kamacite thereby rounding the border. The composition of the iron-nickel-phosphorus melt varied from a relative phosphorus-rich composition of the original schreibersite in the central parts to a phosphorus-poor in the outer parts. Using the iron-phosphorus equilibrium diagram (HANSEN

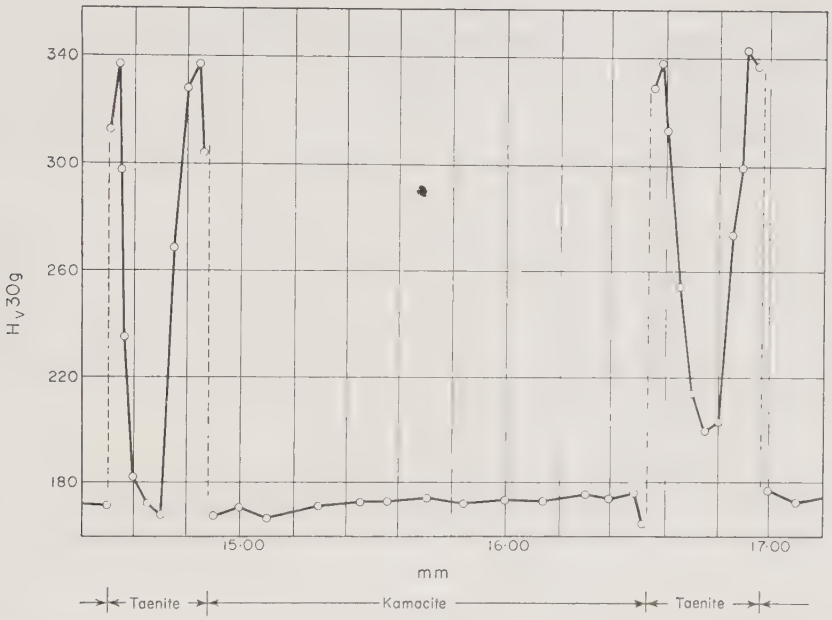

Fig. 4. Microhardness (30 g Vickers) of kamacite and taenite in the Thule meteorite. Judging from the microhardness, the central portions of the taenite should contain only about 10 per cent nickel.

and ANDERKO, 1958) the borderzone can be explained as containing primary kamacite dendrites, while the central parts are a fine-grained eutectic mixture of kamacite and $(Fe,Ni)_3P$.

From laboratory experiments on the Thule meteorite, we know that the granulation takes place upon a short heating to about 800°C and that the Neumann bands disappear simultaneously, as the iron and nickel atoms rearrange themselves. Furthermore, we know from the Fe–P and Ni–P equilibrium diagrams, that the phosphides with 15 per cent P have melting ranges between 1200 and 1080°C. From these data a sketch has been drawn (Fig. 9), which shows the temperature distribution in the outer crust during the last seconds of flight through the atmosphere.

To evaluate the heat flow into the meteorite during its passage through the atmosphere a calculation based on the principles in the paper of MARINGER and MANNING (1960) has been carried out. The data yield a value for the heat transfer rate Q of 410 cal/cm² sec, which corresponds to an ablation rate of 1·6 mm/sec for the meteorite.

The value for the ablation rate is about the double of what MARINGER and MANNING found, but smaller than that which KRUPKA and TAYLOR (1960) have determined by laboratory experiments. They simulated the conditions of re-entry of missiles with a high-intensity plasma discharge (1000 kW) and found an ablation

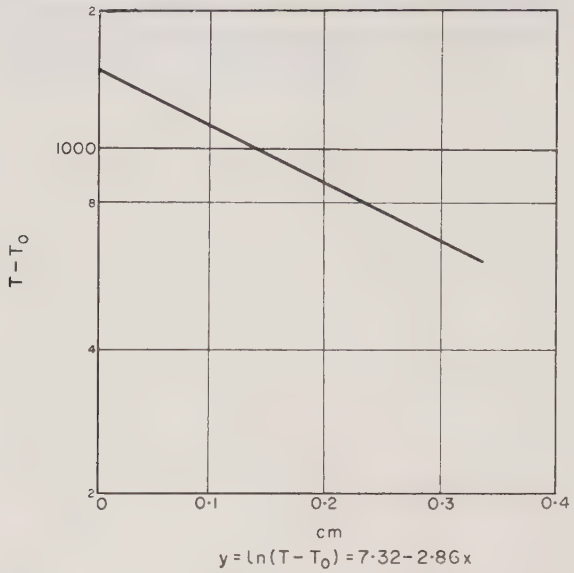

Fig. 9. Graph of temperature distribution in the crust of the Thule meteorite based upon metallurgical evidence. T_0, the temperature of the meteorite before entering the atmosphere, is supposed to be 0°C. (from $T_0 = \frac{277}{\sqrt{R}}$ °K, where R is the distance from the sun, measured in astronomical units).

rate for stainless steel of 2·5 mm/sec. It is interesting to see how different approaches lead to nearly the same ablation rates for iron materials penetrating the atmosphere.

Acknowledgements—The writer wishes to thank Prof. A. NOE-NYGAARD and Mrs. SOLE MUNCK for the specimens from the Mineralogical Museum of Copenhagen; thanks are also due to Dr. H. PAULY, Kryolitselskabet Øresund and to Mr. E. C. WINKEL, Det Danske Stålvalseværk, for discussions and analyses.

REFERENCES

AGRELL S. O. and LONG I. V. P. (1960) *Metall. Rev.* **5,** No. 18, 202.

HANSEN M. and ANDERKO K. (1958) *Constitution of Binary Alloys* pp. 692 and 1027.

KNUTH-WINTERFELDT E. (1952) *Korttidsmetoder til metallografisk elektropolering ved stuetemperatur* København, 115 pp. 42 plates.

KRUPKA R. M. and TAYLOR D. E. (1960) Ablation behaviour of materials subjected to missile re-entry heat flux rates. *Corrosion* **16,** 385–389.

MARINGER R. E. and MANNING G. K. (1960) Aerodynamic heating of the Grant meteorite. *Geochim et Cosmochim. Acta* **18,** 157–161.

PAULY H. (1961) In press.

Geochimica et Cosmochimica Acta, 1961, Vol. 25, pp. 99 to 109. Pergamon Press Ltd. Printed in Northern Ireland

Variation of thorium and uranium in selected granitic rocks

John J. W. Rogers and Paul C. Ragland
Department of Geology, Rice University, Houston, Texas

(*Received* 1 *February* 1961)

Abstract—A selected suite of granitic rocks representing both individual differentiation sequences and a broad sampling of granites from North America have been analysed for thorium, uranium, and potassium by γ-ray spectrometry. In the White Mountain and Oliverian series of New Hampshire both the thorium and uranium contents and the Th/U ratio tend to increase with igneous evolution. In the Southern California batholith the thorium and uranium contents increase during differentiation, but the Th/U ratio is constant. The general tendency for the Th/U ratio to increase with petrogenetic evolution is shown by a comparison of the Th/U ratio with the ratio of potassium feldspar to plagioclase for a broad sampling of granitic rocks. This increase is probably caused by oxidation during magmatic differentiation.

Introduction

A number of recent studies have been concerned with the distribution of thorium and uranium in igneous rocks. In particular, a comparison of thorium and uranium contents and petrographic features of a large suite of granitic rocks was made by Whitfield *et al.* (1959), and Larsen and Gottfried (1960) have described the variation of thorium and uranium in a number of igneous differentiation sequences. All studies, whether of a broad sampling of igneous rocks or of individual local sequences, are in agreement in showing that both thorium and uranium increase in abundance toward later-crystallizing, more acidic rock types. Different studies disagree, however, concerning the behaviour of the thorium to uranium ratio. For example, Whitfield *et al.* proposed that the Th/U ratio increases during petrogenetic evolution; the index of evolution used was the ratio of potassium feldspar to plagioclase, designated as R in that paper and also in the present one. Conversely, Larsen and Gottfried found no significant variation in Th/U ratios in the acidic portions of individual sequences when they plotted Th/U vs. the Larsen differentiation index, a chemical index proposed by Larsen (1938). Larsen and Gottfried did, however, note that the Th/U ratio is generally lower in gabbros than in more acidic rocks.

Possible variations in the Th/U ratio in igneous rocks are important in two regards. First, variations in the ratio may indicate, as discussed later, the significance of oxidative processes in the igneous differentiation mechanism. Secondly, variations in the ratio affect the lead isotopic content of igneous rock reservoirs.

The object of the present study was threefold. The first purpose was to relate the concentrations of thorium and uranium and the Th/U ratio to time of formation in a set of well-known intrusive differentiation sequences. The sequences studied were the Southern California batholith and the White Mountain, New Hampshire, and Oliverian series of New Hampshire. In the Southern California batholith and the White Mountain magma series the sequences of intrusion of various rock types are well known from field studies, and thorium and uranium variations with time of differentiation can be studied directly without the necessity of relating them to petrographic features. Sequence of formation is not determinable in the gneiss domes of the Oliverian series, and consequently thorium and uranium contents and Th/U

ratios have been related to the ratio of potassium feldspar to plagioclase (R). The relatively small number of measured thorium and uranium values and Th/U ratios in the New Hampshire series were found to be completely unrelated to any petrographic or lithologic features; consequently, these data are not reported here pending further investigation.

A second objective in the present study was to investigate the variation in thorium and uranium contents and Th/U ratio across transitional, hypothetically granitized zones between granites and metamorphic wall rocks. Studied sequences include the transition between gneiss and Cathedral Peak granite in the Mount Whitney area of the Sierra Nevadas (see Bradley and Lyons, 1953); the Boundary Peak granite–Pellesier granite–gneiss complex in the Inyo Range (see Anderson, 1937); and the transition between granites and quartzites in the Killarney region of Ontario (see Quirke, 1927, 1940). In no case did the Th/U ratio show any significant difference between the granites and metamorphic rocks, though the granites generally contained larger amounts of both thorium and uranium. The least-altered metamorphic rocks (five samples) had thorium contents ranging from 3·4 to 11 p.p.m., uranium contents from 0·7 to 6·6 p.p.m., and Th/U ratios from 0·8 to 4·8. In the granites the thorium content ranged from 8·2 to 21 p.p.m., the uranium content from 1·9 to 7·4 p.p.m., and the Th/U ratios from 2·2 to 5·9. Plots of thorium and uranium content vs. position in the transition zones are completely erratic, possibly owing to insufficient sampling, and no significance could be attached to them; the data, therefore, are not reported here.

The third purpose of the present study was to combine the new data reported here with the measurements made by Whitfield *et al.* to provide a larger generalized picture of the behaviour of thorium, uranium, and the Th/U ratio in granitic rocks. For this purpose a number of graphs have been constructed relating the thorium, uranium, and potassium contents, the Th/U ratio, and the potassium feldspar to plagioclase ratio.

All samples studied came from the collection made by Whitfield and used in part for previous studies. Thorium, uranium, and potassium contents were measured by gamma ray spectrometry by methods described by Whitfield *et al.* (1959). Measurements were made on a single-channel instrument equipped with a 3-in. thallium-activated sodium iodide crystal. All samples were crushed to −100 mesh, and spectrometry was performed on 350 g of the powder packed in 8-oz cans. The packed material was allowed to attain secular radioactive equilibrium before counting. Counting rates were determined in the 2·62 MeV channel for thorium, the 1·76 MeV channel for uranium, the 1·47 MeV channel for potassium, and the 0·61 MeV channel as an internal check. Accuracy is adjudged to be well within ±15 per cent.

Modal analyses were made by point counts of 1000 to 1500 points.

Data are presented in three tables. Table 1 shows the thorium, uranium, and potassium contents, the Th/U ratio, and the ratio of potassium feldspar to plagioclase (R) in the samples used in the present study. Table 2 gives the results of modal analyses of thin sections of the various samples. Table 3 provides locations and identifications of all samples. In Table 3 the rock names are those used commonly to identify the formation in the field and do not necessarily correspond to the most appropriate names based on the compositions shown in Table 2.

Table 1. Thorium, (p.p.m.) uranium, (p.p.m.) and potassium (%) contents and R values of analysed granitic rocks*

	Th†	U†	K†	Th/U	R‡
MW–1–74	16	6·6	3·1	2·3	0·52
MW–4–77	21	7·4	3·2	2·8	0·80
MW–5–78	53	14	3·4	3·8	0·63
MW–7–80	24	11	3·3	2·3	0·31
I–1–86	8·2	2·5	2·3	3·3	0·22
I–2–87	9·3	2·7	3·1	3·4	0·43
I–8–93	11	1·9	4·1	5·9	1·1
K–13–251	12	5·5	3·2	2·2	1·05
NH–4–306	65	14	4·4	4·7	2·4
NH–6–308	32	7·2	4·8	4·4	3·1
NH–7–309	24	7·1	4·9	3·3	2·6
NH–8–310	24	7·1	4·6	3·4	2·0
NH–9–311	29	7·1	4·0	4·1	13
NH–10–13	23	7·6	4·2	3·0	12
NH–14–316	10	2·3	2·3	4·2	44
NH–15–317	3·4	0·7	4·8	4·8	2·7
NH–17–319	98	8·3	4·2	11·7	1·5
NH–19–321	20	3·0	3·7	6·7	0·55
NH–20–322	14	3·7	3·8	3·8	0·78
NH–22–324	2·3	1·2	5·4	1·9	0·09
NH–23–325	not detectable				
NH–24–326	not detectable				
NH–27–329	19	2·7	3·9	6·9	0·21
NH–28–330	16	6·2	3·2	2·5	0·36
NH–30–332	32	6·5	4·3	4·9	0·95
NH–31–333	26	5·1	4·3	5·1	1·1
NH–34–336	6·2	2·1	0·5	2·9	0·01
NH–36–338	32	4·8	5·0	6·6	1·4
NH–37–339	28	5·9	4·8	4·7	1·4
Sc–4–52	10	2·4	2·4	4·3	0·38
Sc–5–53	11	2·1	2·1	5·1	0·19
Sc–9–57	14	6·8	3·1	2·1	0·49
Sc–10–58	11	1·9	2·8	5·7	0·47
Sc–11–59	12	2·0	2·4	5·8	0·13
Sc–19–66	0·8	0·3	0·4	2·6	0
Sc–20–67	4·2	1·5	1·8	2·8	0·17
Sc–21–68	4·2	1·3	1·6	3·2	0·10
Sc–23–70	3·1	1·9	1·8	1·6	0·01
Sc–24–71	17	5·3	3·4	3·2	2·2

* All values are reported to two significant figures and are rounded off after calculation of Th/U and R.
† Thorium and uranium values are reported as parts per million of the metal, and potassium is reported as per cent of the metal.
‡ R is the ratio of potassium feldspar to plagioclase as determined from modal analyses.

This study was financed by Grant C–009 from the Robert A. Welch Foundation.

Thorium and Uranium in Individual Igneous Sequences

Figs. 1 to 3 show the variation of thorium, uranium, and Th/U ratio in three separate igneous sequences. For the Southern California batholith and the White

Table 2. Modal analyses of granitic rocks*†

Slide no.	Quartz	K feldspar	Plagioclase	Biotite	Horn blende	Opaques	Zircon	Apatite	Sphene	Epidote	Allanite	Muscovite	Pyroxene
MW–1–74	33	22	41	2·9		0·4		tr.	0·1				
MW–4–77	22	32	40	3·6	1·0	0·8		tr.	0·1				
MW–5–78	17	29	46	4·4	1·6	1·1		tr.	0·8		tr.		
MW–7–80	20	14	46	8·5	6·8	0·2	tr.	tr.	tr.				
I–1–86	19	12	55	8·7		0·7	tr.	tr.	0·3	2·0	tr.	0·6	
I–2–87	25	19	45	7·0	0·5	0·1			0·3	0·4			
I–8–93	20	39	35	2·7		0·8			0·2	0·1		0·2	
K–13–251	28	34	32	tr.					tr.			5·8	
NH–4–306	35	43	18	2·8		0·7	tr.	tr.	tr.				
NH–6–308	29	48	15	3·1	4·3	0·5	tr.	tr.	tr.				
NH–7–309	29	50	19	0·7	0·9	0·5	tr.	tr.					
NH–8–310	28	45	23	2·0	0·6	0·8	tr.	tr.					
NH–9–311	27	66‡	5·1		1·8	0·2	tr.	tr.					
NH–10–13	26	65‡	5·6		3·4	0·3	tr.	tr.					
NH–14–316	1·1	89‡	2·1			1·7	tr.	tr.		0·4			6·1
NH–15–317	1·5	59‡	22		1·2	1·9	tr.	tr.					14
NH–17–319	29	41	28	1·9		0·1	tr.	tr.			tr.		
NH–19–321	4·3	32	59	0·1	4·3	0·2	tr.	tr.					
NH–20–322	5·4	38	49	0·1	5·8	1·4	tr.			tr.			
NH–22–324	3·5	7·1	83	2·0		1·2		tr.		tr.			
NH–23–325			67	4·3		9·2		0·7		tr.			18
NH–24–326			77	1·2		2·2		tr.		3·2			15
NH–27–329	41	8·5	41	7·0		tr.	tr.	tr.	tr.	1·3			
NH–28–330	34	15	41	7·0		tr.				1·9			
NH–30–332	34	32	33	0·3		0·1				0·1		0·1	
NH–31–333	41	30	26	1·6		tr.							
NH–34–336	32	0·5	65	0·6		0·6		tr.				0·6	
NH–36–338	36	35	25			tr.	tr.	tr.	tr.	0·7		2·7	
NH–37–339	38	31	23	0·5		tr.	tr.	tr.	tr.	1·0		4·9	
Sc–4–52	25	18	48	7·7	1·4	tr.	tr.	tr.					
Sc–5–53	32	9·4	49	7·4	1·8	0·2	tr.	tr.					
Sc–9–57	35	19	39	6·3	1·1	0·1	tr.	tr.					
Sc–10–58	40	17	36	4·9	1·4	0·3	tr.		tr.				
Sc–11–59	28	7·6	58	5·9	0·5	0·1		tr.	tr.		tr.		
Sc–19–66			53		39	1·0							7·2
Sc–20–67	38	7·7	45	7·5	1·0	tr.				0·4			
Sc–21–68	35	4·2	44	10	6·2	0·2	tr.						
Sc–23–70	27	0·5	52	14	7·5	0·5	tr.						
Sc–24–71	38	41	19	1·0		0·4				tr.			

* Alteration products generally constitute less than one per cent of each sample and are omitted from the table.
† All values are reported to two significant figures and are rounded off after calculation of *R*.
‡ Highly perthitic feldspar.

Table 3. Locations and identifications of all samples

Sample no.	Location	Name
MW–1–74	Mt. Whitney, Calif.	Cathedral Peak granite
MW–4–77	Mt. Whitney, Calif.	Cathedral Peak granite
MW–5–78	Mt. Whitney, Calif.	granodiorite
MW–7–80	Mt. Whitney, Calif.	tonalite
I–1–86	Inyo Range, Calif.	Boundary Peak granite
I–2–87	Inyo Range, Calif.	Pellesier granite
I–8–93	Inyo Range, Calif.	Boundary Peak granite
K–13–251	Killarney, Ontario	granite
	New Hampshire	
NH–4–306	White Mt. Series	biotite granite (Conway)
NH–6–308	White Mt. Series	biotite granite (Conway)
NH–7–309	White Mt. Series	biotite granite (Conway)
NH–8–310	White Mt. Series	biotite granite (Conway)
NH–9–311	White Mt. Series	hastingsite granite
NH–10–13	White Mt. Series	hastingsite granite
NH–14–316	White Mt. Series	quartz syenite
NH–15–317	White Mt. Series	quartz syenite
NH–17–319	White Mt. Series	biotite granite (Conway)
NH–19–321	White Mt. Series	monzonite
NH–20–322	White Mt. Series	monzonite
NH–22–324	White Mt. Series	monzodiorite
NH–23–325	White Mt. Series	gabbro
NH–24–326	White Mt. Series	gabbro
NH–27–329	Oliverian Series	Mascoma quartz monzonite
NH–28–330	Oliverian Series	Mascoma quartz monzonite
NH–30–332	Oliverian Series	Mascoma quartz monzonite
NH–31–333	Oliverian Series	Mascoma quartz monzonite
NH–34–336	Oliverian Series	Mascoma quartz diorite
NH–36–338	Oliverian Series	Lebanon granite
NH–37–339	Oliverian Series	Lebanon granite
	Southern California Batholith	
Sc–4–52		Mt. Hole granodiorite
Sc–5–53		Mt. Hole granodiorite
Sc–9–57		Woodson Mt. granodiorite
Sc–10–58		Woodson Mt. granodiorite
Sc–11–59		Woodson Mt. granodiorite
Sc–19–66		San Marcos gabbro
Sc–20–67		Bonsall tonalite
Sc–21–68		Bonsall tonalite
Sc–23–70		Bonsall tonalite
Sc–24–71		Roblar leucogranite

Mountain magma series the values are plotted against sequence of intrusion, as determined largely by field evidence and reported by Larsen (1948) for Southern California and by Billings and Keevil (1946) for the White Mountain series. Owing to the impossibility of establishing a sequence of formation for the rocks in the

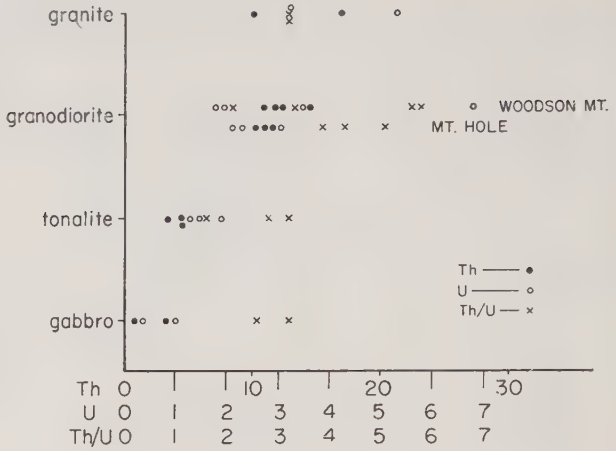

Fig. 1. Distribution of thorium, uranium, and Th/U ratio in the Southern California batholith. Thorium and uranium contents are in parts per million. Progressively younger rocks are toward the top of the diagram.

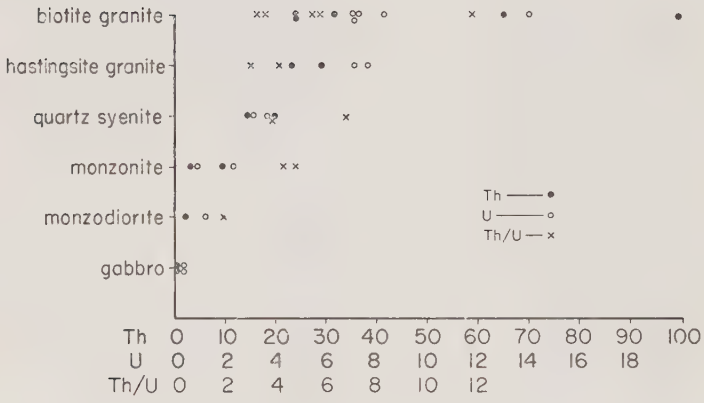
biotite granite
hastingsite granite
quartz syenite
monzonite
monzodiorite
gabbro
Th ——— •
U ——— ○
Th/U — ×
Th 0 10 20 30 40 50 60 70 80 90 100
U 0 2 4 6 8 10 12 14 16 18
Th/U 0 2 4 6 8 10 12

Fig. 2. Distribution of thorium, uranium and Th/U ratio in the White Mountain magma series. Thorium and uranium contents are in parts per million. Progressively younger rocks are toward the top of the diagram.

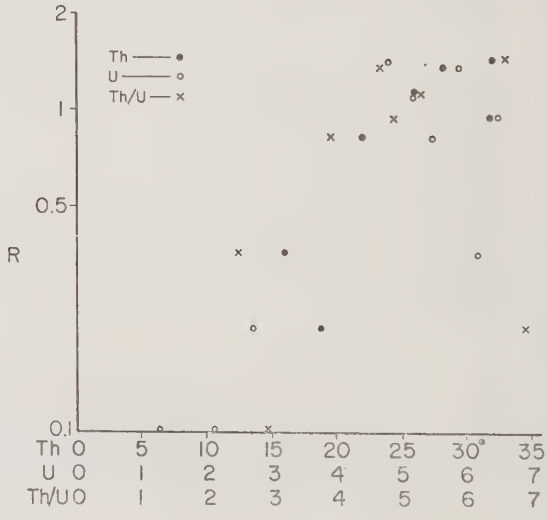

Fig. 3. Distribution of thorium, uranium and Th/U ratio in the Oliverian series. Thorium and uranium contents are in parts per million. Data are plotted against the ratio of potassium feldspar to plagioclase (R).

gneiss domes of the Oliverian series, the radioactivity data have been plotted against the ratio of potassium feldspar to plagioclase (R), which is considered to represent stage of petrogenetic evolution. Several of the values plotted were reported by Whitfield *et al.* and are not repeated here, but most of the measurements were made for this study and are shown in Tables 1 and 2.

In all three sequences the abundances of thorium and uranium increase toward the later-forming rocks. In the White Mountain series the later-crystallizing rocks exhibit the only large Th/U ratios and exhibit the greatest range of ratios; in the Southern California batholith the ratio is apparently unchanged during differentiation, though data for the San Marcos gabbro were not obtainable owing to the low radioactivity of the two samples measured. In the Oliverian series, with the exception of one aberrant sample, the Th/U ratio exhibits a reasonably steady increase with increasing R. Thus, in two of the three studied sequences, the Th/U ratio shows a weak tendency to increase with petrogenetic evolution, but the reasons for the differences between the behaviour of the Th/U ratio in the Southern California batholith and in the two series from New Hampshire are not known.

General Distribution of Thorium and Uranium in Granitic Rocks

Figs. 4 to 10 illustrate the general relationships among the thorium, uranium and potassium contents, the Th/U ratio, and the ratio of potassium feldspar to plagioclase (R) in granitic rocks. The graphs are based on data reported in the present paper and also by Whitfield *et al.* (1959). The graphs thus encompass the broad suite of granitic rocks studied by Whitfield, the new measurements from the Southern California batholith, the White Mountain magma series, and the Oliverian series, and measurements made on the granitic rocks in the transition zones in the Sierra Nevada, the Inyo Range, and at Killarney, Ontario. Whether or not this selectivity biases the data is a matter for individual judgment.

The behaviour of thorium is shown by Figs. 4 to 6. The tendency for thorium and uranium to vary together is shown in Fig. 4. Note, however, that high values of thorium are not accompanied by proportionally high values of uranium. Thus, for rocks with an abnormally high thorium content, the Th/U ratio is higher than average; inasmuch as these rocks are also commonly later-crystallizing members of igneous sequences, the relationships shown in Fig. 4 support the contention that the Th/U ratio increases during igneous evolution. The tendency for the absolute amounts of thorium to increase during differentiation is shown in Figs. 5 and 6, where thorium content is plotted against potassium content, a weak chemical index of differentiation, and R, a petrographic index. Note that the spread of thorium values is much larger in the more highly differentiated rocks, possibly indicating variability of differentiation mechanisms.

Figs. 7 and 8 show the variation in uranium content of igneous rocks. Plots of uranium vs. both potassium content and R show the tendency of uranium to increase with igneous evolution. The relationships are much more uncertain in the case of uranium, however, than in the case of thorium. Plots of uranium content are invariably more diffuse than those of thorium, and it appears that uranium is much less related to major lithologic features than thorium. One possible explanation for the erratic behaviour of uranium is its presumed high mobility in oxidized form, which

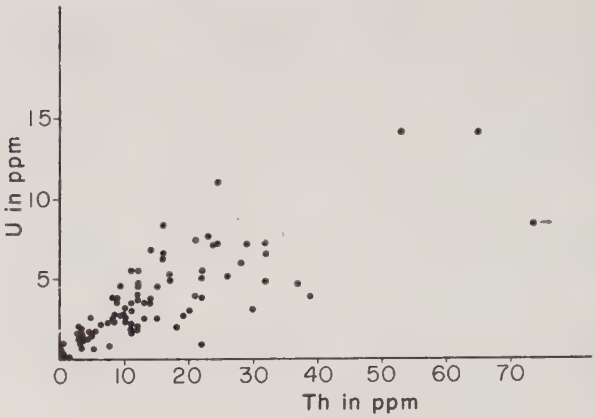

Fig. 4. Thorium content vs. uranium content of granitic rocks.

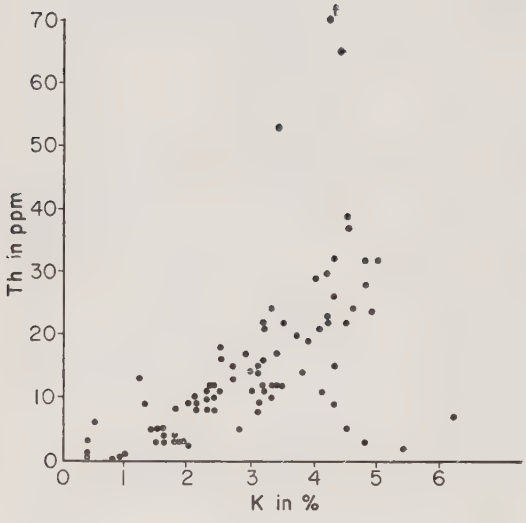

Fig. 5. Thorium content vs. potassium content of granitic rocks.

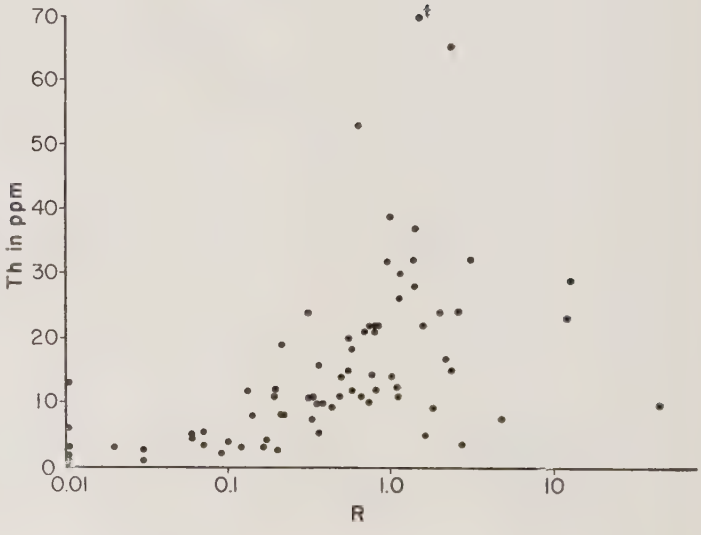

Fig. 6. Thorium content vs. ratio of potassium feldspar to plagioclase (R) of granitic rocks. Rocks with R values of less than 0·01 are plotted along the 0·01 line.

might permit its selective removal from magmas in volatile phases. This erratic distribution and possibility of selective removal may also explain the hypothesized increase in the Th/U ratio in the more differentiated rocks.

Plots of the Th/U ratio versus potassium content and R are shown in Figs. 9 and 10. All ratios (Th/U and R) are plotted on logarithmic scales. Both plots are diffuse,

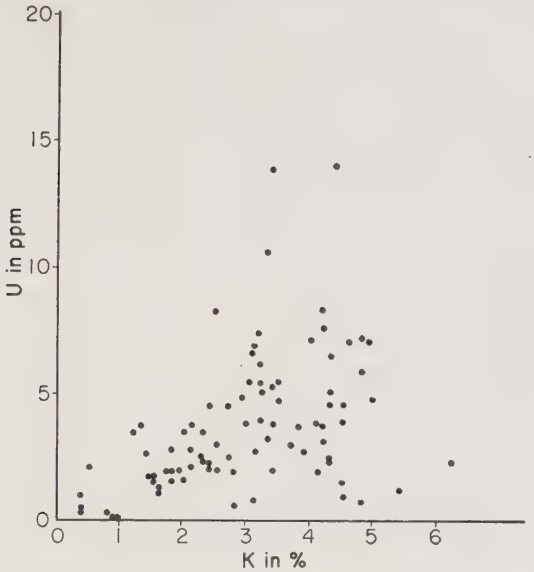

Fig. 7. Uranium content versus potassium content of granitic rocks.

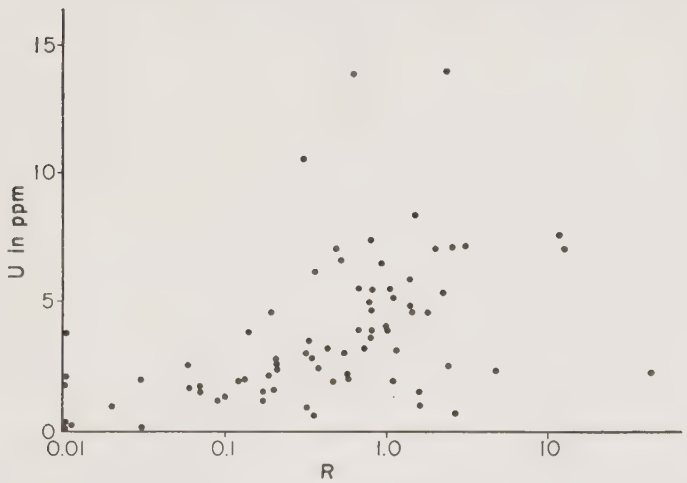

Fig. 8. Uranium content vs. ratio of potassium feldspar to plagioclase (R) of granitic rocks. Rocks with R values of less than 0·01 are plotted along the 0·01 line.

and the relationships are not absolutely certain, and in particular, the relationship between potassium content and the Th/U ratio seems quite indefinite. The possibility of a linear relationship between Th/U and R, both plotted logarithmically, may be tested by calculation of the linear correlation coefficient. This coefficient for Fig. 10

is 0·31. If the Th/U and R values are derived from normally distributed populations, this coefficient is significant at a confidence level greater than 99 per cent. Even if the logarithmic transformations used here are not sufficient to normalize the data, the correlation coefficient is almost certainly significant at a high confidence level.

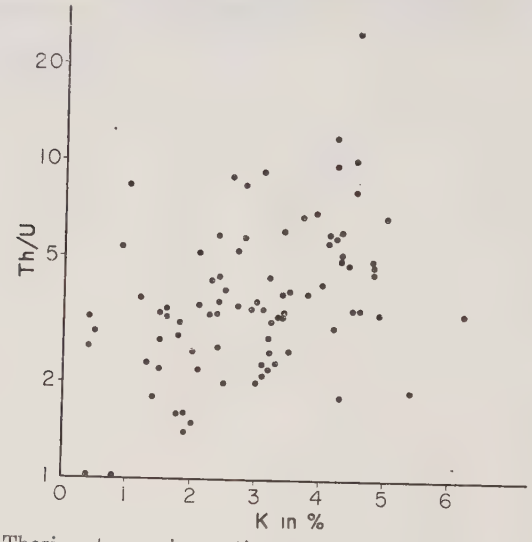

Fig. 9. Thorium to uranium ratio vs. potassium content of granitic rocks.

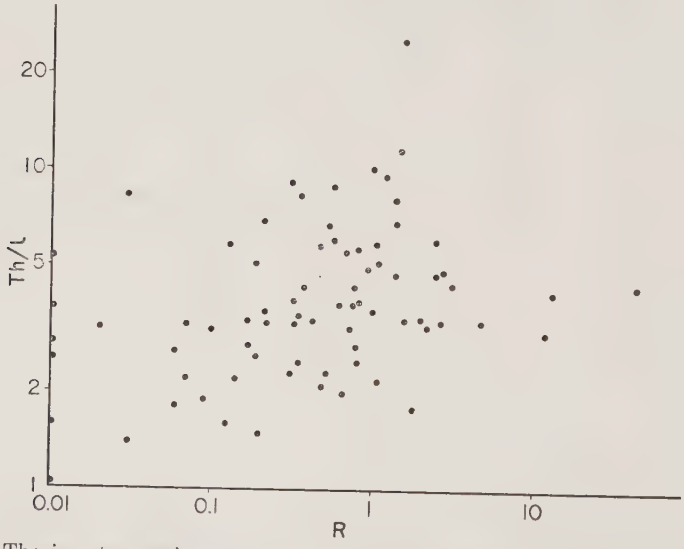

Fig. 10. Thorium to uranium ratio vs. ratio of potassium feldspar to plagioclase (R) of granitic rocks. Rocks with R values of less than 0·01 are plotted along the 0·01 line.

The fact that the correlation coefficient is less than 1 does not, of course, negate the validity of a relationship between Th/U and R; a low but significant coefficient merely indicates that Th/U is related to more variables than just R. A higher correlation coefficient might, of course, be obtained by comparison of the relationship with some curve other than a straight line, and no claim is made that Th/U and

R are linearly related. The evidence, however, appears to show that the Th/U ratio increases with igneous differentiation, though the increase is erratic and probably controlled by more than one process.

Whether the comparatively high Th/U ratios in rocks with a high R value result from loss of uranium or addition of thorium is uncertain. The likelihood of uranium loss is mentioned above. The possibility that thorium has been added to such rocks as the Conway granite, which is exceptionally rich in allanite (Billings and Keevil, 1946) must not be discounted. The relatively more erratic distribution of uranium than of thorium, however, as shown by comparison of Figs. 5 and 7 and Figs. 6 and 8, makes loss of uranium more plausible than secondary addition of thorium except for such extremely high thorium rocks as the Conway granite.

The possible loss of uranium during the later stages of igneous differentiation may result from oxidation to the uranyl ion during the evolution of suites of igneous rocks. This conclusion is based on the assumed, though not proven, greater solubility of uranyl ion than of tetravalent uranium or thorium in volatile igneous phases. It is, however, possible that fractionation occurs between the tetravalent uranium and thorium ions, for the two ions are not identical, though they are quite similar. The mere presence of ferric iron in igneous rocks, e.g. in the form of the early-crystallizing magnetite of many granites, indicates that oxidizing capacity is present in magmas. Whether or not the oxidation potential varies during igneous evolution is not known, and the problem is of considerable interest in connection with the studies of Osborn (1959) on the significance of oxygen pressure in the differentiation of basaltic magma. Osborn found that the maintenance of a constant oxygen pressure on a melt with a composition analogous to that of basalt caused oxidation of iron and production of a highly silicic (granitic) liquid. This importance of oxidation in the differentiation of granitic materials may be substantiated by the apparent variation in Th/U ratios.

References

Anderson G. H. (1937) Granitization, albitization, and related phenomena in the northern Inyo Range of California–Nevada. *Bull. Geol. Soc. Amer.* **48,** 1–74.

Billings M. P. and Keevil N. B. (1946) Petrography and radio-activity of four Paleozoic magma series in New Hampshire. *Bull. Geol. Soc. Amer.* **57,** 797–828.

Bradley C. and Lyons E. J. (1953) A mode of evolution of a granitic texture. *in* Emmons R. C. (ed.) *Selected* petrogenic relationships of plagioclase. *Geol. Soc. Amer. Mem.* **52,** 101–110.

Larsen E. S., Jr. (1938) Some new variation diagrams for groups of igneous rocks. *J. Geol.* **46,** 505–520.

Larsen E. S., Jr. (1948) Batholith and associated rocks of Corona, Elsinore, and San Luis Rey quadrangles, Southern California. *Geol. Soc. Amer. Mem.* **29,** 182pp.

Larsen E. S. III and Gottfried D. (1960) Uranium and thorium in selected suites of igneous rocks. *Amer. J. Sci.* **258-A,** 151–169.

Osborn E. F. (1959) Role of oxygen pressure in the crystallization and differentiation of basaltic magma. *Amer. J. Sci.* **257,** 609–647.

Quirke T. T. (1923) Killarney gneisses and magmatites. *Bull. Geol. Soc. Amer.* **38,** 753–770.

Quirke T. T. (1940) Granitization near Killarney, Ontario. *Bull. Geol. Soc. Amer.* **51,** 237–253.

Whitfield J. M., Rogers J. J. W. and Adams J. A. S. (1959) The relationship between the petrology and the thorium and uranium contents of some granitic rocks. *Geochim. et Cosmochim. Acta* **17,** 248–271.

Geochimica et Cosmochimica Acta, 1961, Vol. 25, pp. 110 to 146. Pergamon Press Ltd. Printed in Northern Ireland

Chemical and mineralogical studies of deep-sea sediments

S. K. El Wakeel* and J. P. Riley
Dept. of Oceanography, The University of Liverpool

(*Received* 26 *July* 1960)

Abstract—Chemical and spectrographic analyses are presented for the major and several minor elements in ten calcareous, twelve argillaceous and three siliceous deep-sea sediments from the Atlantic, Pacific and Indian Oceans and Mediterranean Sea; a 5 m core from the Atlantic; three deep-sea volcanic sediments; an unusual calcareous manganiferous ooze, and the $<2\ \mu$ fractions from two near-shore muds. The distribution of the minor elements was very similar to that described by Goldberg and Arrhenius for Pacific sediments. Except for their higher content of ferrous iron and organic carbon the chemical composition of the $<2\ \mu$ fraction of the near shore clays closely resembled that of the deep-sea argillaceous sediments. This resemblance and the similarity of the abundances of certain of the minor elements, such as Ti, Zr, Cr and V, in the pelagic to their abundances in igneous rocks, suggests a mainly terrigenous origin for red clay. The argillaceous material of two globigerina oozes from the Mediterranean was very similar in composition to that of the deep ocean sediments. The proportions of all the major elements down the length of the 5·05 m core of red clay from off the Bermuda rise in the Atlantic were very constant. Niggli values have been used to compare the sediments, on a carbonate-free basis, the sediments from the Atlantic are characterized by their higher al and lower fm values compared with those from the Pacific and Indian Oceans. Illite and chlorite, with lesser amounts of montmorillonite, are the principal clay minerals in the deep-sea sediments. The near shore clays are richest in kaolinite, but illite and montmorillonite are also present.

Although deep sea sediments cover more than 50 per cent of the surface of the earth, there is surprisingly little accurate information available about their chemical composition. Much of the earlier analytical data is incomplete and often only semi-quantitative owing to the use of faulty analytical techniques; frequently, even in recent work, only selected elements have been determined.

As new methods of study, microscopical, chemical and physical have been developed, the emphasis of investigations has changed from a purely descriptive approach, to the consideration of the geochemistry and mineralogy of the samples. The *Discovery* Expedition to the Antarctic Seas (Neaverson, 1934), the *Meteor* Expedition to the Atlantic and Indian Oceans (Correns, 1937; Schott, 1955), the *Snellius* Expedition to the Dutch East Indies (Neeb and Kuenen, 1943) and the last cruise of the *Carnegie* in the Pacific Ocean (Revelle, 1935), have greatly added to our knowledge of the chemistry of marine sediments. The geological findings of these expeditions have been discussed by Sverdrup *et al.* (1942), Shepard (1948) and Kuenen (1950).

The development of the piston corer by Kullenberg (1947) just after the Second World War has added a third dimension to the study of marine sediments. This type of corer was first used on the Swedish Deep Sea Expedition (Pettersson, 1949; Landergren, 1954). It has subsequently been used on the *Galatea* Expedition and on many voyages, among others, of *Discovery II*, and of ships of the Lamont Geological Observatory and of the Scripps Institute of Oceanography (Capricorn, Cusp, Chinook, Mid-Pacific and Downwind Expeditions). The symposium on *Recent Marine Sediments* edited by Trask (1955) contains a valuable bibliography covering the field of deep sea sediments.

* Present address: Oceanography Dept., University of Alexandria, Egypt.

Many rarer elements are concentrated in marine sediments relative to igneous rocks. Much of the earliest systematic work on the occurrence of these elements in deep sea sediments was carried out by GOLDSCHMIDT and his collaborators (GOLDSCHMIDT and PETERS, 1931, 1932a, b 1933; GOLDSCHMIDT and HEFTER, 1933). (Sc Y, Ga, Be, B, Ge, Se, respectively). Since that time further work on this subject has also been mainly confined to the determination of individual trace elements such as boron (LANDERGREN, 1945), germanium (EL WARDANI, 1958) and gallium and germanium (BURTON *et al.*, 1959).

LANDERGREN (1954) has studied the interrelationships between certain of the major and minor elements in a 14 m core from the Romanche deep in the Atlantic.

REVELLE *et al.* (1955) have determined the commoner trace elements in a number of sediments from the Pacific Ocean. They found a marked covariance of manganese with nickel and of iron with titanium in red clay. They attributed the concentration of these elements to the action of negatively charged colloidal hydrous manganese dioxide, which scavenges cationic species such a Ni, Co and Pb from sea-water, and to the action of positively charged colloidal hydrated ferric oxide as a collector for anions. GOLDBERG and ARRHENIUS (1958) now appear to have abandoned the theory that colloidal manganese dioxide adsorbs the cationic species from sea water, since they have found that almost all of the manganese in sea water occurs in true solution in the divalent form. They attribute all the adsorption effects to the action of colloidal hydrous ferric oxide.

ARRHENIUS (1952) considers that the high concentration of barium found in some marine sediments has been produced by a biological mechanism, and is associated with a rapid rate of deposition and dissolution of organic remains. A considerable proportion of the copper present in pelagic sediments has a biological origin and a remarkable covariance exists between the biogenous copper and barium (REVELLE *et al.*, 1955).

GOLDBERG and ARRHENIUS (1958) have made a thorough investigation of the major and minor constituents of about forty Pacific pelagic sediments, many of which contained much basaltic material, using optical and X-ray spectroscopic techniques. Analyses were made of fractions of various grain sizes, separated according to settling velocity, from several of the sediments. The pore water of the sediments and the elements removed from them by chelative dissolution, using ethylenediaminetetra-acetic acid, were also examined. Particular attention was paid to the mode of occurrence of barium in sediments and to the interrelationships between certain trace elements, such as vanadium and chromium, and some of the major components, particularly in sediments rich in basaltic pyroclastics.

Using X-ray diffraction methods REVELLE (1944) was able to show that the fine clay fraction of recent deep marine sediments is mainly crystalline. This confirmed CORRENS' (1937) discovery that a mica (probably illite) was present in all the bottom samples collected by the *Meteor* in the South Atlantic. Some of the samples also contained much kaolinite and a few had halloysite or montmorillonite. LEINZ (1937) examined the blue clay samples collected by the same expedition and found them to contain mica with variable amounts of kaolinite.

DIETZ (1942) reported that illite was the predominant clay mineral in most of the thirty-nine deep-sea sediments which he examined. Kaolinite was present in all the

samples, but was abundant only in those from near-shore stations. Montmorillonite was not detected in most deep-sea sediments, but was present in small amounts in near shore samples. The methods used by Dietz and earlier workers were incapable of detecting small amounts of montmorillonite; it was only after the development of the ethylene glycol–clay mineral X-ray techniques that the identification of as little as 5 per cent montmorillonite became feasible. Grim *et al.* (1949) using a combination of X-ray techniques and differential thermal analysis examined a series of samples collected from the Gulf of California and the Pacific Ocean. They found that all the samples contained, in decreasing order of abundance, illite, montmorillonite and kaolinite; there was also evidence in some samples of the presence of a chloritic clay mineral. There was no evidence of vertical variation of composition in the cores which they studied. Similar results were obtained by Murray and Sayyab (1955) for Recent marine sediments from off the coast of North Carolina.

Suzuki and Kitazaki (1954) have carried out electron microscopic and differential thermal examinations of deep sea clays from the Pacific, which they consider to be of volcanic origin. They consisted chiefly of amorphous clay mineral (allophane) with small amounts of illite, quartz and remains of unicellular organisms.

This paper describes an investigation into the chemical and mineralogical composition of a number of pelagic sediments from the Atlantic, Pacific and Indian oceans, and from the Mediterranean. The samples examined (Table 1, Fig. 1) were mainly of an argillaceous or calcareous-argillaceous type, and except for samples nos. 24, 30 and 31 contained little material identifiable as being of volcanic origin.

Experimental

Preparation of samples

All samples (20–25 g) were dispersed by shaking mechanically for about 30 min with about 500 ml of distilled water. After 24 hr the clear liquid was decanted through a close textured filter held in a Buchner funnel. The clay was transferred to the funnel and washed thoroughly with distilled water to remove soluble salts. It was sucked as dry as possible on the funnel, spread out on filter papers and allowed to dry at room temperature. The dried sample was disintegrated with the fingers, mixed well, and quartered to obtain a representative sample for chemical analysis; the remainder being reserved for mineralogical study. The portion to be used for chemical analysis was again washed as described above until the washings were free from chloride; after air-drying the specimen was ground to pass a 100-mesh sieve and dried at 105°C and stored in a well stoppered tube in a desiccator.

Chemical analysis

The determination of SiO_2, Fe_2O_3, FeO, Al_2O_3, TiO_2, MnO, CaO, MgO, Na_2O, K_2O, P_2O_5 and H_2O were carried out as described by Riley (1958a, b) Carbonate-carbon dioxide was determined as described by Groves (1951); organic carbon was either estimated indirectly by deduction of this value from the total amount of carbon (including carbonate-carbon) found by combustion (Riley, 1958b), or by direct determination of organic carbon by the method of El Wakeel and Riley (1957) which gave similar results. Organic amino-nitrogen was determined by the Micro-Kjeldahl technique. Ferrous oxide was estimated by the conventional method

Sample no.	Expedition	Station	Depth (m)	Lat.	Long.	Type and colour
1	Challenger*	5	5400	24°20′N	24°28′W	Calcareous ooze—light brown-red
2	Challenger	16	4800	20°39′N	50°33′W	Globigerina ooze—pale yellow brown.
3	Challenger†	256	5820	30°22′N	154°56′W	Red clay, light reddish brown.
4	Challenger‡	272	5130	03°48′S	152°56′W	Globigerina ooze—brown-grey.
5	Michael Sars§	10	4700	45°26′N	09°20′W	Globigerina ooze—fawn coloured.
6	Discovery	D	3195	26°08′S	14°36′W	Globigerina ooze—light brown.
7	Discovery	10STB	4402	46°35′S	24°15′W	Diatom ooze**—grey brown.
8	Discovery	2911STPA	3956	35°55′N	17°29′E	Globigerina ooze—buff.
9	Discovery	2911STPB	3956	35°55′N	17°29′E	Globigerina ooze—buff.
10	Discovery	2896STP	4464	01°06′N	85°36′E	Globigerina ooze—buff.
11	Discovery	158	1395	38°55′N	31°35′W	Globigerina ooze—buff.
12	Discovery	2996	4710	48°52′N	15°00′W	Buff coloured clay—60–75 cm of core.
13	Discovery	3498	5582	34°11′N	55°32′E	Calcareous clay—light brown
14	Discovery	3617	5949	24°30′N	64°47′W	Red clay.
15	Downwind	DWHD 81	3200	22°07′S	115°10′W	Calcareous manganiferous—chocolate coloured ooze.
16	John Murray††	166	4793	06°52′N	67°13′E	Red clay—reddish brown.
17	Lamont Geol. Obs.	A172–19	5395	24°35′N	64°02′W	Red clay—dark red‡‡.
18	Swedish Deep Sea (no. 73)	106	5200	04°04′S	152°53′W	Red clay—121·5–129·0 cm of core.
19	Swedish Deep Sea (no. 86)	134	5500	04°02′N	172°19′W	Red clay—102·5–109·0 cm of core
20	Swedish Deep Sea (no. 128)	189	5170	11°28′S	102°24′E	Red clay—261–268 cm of core.
21	Swedish Deep Sea (no. 148)	224	4405	01°20′S	64°00′E	Red clay—112–118·5 cm of core.
22	Swedish Deep Sea (no. 230)	328	5500	10°12′N	26°36′W	Red clay—142–149·5 cm of core.
23	Swedish Deep Sea (no. 262)	365	5480	14°32′N	55°05′W	Red clay—65·5–69·0 cm of core.
24	Capricorn	H24	4685	16°44′S	161°22′W	Chocolate volcanic clay core 4–48 cm.
25	Cusp	1G	4940	31°05′N	135°24′W	Red clay—0–110 cm of core.
26	Cusp	3G	3110	40°56′N	125°38′W	Green mud—4–24 cm of core.
27	Cusp	7G	4090	43°45′N	137°06′W	Brownish-grey mud. 0–20 cm of core.
28	Cusp	14G	4270	43°49′N	143°07′W	Tan clay, 0–120 cm of core.
29	Mid-Pacific	13–2	5080	09°09′N	144°26′W	Siliceous clay—buff. 15–28 cm of core.
30	Mid-Pacific	18A–1	359	19°46′N	154°58′W	Volcanic muddy sand, 2–19 cm of core.
31	Mid-Pacific	20–2	5408	20°27′N	154°55′W	Volcanic clay, brown, 15–23 cm of core.
32	Chinook I§§	3	3460	29°24′N	153°06′W	Brown clay, 140–145 cm of core.
33	Chinook I***	5	6140	42°29′N	162°08′W	Brown clay, 10–28 cm of core.
34	William Herdman	WH1	6	53°22′N	4°15′W	Light brown clay.
35	William Herdman	WH2	5	53°18′N	4°02′W	Light brown clay.

* British Museum Catalogue no. M25. This sample is described as red clay although analyses show it to contain 60 per cent $CaCO_3$. Murray and Renard (1891).

† British Museum Catalogue no. M320. Murray and Renard (1891).

‡ British Museum Catalogue no. M340. Murray and Renard (1891).

§ British Museum Catalogue no. M9711. Murray and Chumley (1924).

** Described as radiolarian ooze in the official report (Matthews, 1934) but the bulk of the sediment is formed of diatom frustules with a few Nasselarian radiolaria.

†† British Museum Catalogue no. A 51. Stubbings (1937).

‡‡ Eleven core samples at 50 cm intervals from 5·05 m core.

§§ Sample no. 1a-c.

*** Sample no. 4.

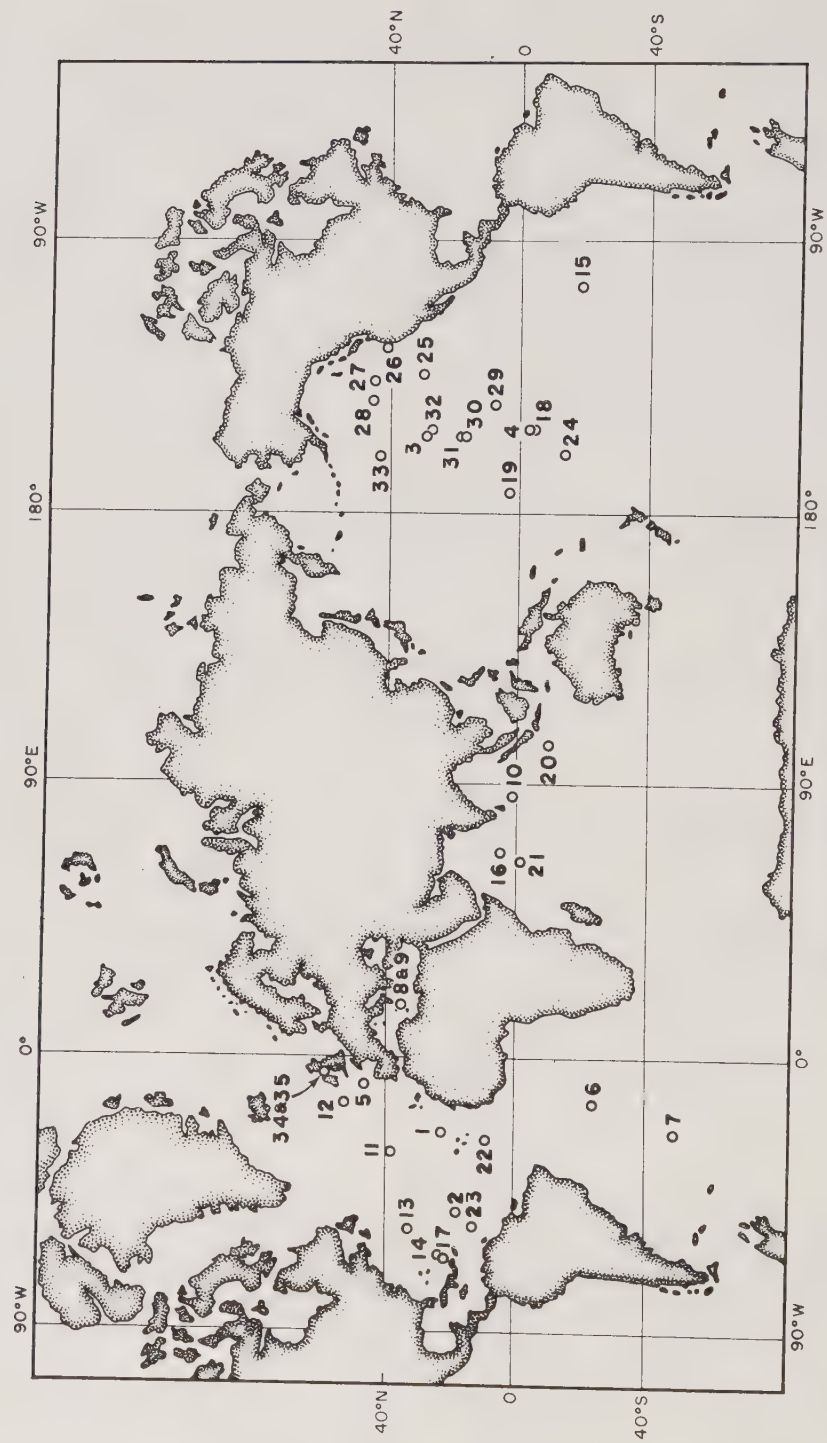

Fig. 1. Sampling stations for marine sediments.

(Groves, 1951). Available oxygen from manganese oxides was determined in a number of samples containing above 0·2 per cent of MnO by microdiffusion using a Cavett flask (cf. Conway, 1950).

Determination of calcium and manganese carbonates

A weight of 0·25 g of the sample was cautiously heated with 25–30 ml of 0·2 N acetic acid and warmed on the water bath until the evolution of gas had ceased. The insoluble residue was filtered off using a sintered glass filter and washed with water. The filtrate and washings were combined and diluted to 250 ml. Calcium and magnesium were determined in aliquots of this solution by titration with diaminoethanetetra-acetic acid. In all cases the percentages of chemically determined carbon dioxide was in good agreement with the carbon dioxide content calculated from the acetic acid-soluble calcium and magnesium.

Trace element analysis

The majority of trace elements were determined spectrographically by a modification of the procedure of Ahrens (1954). Determinations of gallium and germanium were made as described by Burton *et al.* (1959). Determinations of thorium, zirconium, hafnium and cerium were performed by an unpublished method.

Differential thermal analysis

Differential thermal analysis of the air-dried sample was performed as described by Hillier (1955) over the range 50–1000°C. The interpretation of the curves was based upon the following criteria determined from curves obtained from standard clay minerals on the same apparatus.

(a) A definite fairly sharp endothermic peak at 110–150°C indicates the presence of illite. If a low peak occurs at 110°C it may be due to adsorbed water on kaolinite.

(b) An endothermic peak at 585°C indicates that over 75 per cent of illite is present. This peak is subject to interference by the kaolinite peak at 625°C.

(c) A small endothermic peak at 890–910°C is diagnostic of illite and is sensitive to <25 per cent of this mineral.

(d) A rather broad low endothermic peak at 930–960°C indicates illite, as the proportion of illite increases, the peak height increases rapidly. Pure kaolinite has a very sharp exothermic peak at 1000°C.

(e) Montmorillonite has three endothermic reactions at 160°C 715°C and 900°C, respectively, and an exothermic peak at 940°C. The peak at 715°C serves to distinguish it from illite.

(f) Calcite shows a rather intense broad exothermic reaction with a peak at *ca.* 840°C. As the proportion of calcite decreases this peak moves to a higher temperature.

(g) Quartz shows a sharp but weak endothermic peak at 580°C, corresponding to the transition of α- to β-quartz. This peak is only detectable when more than 40 per cent of quartz is present in the sample.

X-ray diffraction analysis

The air-dried samples were examined as described by Grim *et al.* (1951) using CuK_α radiation and using a 19 cm diameter X-ray powder camera. Sediments

containing more than 2 per cent of carbonates were treated with dilute acetic acid to remove carbonates. In the case of samples 16, 17 and 3, more detailed studies both optical and X-ray, were carried out by Paul D. Blackmon of the Geochemistry and Petrology Branch of the U.S. Geological Survey through the courtesy of Dr. Preston E. Cloud.

Results of chemical analyses for major constituents

The detailed analyses of all samples examined, together with the corresponding Niggli values are given in Table 2. In order to facilitate the interpretation of results they are arranged according to composition, calcareous samples first, in order of decreasing carbonate content, followed by argillaceous clays and then by siliceous clays. The samples of volcanic origin 30, 31 and 24, and the acetic acid-insoluble residues of 2 and 6 are similar in composition and are grouped together. The remainder of the samples comprise the green mud 26, the calcareous manganiferous mud 15 and the $<2\mu$ clay fractions from two near shore muds (34 and 35). In order to compare the inorganic and non-calcareous contents of the samples, the analyses were recalculated to 100 per cent after deduction of carbonates, water, and organic carbon and nitrogen. The results are shown in Table 3, together with their Niggli values. Analyses of eleven samples taken at 50 cm intervals down the core 17 from the Atlantic ocean are given in Table 5. The corresponding values on a carbonate, organic carbon and water-free basis are shown in Table 6, together with their average and standard deviations. The average compositions of the three main types of deep-sea pelagic deposits deduced in the present work are shown in Table 4.

Discussion of Results for the Major Components

1. *Carbonate content*

The relationship between the calcium and magnesium carbonate contents of the sediments is not consistent, but it is generally true that in carbonate-rich sediments the greater the percentage of total carbonate in the sediment, the smaller is the percentage of magnesium carbonate present. The magnesium carbonate content of the sediments depends on the nature and type of calcareous organisms predominant in the sediment. It is particularly high in the two globigerina oozes from the Mediterranean.

The average magnesium carbonate contents of the calcareous, argillaceous and siliceous samples examined were 2·16 per cent, 0·83 per cent and 1·04 per cent, which give an average of 1·5 per cent for pelagic deep-sea sediments. This is in good agreement with the value of 1·4 per cent found by Gebling (cited by Vinogradov, 1953).

2. *Organic carbon and nitrogen contents*

The data shown in Tables 2 and 4 indicate that in general the organic carbon content of the deep-sea sediments is fairly constant. Average values for calcareous, argillaceous and siliceous samples are 0·31 per cent, 0·24 per cent and 0·22 per cent, respectively. Comparatively little is known about the nature of the organic matter in marine sediments, but since 50–60 per cent of it consists of carbon the weight ratio of organic matter to carbon varies from 1·67–2·0 (Trask, 1955). If a mean ratio of 1·8 is assumed, the average content of organic matter in calcareous, argillaceous,

Table 2. Analyses of samples (dried at 110°C) for major constituents (% weight) and Niggli values

	6	11	2	1	8	10	5	9	21	12	4	13	14
SiO_2	2·24	9·55	21·44	21·82	22·14	24·23	24·57	25·10	29·48	46·26	47·23	50·34	51·81
TiO_2	0·07	0·22	0·40	0·38	0·32	0·25	0·30	0·35	0·45	0·62	0·44	0·79	0·82
Al_2O_3	0·75	3·12	8·03	6·87	7·56	6·60	7·24	8·73	9·63	13·52	8·79	15·09	19·12
Fe_2O_3	0·78	2·16	4·65	2·55	2·73	2·43	2·04	3·16	4·63	3·27	4·56	3·12	6·15
FeO	0·10	n.d.	0·39	0·44	0·45	0·64	0·61	0·57	0·35	2·26	0·51	3·27	1·97
MnO	0·12	0·07	0·48	0·12	0·11	0·31	0·08	0·14	0·55	0·11	1·16	0·066	0·59
CaO	0·14	0·13	1·14	0·24	0·21	0·20	0·38	0·22	0·30	0·68	0·53	0·47	0·72
MgO	0·20	0·65	1·39	0·93	0·97	1·07	0·68	1·28	2·00	2·14	1·37	2·83	2·83
Na_2O	0·38	0·94	1·02	0·73	0·53	0·75	0·63	0·65	0·76	0·90	0·93	1·38	1·17
K_2O	0·16	0·46	0·57	1·34	1·35	1·40	1·48	1·49	1·50	3·05	1·43	3·52	3·70
P_2O_5	0·07	0·15	0·16	0·11	0·10	0·10	0·09	0·11	0·21	0·02	0·62	0·077	0·092
H_2O	2·36	2·07	3·62	3·03	3·29	3·31	2·64	3·49	4·50	7·41	4·66	6·60	8·70
$CaCO_3$	90·57	79·74	54·66	59·98	56·35	56·73	56·25	51·05	44·87	16·77	25·06	10·68	1·11
$MgCO_3$	2·05	0·88	1·94	1·32	3·85	1·78	2·91	3·49	0·98	2·51	2·55	1·68	1·07
Available O	n.d.	n.d.	n.d.	n.d.	n.d.	0·050	n.d.	n.d.	n.d.	n.d.	0·24	n.d.	n.d.
Organic C	0·21	n.d.	0·22	0·28	0·31	0·30	0·32	0·31	0·17	0·49	0·45	0·33	0·30
Organic N	n.d.	n.d.	n.d.	0·012	0·012	0·017	0·010	0·012	0·017	0·009	0·030	0·008	0·010
Total	100·20	100·14	100·11	100·15	100·28	100·17	100·23	100·15	100·40	100·02	100·56	100·26	100·16
Total Fe_2O_3	0·89	2·16	5·08	3·04	3·23	3·14	2·72	3·79	5·02	5·78	5·13	6·75	8·35
si	3·8	17·6	44·9	46·8	47·5	53·6	54·4	55·8	69·3	149·2	150·9	168·1	184·5
al	0·8	3·4	9·9	8·7	9·6	8·6	9·4	11·5	13·3	25·7	16·6	29·7	40·1
fm	4·4	6·0	16·1	10·1	14·4	12·1	11·5	16·4	18·6	30·4	27·8	35·3	42·2
c	94·0	88·4	71·2	77·8	73·1	75·7	75·6	68·6	64·1	34·8	49·8	23·1	5·1
alk	0·8	2·2	2·8	3·4	2·9	3·6	3·5	3·5	4·0	9·1	5·8	11·9	12·6
k	0·21	0·24	0·27	0·55	0·63	0·55	0·61	0·60	0·57	0·69	0·51	0·62	0·67
mg	0·70	0·49	0·45	0·49	0·62	0·52	0·59	0·60	0·46	0·53	0·44	0·51	0·42
h	13·6	12·7	25·3	21·7	23·5	24·4	19·5	25·8	35·3	79·5	49·6	73·4	103·4
CO_2	96·3	89·3	71·5	79·3	78·5	78·1	79·3	73·7	64·9	37·2	53·9	25·1	5·4
ti	0·07	0·31	0·63	0·62	0·54	0·43	0·53	0·60	0·78	1·2	1·04	2·0	2·1
p	0·05	0·13	0·15	0·11	0·10	0·10	0·09	0·11	0·22	0·0	0·84	0·1	0·1
al-alk	0·0	1·2	7·1	5·3	6·7	5·0	5·9	8·0	9·3	16·6	10·8	17·8	27·5

Table 2—(*contd.*)

	17*	25	23	16	28	3	32	27	19	33	29	22
SiO_2	53·16	53·93	54·70	54·74	55·24	55·35	55·50	57·33	57·69	57·94	58·27	59·88
TiO_2	0·80	0·96	0·85	0·86	0·92	0·87	0·97	0·90	0·61	0·84	0·73	0·84
Al_2O_3	19·09	17·46	19·82	16·26	17·35	19·13	17·45	16·38	16·50	16·59	15·10	16·76
Fe_2O_3	8·19	8·53	8·27	8·38	6·72	6·25	6·93	5·17	7·80	5·91	6·44	6·93
FeO	0·53	0·45	0·55	n.d.	1·18	1·70	1·24	2·32	0·23	1·36	0·88	0·28
MnO	0·69	0·78	0·38	0·27	0·56	0·45	0·55	0·30	0·88	0·21	0·08	0·16
CaO	0·60	1·34	0·72	0·76	1·15	0·62	0·73	2·05	0·76	0·84	0·88	0·62
MgO	2·96	4·35	2·42	4·56	4·00	2·95	3·41	3·43	3·95	3·09	3·20	2·42
Na_2O	1·05	1·27	0·90	2·72	1·55	1·97	1·44	2·31	1·02	1·62	1·40	0·84
K_2O	3·63	3·65	2·95	3·08	3·55	3·68	3·95	2·68	1·48	3·60	3·25	2·05
P_2O_5	0·06	0·09	0·16	0·11	0·06	0·08	0·17	0·16	0·45	0·09	0·22	0·11
H_2O	6·61	6·30	7·42	5·87	6·56	5·22	6·23	5·08	6·82	6·48	7·49	7·37
$CaCO_3$	1·70	0·39	0·50	1·32	0·52	0·70	0·43	0·87	0·80	0·64	0·57	0·77
$MgCO_2$	1·02	0·44	0·44	1·17	0·54	1·13	0·52	0·90	0·94	0·61	1·17	1·07
Available O	0·06	0·11	n.d.	n.d.	n.d.	n.d.	n.d.	n.d.	0·21	n.d.	n.d.	0·040
Organic C	0·08	0·13	0·22	0·25	0·15	0·33	0·41	0·25	0·07	0·43	0·26	0·21
Organic N	0·006	0·016	0·018	n.d.	0·009	0·028	0·021	0·013	0·014	0·008	0·006	0·017
Total	100·24	100·20	100·32	100·35	100·06	100·46	99·95	100·14	100·22	100·26	99·95	100·37
Total Fe_2O_3	8·78	9·02	8·88	8·38	8·03	8·14	8·51	7·75	8·05	7·42	7·42	7·24
si	186·1	181·3	207·1	182·8	194·5	195·4	201·3	203·7	219·4	225·1	234·3	259·4
al	39·4	34·6	44·2	32·0	36·0	39·8	37·3	34·3	37·0	38·0	35·7	42·8
fm	43·1	47·8	41·3	47·2	45·3	41·3	44·7	42·0	50·8	42·0	45·3	43·1
c	5·9	5·6	4·1	5·4	5·5	3·9	3·8	9·7	4·9	5·0	5·2	4·9
alk	11·7	12·0	10·4	15·4	13·2	15·0	14·2	14·0	7·3	15·0	13·8	9·2
k	0·70	0·65	0·68	0·43	0·60	0·55	0·64	0·43	0·49	0·59	0·61	0·62
mg	0·42	0·48	0·36	0·54	0·49	0·44	0·44	0·49	0·49	0·46	0·50	0·44
h	77·2	70·7	96·2	65·3	77·1	61·4	75·4	60·2	86·4	83·9	100·3	106·5
CO_2	6·1	1·8	2·3	5·4	2·5	4·4	2·3	4·1	4·4	3·2	4·7	5·3
ti	2·1	2·40	2·39	2·13	2·39	2·27	2·63	2·35	1·75	2·43	2·25	2·71
p	0·1	0·14	0·27	0·17	0·10	0·13	0·28	0·26	0·71	0·16	0·39	0·22
al-alk	27·7	22·6	33·8	16·6	22·8	24·8	23·1	20·3	29·7	23·0	21·9	33·6

* Average for whole core.

Table 2—(*contd.*)

	20	18	7	30	31	24	26	15	34	35	Residues 2	Residues 6
SiO_2	63·27	65·94	67·36	39·21	49·60	46·50	59·42	3·32	55·44	47·61	43·75	48·81
TiO_2	0·62	0·57	0·59	2·61	2·36	1·51	0·71	0·07	0·70	0·81	0·97	0·96
Al_2O_3	14·84	10·45	11·33	10·91	13·96	15·40	14·01	0·64	11·40	14·51	15·82	18·44
Fe_2O_3	6·30	6·09	3·40	5·39	6·30	12·32	1·55	13·88	3·10	3·66	17·11	11·76
FeO	0·58	0·40	1·42	7·11	5·73	0·00	4·82	—	1·89	2·66	n.d.	n.d.
MnO	0·11	1·54	0·19	0·18	0·24	2·38	0·07	4·80	0·09	0·08	1·50	0·84
CaO	0·82	0·69	0·89	6·79	5·74	2·54	0·89	0·01	0·43	0·44	2·94	2·99
MgO	1·88	1·82	1·71	10·66	6·01	3·38	3·86	1·23	2·01	1·86	3·34	3·31
Na_2O	0·70	0·57	1·64	1·62	2·14	1·88	1·68	0·49	1·01	0·78	1·42	1·82
K_2O	1·93	1·49	2·15	0·36	1·20	2·90	2·30	0·10	2·55	3·10	2·44	1·30
P_2O_5	0·14	0·75	0·10	0·21	0·20	0·49	0·08	0·13	0·14	0·18	0·48	0·26
H_2O	7·52	7·41	6·33	2·50	3·49	7·24	7·10	2·20	4·45	7·02	8·14	9·12
$CaCO_3$	0·66	1·43	1·52	10·83	1·84	1·75	0·79	70·62	13·98	13·42	—	—
$MgCO_3$	0·82	1·07	1·21	1·15	1·09	1·57	1·23	1·53	2·47	2·18	—	—
Available O	n.d.	0·24	n.d.	n.d.	n.d.	0·30	n.d.	0·71	n.d.	n.d.	n.d.	n.d.
Organic C	0·30	0·11	0·26	0·48	0·16	0·00	1·59	0·00	0·64	1·75	2·42	0·53
Organic N	0·024	0·006	—	0·0022	0·0034	0·0053	0·059	n.d.	0·010	0·030	n.d.	n.d.
Total	100·51	100·57	100·10	100·01	100·06	100·16	100·16	99·73	100·31	100·09	100·33	100·14
Total Fe_2O_3	6·94	6·53	4·98	13·29	12·67	12·32	6·91	13·88	5·21	6·62	17·11	11·76
si	306·7	347·7	357·9	80·3	131·3	136·9	241·2	5·4	206·0	162·9		
al	42·4	32·5	35·5	13·2	21·8	26·7	33·4	0·6	25·0	29·3		
fm	42·2	51·1	38·9	55·0	51·5	51·4	48·3	28·8	32·5	32·1		
c	6·2	8·5	9·8	28·2	19·2	11·1	5·7	69·7	32·9	29·2		
alk	9·2	8·0	15·8	3·7	7·5	10·8	12·6	0·9	9·6	9·4		
k	0·64	0·63	0·46	0·13	0·27	0·50	0·47	0·11	0·63	0·72		
mg	0·39	0·36	0·47	0·63	0·50	0·35	0·56	0·17	0·54	0·46		
h	121·5	130·3	112·2	17·1	30·8	71·1	96·1	12·1	55·1	80·1		
CO_2	4·8	8·5	9·4	15·0	5·0	6·4	5·7	71·6	37·7	32·8		
ti	2·27	2·23	2·35	4·01	4·71	3·38	2·22	0·10	2·01	2·08		
p	0·31	1·66	0·24	0·19	0·24	0·61	0·15	0·05	0·23	0·28		
al-alk	33·2	24·5	19·7	9·5	14·3	15·9	20·8	−0·30	15·4	19·9		

Table 3. Analyses for major constituents on a carbonate, organic C and N, and water free basis (% weight)

	6	Residue 6	2	Residue 2	11	25	17†	14	21	3	23	16	28	32
SiO_2	44·62	48·74	53·99	53·93	54·73	58·10	58·52	58·70	59·08	59·37	59·60	59·68	59·77	59·89
TiO_2	1·40	1·08	1·01	1·06	1·26	1·03	0·88	0·92	0·90	0·93	0·93	0·94	1·00	1·05
Al_2O_3	14·94	17·62	20·22	20·38	17·88	18·80	21·02	21·12	19·30	20·52	21·60	17·72	18·78	18·83
Fe_2O_3*	17·73	19·07	12·79	13·00	12·38	9·71	9·67	8·98	10·06	8·73	9·68	9·13	8 69	9·18
MnO	2·39	1·67	1·21	0·93	0·40	0·84	0·76	0·67	1·10	0·48	0·41	0·29	0·61	0·59
CaO	2·78	3·27	2·87	3·30	0·75	1·44	0·66	0·81	0·60	0·66	0·78	0·83	1·24	0·79
MgO	3·98	3·72	3·50	3·66	3·72	4·68	3·26	3·20	4·01	3·16	2·64	4·97	4·33	3·68
Na_2O	7·57	1·58	2·57	2·01	5·38	1·37	1·16	1·32	1·52	2·11	0·98	2·96	1·68	1·55
K_2O	3·19	2·72	1·44	1·44	2·64	3·93	4·00	4·18	3·01	3·95	3·21	3·36	3·84	4·26
P_2O_5	1·40	0·53	0·40	0·28	0·86	0·10	0·07	0·10	0·42	0·09	0·17	0·12	0·06	0·18
si		126·6		156·7	163·4	184·7	198·0	194·9	197·6	206·1	212·1	193·5	196·6	206·3
al		27·0		34·9	31·6	35·2	41·9	42·6	38·1	44·0	45·3	33·9	36·9	38·2
fm		55·4		46·5	45·4	47·7	43·2	41·3	48·3	39·8	41·1	47·0	45·0	44·4
c		9·1		10·3	2·5	4·9	2·5	2·9	2·2	2·5	3·0	2·8	4·5	2·9
alk		8·5		8·3	20·5	12·2	12·4	13·2	11·4	15·7	10·7	16·3	13·6	11·5
k		0·53		0·32	0·24	0·65	0·67	0·68	0·57	0·55	0·68	0·43	0·60	0·64
mg		0·26		0·34	0·37	0·47	0·38	0·39	0·41	0·40	0·34	0·51	0·48	0·42
ti		2·05		2·29	2·90	2·45	2·24	2·21	2·21	2·37	2·44	2·25	2·45	2·69
p		0·57		0·35	1·16	0·14	0·10	0·12	0·62	0·13	0·28	0·18	0·10	0·29
h		118·4		97·6	118·0	7·20	82·1	109·1	100·7	64·1	95·9	69·2	79·1	77·2
al-alk		18·5		26·6	11·1	23·0	29·5	29·4	26·7	25·9	34·6	17·6	23·3	23·7

* Total iron as Fe_2O_3.
† Average of whole core.

Table 3—(*contd.*)

	9	8	1	27	13	33	19	10	12	29	5	22	20
SiO_2	59·96	60·20	61·34	61·45	62·50	62·81	63·13	63·68	63·75	64·35	64·38	65·86	69·33
TiO_2	0·84	0·88	1·06	0·96	0·98	0·91	0·67	0·66	0·85	0·81	0·79	0·92	0·68
Al_2O_3	20·86	20·70	19·31	17·56	18·72	17·99	18·05	17·35	18·65	16·68	18·98	18·44	16·26
Fe_2O_3*	9·05	8·84	8·54	8·31	7·51	8·04	8·81	8·25	7·39	8·19	7·13	7·96	7·61
MnO	0·33	0·30	0·34	0·32	0·08	0·23	0·96	0·81	0·15	0·09	0·21	0·18	0·12
CaO	0·53	0·58	0·67	2·20	0·58	0·91	0·83	0·53	0·93	0·97	0·96	0·68	0·90
MgO	3·06	2·66	2·61	3·68	3·49	3·35	4·32	2·81	2·93	3·53	1·78	2·67	2·06
Na_2O	1·55	1·45	2·05	2·48	1·70	1·76	1·12	1·97	1·23	1·55	1·65	0·92	0·77
K_2O	3·56	3·70	3·77	2·87	4·35	3·90	1·62	3·68	4·19	3·59	3·88	2·25	2·12
P_2O_5	0·26	0·27	0·31	0·17	0·09	0·10	0·49	0·26	0·03	0·24	0·24	0·12	0·15
si	212·0	221·0	226·2	212·5	226·5	232·4	229·4	244·1	242·1	246·0	262·2	273·8	322·3
al	43·5	44·5	42·0	35·8	39·8	39·2	38·7	39·2	41·6	37·5	45·4	45·2	44·5
fm	41·1	39·6	39·1	41·4	41·9	41·7	50·0	42·3	39·8	44·1	33·6	42·0	41·4
c	2·0	2·2	2·7	8·2	2·4	3·6	3·2	2·1	3·8	4·0	4·3	3·1	4·4
alk	13·4	13·7	16·2	14·6	15·9	15·5	7·7	16·4	14·8	14·4	16·7	9·7	9·7
k	0·60	0·63	0·55	0·43	0·63	0·59	0·49	0·55	0·69	0·61	0·61	0·62	0·64
mg	0·39	0·36	0·36	0·46	0·45	0·44	0·46	0·38	0·42	0·46	0·32	0·39	0·34
ti	2·28	2·52	2·99	2·45	2·60	2·51	1·83	1·96	2·50	2·36	2·56	2·86	2·39
p	0·42	0·45	0·52	0·27	0·11	0·16	0·75	0·45	0·00	0·41	0·44	0·23	0·32
h	98·2	109·4	104·6	62·8	98·9	86·7	90·4	111·1	129·3	105·3	92·4	112·4	127·7
al-alk	30·1	30·8	25·8	21·2	23·9	23·7	31·0	22·8	26·8	23·1	28·7	35·5	34·8

* Total iron as Fe_2O_3.

Table 3—(*contd.*)

	4	18	7	26	30	24	31	15	34	35
SiO_2	69·82	72·98	74·07	66·07	45·68	52·06	52·71	13·08	70·20	62·64
TiO_2	0·65	0·63	0·65	0·79	3·04	1·69	2·51	0·28	0·89	1·07
Al_2O_3	13·00	11·57	12·46	15·58	12·71	17·25	14·83	2·52	14·44	19·09
Fe_2O_3*	7·59	7·24	5·48	7·68	15·48	13·80	13·46	54·71	6·60	8·71
MnO	1·72	1·70	0·21	0·08	0·21	2·67	0·25	18·91	0·10	0·11
CaO	0·78	0·76	0·98	0·99	7·91	2·84	6·10	0·04	0·54	0·58
MgO	2·03	2·01	1·88	4·29	12·42	3·78	6·39	4·84	2·54	2·45
Na_2O	1·38	0·63	1·80	1·87	1·89	2·11	2·27	1·93	1·28	1·03
K_2O	2·11	1·65	2·36	2·56	0·42	3·25	1·27	0·39	3·23	4·08
P_2O_5	0·92	0·83	0·11	0·09	0·24	0·55	0·21	0·51	0·18	0·24
							Available Oxygen	2·79		
si	327·6	380·5	395·1	254·7	94·5	146·4	138·1	19·2	330·8	243·0
al	36·0	35·5	39·2	35·4	15·5	28·6	22·9	2·2	40·1	43·6
fm	47·4	51·5	37·8	47·2	62·7	51·3	52·1	94·6	41·7	40·0
c	4·0	4·3	5·6	4·1	17·5	8·6	17·1	0·1	2·7	2·4
alk	12·6	8·7	17·4	13·3	4·3	11·5	7·9	3·1	15·5	14·0
k	0·51	0·63	0·46	0·47	0·13	0·50	0·27	0·11	0·63	0·72
mg	0·29	0·30	0·39	0·52	0·61	0·31	0·48	0·11	0·43	0·35
ti	2·25	2·44	2·59	2·34	4·72	3·16	4·95	0·29	3·22	3·10
p	1·83	1·82	0·26	0·15	0·22	0·65	0·25	0·29	0·38	0·41
h	107·7	142·6	123·8	101·4	20·1	76·0	32·4	42·6	88·5	119·4
al-alk	23·4	26·8	21·8	22·1	11·2	17·1	15·0	−0·9	24·6	29·6

* Total iron as Fe_2O_3.

Table 4. Average compositions of sediments

	Original compositions					Composition on carbonate, water and organic C-free basis				
	Calcareous†	Calcareous‡	Argillaceous	Siliceous	Oceanic average*	Calcareous†	Calcareous†	Argillaceous	Siliceous	Oceanic average*
SiO_2	26·96	31·21	55·34	63·91	42·72	59·86	61·86	60·44	70·61	61·52
TiO_2	0·38	0·43	0·84	0·65	0·59	0·94	0·86	0·92	0·72	0·90
Al_2O_3	7·97	9·19	17·48	13·30	12·29	18·34	18·71	19·06	14·72	18·12
Fe_2O_3	3·00	3·31	7·04	5·66	4·89	9·77	8·72	8·93	7·08	9·09
FeO	0·87	0·95	1·13	0·67	0·94	—	—	—	—	—
MnO	0·33	0·37	0·48	0·50	0·41	0·75	0·63	0·52	0·55	0·64
CaO	0·30	0·34	0·93	0·75	0·60	1·04	0·93	1·01	0·83	1·00
MgO	1·29	1·46	3·42	1·95	2·18	3·05	2·89	3·73	2·17	3·19
Na_2O	0·80	0·83	1·53	0·94	1·10	2·50	1·71	1·67	0·93	1·98
K_2O	1·48	1·71	3·26	1·90	2·10	3·29	3·37	3·56	2·09	3·23
P_2O_5	0·15	0·16	0·14	0·27	0·16	0·46	0·32	0·16	0·30	0·33
H_2O	3·91	4·25	6·54	7·13	5·35	—	—	—	—	—
$CaCO_3$	50·09	43·16	0·79	1·09	24·87	—	—	—	—	—
$MgCO_3$	2·16	2·30	0·83	1·04	1·51	—	—	—	—	—
Org.C	0·31	0·32	0·24	0·22	0·27	—	—	—	—	—
Org.N	—	0·014	0·016	0·016	0·015	—	—	—	—	—
Total	100·00	100·00	100·00	100·00	100·00	100·00	100·00	100·00	100·00	100·00
Total Fe_2O_3	3·89	4·37	8·23	6·42	—	—	—	—	—	—

* Weighted mean calculated on an areal basis (including samples 6 and 11). Percentage of deep ocean floor covered by sediments, 48·7 per cent calcareous, 37·8 per cent argillaceous, 13·5 per cent siliceous.

† Including highly calcareous samples nos. 6 and 11.

‡ Excluding highly calcareous samples nos. 6 and 11.

siliceous and average pelagic deposits will be 0·49 per cent, 0·40 per cent and 0·47 per cent, respectively. These values are in excellent agreement with the averages of 0·45 per cent reported by Correns (1937) and 0·5 per cent recorded by Trask (1955).

The organic carbon content of the Atlantic core (sample 17) was low and showed no significant variation with depth. Samples existing under conditions of low redox potential and containing much ferrous iron such as the green mud (26) and nearshore samples (34 and 35) are, as would be expected, rich in organic carbon. On the other hand, sediments having high redox potentials, characterized by the presence of considerable amounts of higher oxides of manganese are often, but not always, depleted in organic matter (samples 15, 18, 24, 25, but cf. 4).

A statistical study of the data showed that there was no correlation between either the carbonate and organic carbon contents of the sediments or their carbonate and phosphate contents.

The mean organic carbon : nitrogen ratios for the calcareous and argillaceous sediments were 21 and 15, respectively. Owing to a number of extremely high values, the average ratio of 26 for siliceous sediments must be regarded as a maximum.

3. *Distribution of other major components*

The intercomparison of the analyses shown in Table 2 is made difficult by the presence of varying amounts of water, organic carbon, and carbonates, derived from the skeletons of calcareous organisms. Table 3 shows the compositions of the sediments recalculated on a water, organic carbon, and carbonate-free basis, arranged in order of increasing SiO_2 content. Average values for the sediments examined calculated on both bases, are given in Table 4, using the values given by Sverdrup *et al.* (1942) for the proportions of the various sediment types. The following samples have been excluded from the calculation of the averages and from the general discussion: (i) samples 24, 30 and 31, which are of volcanic origin, (ii) the calcareous–manganiferous ooze (15), (iii) the two nearshore sediments (34, 35).

For the purposes of this discussion and in Table 4, the following nomenclature will be employed. The term calcareous clay is used to designate a deep-sea clay having a total $CaCO_3 + MgCO_3$ content of 5–60 per cent, those sediments with more than 60 per cent of carbonates are termed calcareous oozes. Samples low in carbonates and which contain between 52 and 58 per cent of SiO_2 are termed argillaceous, and those which contain more than this amount of SiO_2 are called siliceous oozes, the latter consist mainly of clay diluted with organically derived silica. This classification is not entirely satisfactory, since, for example, sample 4 with 27·61 per cent of carbonates would be described as a calcareous clay. On a carbonate and water-free basis it has a silica content (69·84 per cent) considerably greater than the argillaceous samples; and should therefore be classified as a calcareous–siliceous clay.

Table 3 shows that on a carbonate, carbon and water-free basis, the SiO_2 contents of sediments with less than 60 per cent of carbonates from the Atlantic, Pacific and Indian Oceans are very similar. On this basis, the calcareous oozes nos. 2, 6 and 11 (and the acetic acid insoluble residues of 2 and 6) from the Atlantic have a relatively low SiO_2 content and correspondingly higher Al_2O_3 and Fe_2O_3 concentrations than the remaining samples from this ocean.

On a carbonate and water-free basis, the alumina contents of the calcareous and

argillaceous sediments are similar. On the other hand the siliceous oozes are relatively deficient in alumina in inverse proportion to their content of biogenic silica sediments. The sediments of the Atlantic Ocean are on the average richer in alumina than those of the Pacific and Indian Oceans.

With the exception of the highly calcareous sediments, the iron content of the deep-sea sediments, calculated as Fe_2O_3, on a carbonate and water-free basis, is surprisingly uniform. This is particularly true of the argillaceous samples, which contain average concentrations of 8·23 per cent total Fe_2O_3 (7·04 per cent Fe_2O_3 and 1·13 per cent FeO on original clay). The mean iron contents of the sediments of the three oceans are similar, but those from the Pacific are slightly higher.

Ferrous iron is present in all the samples examined, except those containing appreciable amounts of higher oxides of manganese. Usually less than 1 per cent FeO is present, but it is present in larger concentrations in sediments of low redox potential, containing large amounts of organic matter, such as green mud (sample 26), and near shore clays (samples 34 and 35). Large amounts of ferrous iron are also found in sediments containing much unaltered volcanic material (samples 30 and 31).

Certain of the highly calcareous samples from the Atlantic (nos. 2, 6 and 11) and their acid-insoluble residues have Fe_2O_3 contents (on a water and carbonate-free basis) considerably higher than the argillaceous sediments. This effect has been observed previously by Revelle (1944), who found that sediments containing less than 30 per cent of carbonates contained on average about 7·0 per cent of Fe_2O_3 (on a water and carbonate-free basis), whereas those containing over 80 per cent of carbonates had much greater concentrations of Fe_2O_3 amounting to as much as 16 per cent in some cases. This excess iron over that contained in the argillaceous sediments is probably mainly derived from globigerina or other organisms, the highly insoluble iron oxide or hydroxide content of which remains after their calcareous parts have dissolved away during sedimentation. When it is remembered that marine foraminifera usually contain less than 1 per cent of Fe_2O_3 (Clarke and Wheeler, 1922) it will be realized that at least 85 per cent of the carbonates of the original organisms must have dissolved away to yield a sediment containing an acetic acid-insoluble residue containing 17 per cent of iron. These facts imply sedimentation under conditions in which carbonates are readily dissolved, i.e. a high content of dissolved carbon dioxide in the sea water.

Many of the shells and pieces of calcareous debris in these sediments were observed under the microscope to be stained dark red with iron derivatives and this has also been observed by Bradley and Bramlette (1942).

A linear relationship exists between the TiO_2 content of the sediments and their total iron content expressed as Fe_2O_3 (Fig. 2) such that $TiO_2 = 0{\cdot}1046\ Fe_2O_3 - 0{\cdot}02$. This relationship seems to hold regardless of the type of sedimentation in the ocean from which it originated. Similar correlations have been previously observed by Hamaguchi *et al.* (1954) and by Revelle *et al.* (1955) for deep sea-clays.

On a carbonate and water-free basis the average TiO_2 contents of the argillaceous and calcareous sediments are similar (0·94 and 0·92 per cent, respectively). The siliceous oozes give a lower average (0·72 per cent) which is attributable to the diluting effect of their organically derived silica, as the average Niggli ti value (2·41) is similar to those of the argillaceous (2·35) and calcareous sediments (2·53). The average for

pelagic sediments (0·90 per cent) is similar to that of other sedimentary rocks. The sediments from the Pacific Ocean are slightly richer in titanium (av. 0·95 per cent) than those from the other oceans. Correns (1954) has found that euhedral, anatase and rutile account for much of the titanium occurring in pelagic sediments of non-volcanic origin.

Manganese is concentrated considerably in deep-sea pelagic sediments compared with continental igneous rocks. Much controversy has arisen over the processes by

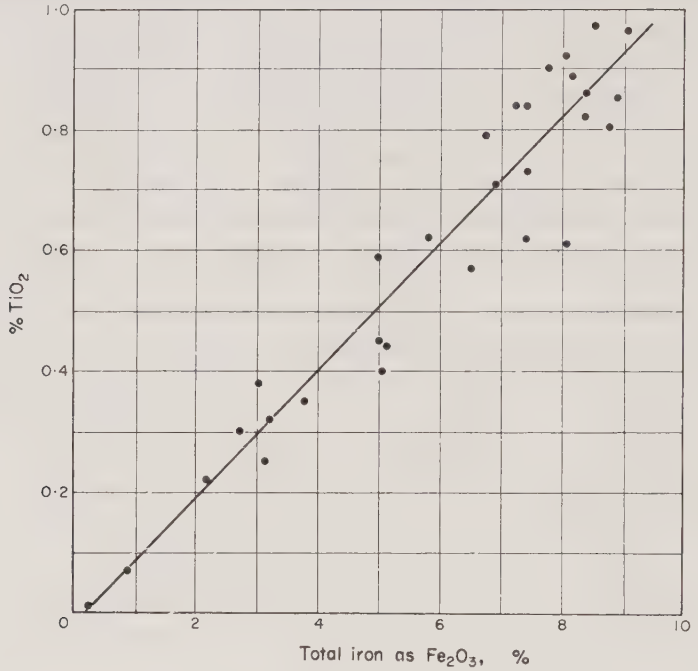

Fig. 2. Relationship between titanium dioxide and total iron (expressed as Fe_2O_3) in marine sediments.

which the manganese originated and was concentrated in the sediments, and both biological and submarine volcanic mechanisms have been suggested (Pettersson, 1959).

Although on a carbonate and water-free basis, the average manganese contents of the three types of sediments were similar, the manganese contents of the individual samples were very variable and ranged from 0·09 to 2·39 per cent MnO. This variation, which is much greater than that of any of the other major constituents, is probably caused by the fact that in the sediments most of the manganese is an adventitious impurity and occurs mainly as discreet ferro-manganese minerals: their calcareous and argillaceous fractions contain only small amounts of manganese. Micro-manganese nodules are easily visible under the microscope in samples which are relatively rich in manganese (e.g. sample 4). The samples from the Pacific Ocean are, on average, almost twice as rich in manganese as those from the Atlantic, a finding which agrees with the much wider occurrence of manganese nodules in the Pacific.

The average value found in this work for all Pacific Ocean argillaceous sediments (0·85% MnO) is similar to the average of 0·67% MnO found by REVELLE (1944) for ten red clay samples from the North Pacific. Statistical examination of the data for sediments containing more than 5 per cent of total carbonates, all but one of which are from the Atlantic, has shown that there is an inverse relationship between their manganese and total carbonate contents. It is probable that this effect is mainly one of dilution of manganese associated with the argillaceous fraction with organically derived carbonate. The same samples also show a correlation between their manganese and total iron contents (Fig. 3) similar to that found by REVELLE (1944).

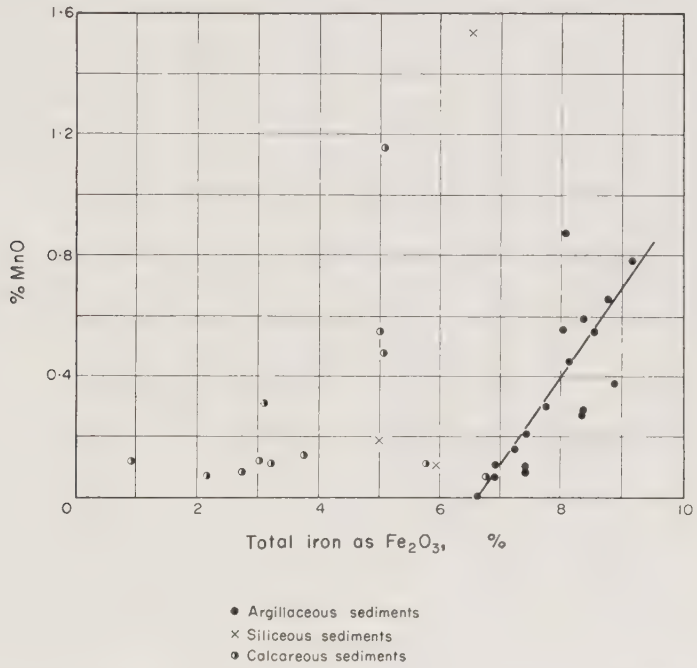

Fig. 3. Relationship between manganese oxide and total iron (expressed as Fe_2O_3) in marine sediments.

The relationship of manganese to total carbonate in the argillaceous and siliceous sediments appears to be a purely random one. Over the range of total iron contents of 6·8–9 per cent Fe_2O_3, which covers the bulk of the argillaceous samples, there is a linear relationship between total iron and manganese, with much steeper slope than that found for calcareous sediments, so that $Fe_2O_3 = 3{\cdot}47\ MnO + 6{\cdot}58$. Most of the manganese in the argillaceous sediments is contained in discreet manganese minerals in which MnO is associated with, on average, about three to four times its weight of Fe_2O_3. The average total Fe_2O_3 and MnO contents of argillaceous sediments free from manganese–iron minerals are probably about 6·8 per cent and $<0{\cdot}1$ per cent, respectively. It is therefore easy to see why there is a linear relationship between manganese and iron only above this level, since, in any addition of manganese minerals, MnO will be accompanied by three to four times its weight of Fe_2O_3.

Goldberg and Arrhenius (1958) have suggested that up to ca. 0·1 per cent of manganese in a sediment may be bound in the clay minerals.

The oxidation state of the manganese in certain of the sediments has been determined. The results expressed as percentage of "available oxygen" are shown in Table 2. These percentages correspond to formulae of $MnO_{2\cdot1}$, $MnO_{1\cdot9}$, $MnO_{1\cdot6}$, $MnO_{1\cdot4}$, $MnO_{2\cdot0}$, $MnO_{2\cdot1}$, $MnO_{1\cdot7}$, for the manganese oxides in samples 10, 4, 25, 17, 19, 22 and 18, respectively. In the majority of cases manganese is in the tetravalent state and presumably exists as δ-MnO_2 (cf. Buser and Grütter, 1956). In samples 17, 18 and 25 manganese in lower valency states must be present, perhaps associated with iron in the form of ferric manganite, as found by Buser and Grütter (1956) in manganese nodules. The valency of manganese in these samples is similar to the average value of 3·34 found for three manganese nodules from the Pacific Ocean (Riley and Sinhaseni, 1958).

Calcium and magnesium oxides are fairly uniformly distributed in the three groups of sediments (on a carbonate, water and organic carbon-free basis). Magnesium oxide is approximately three times as abundant as calcium oxide. The sediments from the Pacific Ocean are considerably richer in both magnesium and calcium than those of the Atlantic.

The distribution of alkali metals in the samples is similar to that in sediments in general, in which K_2O preponderates over Na_2O. Only the two calcareous samples with ca. 80 per cent or more of carbonates are exceptional and contain more Na_2O than K_2O.

On a carbonate-free basis, the calcareous sediments, on average, contain approximately twice as much P_2O_5 as the argillaceous samples, which suggests that a large part of the P_2O_5 in the former is of biological origin. There is, however, no correlation between the P_2O_5 and total carbonate contents of the calcareous sediments. This does not necessarily preclude a biological origin, since calcium phosphate and apatite are considerably less soluble than calcium carbonate in water containing CO_2, and would dissolve less readily during the process of sedimentation. Owing to the fact that calcium minerals other than apatite are present in the non-carbonate fractions of most of the sediments, there is no correlation between their CaO and P_2O_5 contents.

Chemical composition of deep sea-core sample 17

In order to study the vertical variation of composition of a typical argillaceous sediment, a core from the North Atlantic was examined. It was taken from the top of a small hill at the end of the Bermuda Rise and showed no evidence of having been disturbed by turbidity currents. Its length was 5·05 m and eleven 4 cm sections were taken at 50 cm intervals from the sediment–water interface down to a depth of 5·00 m. Each section was well washed, dried and thoroughly mixed before analysis. The analyses are shown in Tables 5 and 6.

The maximum content of calcium carbonate occurs at the surface of the sediment; down to a depth of 1·5 m there is a progressive decline followed by lesser maxima at 2 and 4 m.

Magnesium carbonate follows a similar trend. These maxima are associated with the presence in the sediment of layers of calcareous foraminiferal shells. On a carbonate, water, and organic carbon-free basis, the composition of the core is fairly uniform from

Table 5. Analysis of core sample no. 17 for major constituents

Depth in core	Top 4 cm	50 cm	100 cm	150 cm	200 cm	250 cm	300 cm	350 cm	400 cm	450 cm	500 cm	Average
SiO_2	50·82	53·85	53·56	53·42	53·25	53·47	53·64	53·25	52·44	53·39	53·65	53·16
TiO_2	0·81	0·82	0·82	0·81	0·78	0·81	0·81	0·79	0·79	0·83	0·78	0·80
Al_2O_3	17·80	18·24	18·72	19·34	18·39	19·43	19·29	19·20	19·50	19·75	20·30	19·09
Fe_2O_3*	8·52	8·59	9·01	8·83	8·29	9·23	8·69	8·69	8·80	9·01	8·90	8·78
MnO	0·69	0·73	0·80	0·65	0·63	0·65	0·65	0·68	0·64	0·75	0·71	0·69
CaO	0·55	0·63	0·61	0·63	0·60	0·66	0·62	0·59	0·57	0·62	0·54	0·60
MgO	2·92	2·91	3·16	2·92	2·83	3·05	3·12	2·99	2·92	2·86	2·88	2·96
Na_2O	1·08	1·16	1·27	1·06	1·27	0·93	1·10	0·94	1·19	0·78	0·75	1·05
K_2O	3·61	3·79	3·76	3·72	3·65	3·54	3·61	3·61	3·64	3·63	3·43	3·63
P_2O_5	0·08	0·06	0·06	0·07	0·07	0·07	0·06	0·05	0·07	0·07	0·06	0·06
H_2O	6·31	6·15	6·60	6·71	6·18	6·78	6·71	6·58	6·56	7·09	7·05	6·61
$CaCO_3$	5·41	1·98	1·04	0·93	2·58	0·64	0·86	1·89	2·05	0·80	0·57	1·70
$MgCO_3$	1·69	1·36	0·79	0·96	1·57	0·69	0·92	1·05	0·86	0·67	0·59	1·02
Org.C	0·16	0·08	0·16	0·02	0·07	n.d.	0·09	0·10	0·15	n.d.	0·08	0·08
Total	100·45	100·36	100·38	100·07	100·14	99·95	100·17	100·41	100·18	100·29	100·29	100·23

* Total iron as Fe_2O_3.

Table 6. Analysis of core 17 on carbonate, water and organic carbon free basis

Depth in core	Top 4 cm	50 cm	100 cm	150 cm	200 cm	250 cm	300 cm	350 cm	400 cm	450 cm	500 cm	Average	Standard deviation	Coefficient of variation (%)
SiO_2	58·50	59·33	58·37	58·40	59·32	58·22	58·56	58·64	57·91	58·20	58·31	58·52	0·36	0·6
TiO_2	0·93	0·90	0·89	0·89	0·87	0·88	0·88	0·87	0·87	0·90	0·85	0·88	0·02	2·5
Al_2O_3	20·49	20·09	20·40	21·15	20·49	21·16	21·06	21·15	21·53	21·57	22·06	21·02	0·59	2·8
Fe_2O_3	9·81	9·46	9·82	9·66	9·24	10·05	9·49	9·57	9·72	9·82	9·67	9·67	0·22	2·3
MnO	0·79	0·80	0·87	0·71	0·70	0·71	0·71	0·75	0·71	0·82	0·77	0·76	0·06	7·5
CaO	0·63	0·69	0·66	0·69	0·67	0·72	0·68	0·65	0·63	0·68	0·59	0·66	0·04	5·5
MgO	3·36	3·21	3·44	3·19	3·15	3·32	3·41	3·29	3·22	3·12	3·13	3·26	0·11	3·5
Na_2O	1·24	1·28	1·38	1·16	1·41	1·01	1·20	1·04	1·31	0·85	0·82	1·16	0·20	17·3
K_2O	4·16	4·17	4·10	4·07	4·07	3·85	3·94	3·98	4·02	3·96	3·73	4·00	0·13	3·3
P_2O_5	0·09	0·07	0·07	0·08	0·08	0·08	0·07	0·06	0·08	0·08	0·07	0·07	0·01	14·3
Total	100·00	100·00	100·00	100·00	100·00	100·00	100·00	100·00	100·00	100·00	100·00	100·00	—	—

top to bottom. The silica content of the core on this basis shows small variations which are indicative of changes in the amounts of siliceous organisms and quartz present, the maximum at 2·00 m is associated with the presence of the former. These variations are largely counterbalanced by corresponding changes in Fe_2O_3 and Al_2O_3. There is, however, a tendency for the latter to increase with depth. On the other hand, the K_2O content of the core decreases with depth. The manganese concentration down the core remained surprisingly constant, and showed no sign of the very large variations found by Landergren (1954) and Berrit and Rotschi (1956) for cores from the central Atlantic and Western Pacific respectively. Levels of maximum manganese content in these cores were associated by Pettersson (1959) with nearby volcanic outbreaks.

Composition of the clay fractions of the near shore muds nos. 34 *and* 35

The $<2\ \mu$ fractions separated from the two near shore muds (nos. 34 and 35), on a carbonate-free basis, are quite similar in composition to siliceous deep-sea oozes. There are, however, three principal differences: (i) their ferrous iron content is much higher than that of the deep-sea oozes, but their total iron content is similar; (ii) their organic carbon content is again much higher than that of the pelagic sediments; (iii) they contain concentrations of manganese similar to shales and igneous rocks and much lower than the pelagic sediments.

Composition of green mud (*sample* 26)

Except for its high organic carbon content and the fact that most of its iron is in the ferrous state, the green mud from deep water off the North American coast (sample 26) closely resembles the deep-sea argillaceous sediments.

Composition of samples of volcanic origin from Pacific ocean

Samples nos. 30 and 31 have compositions very different from the other deep-sea sediments and proved on microscopic examination to be of volcanic origin. Sample 30 contained abundant shards of brown glass, amphibole, plagioclase, optically negative feldspar, chlorite, chips of feldspar–augite rock, together with some calcite and small amounts of iron-manganese granules. Sample 31 contained much brown glass, feldspar and augite, together with considerable amounts of the skeletons of siliceous organisms and sponge spicules. Minor amounts of micro-manganese nodules, olivine and some much altered hornblende were also present.

Both samples are characterized by their low silica and alumina and water contents and their high contents of TiO_2 (2·5–3·0 per cent), CaO and MgO. They are rich in iron, most of which is in the ferrous state. Their manganese content is only slightly higher than the average for igneous rocks, and considerably lower than the average for Pacific Ocean sediments. In addition Na_2O preponderates over K_2O as in igneous rocks. These samples represent an early stage in the process by which volcanic products are altered to so-called palagonite. Most of the minerals are little altered and the iron is still mainly in the ferrous state. The absence of free quartz and the presence of olivine and augite is almost certainly an indication that they have been derived mainly from basic volcanic materials.

Sample no. 24 is intermediate in composition between these volcanic types and the

argillaceous deep-sea sediments. It contained much volcanic glass, decomposed feldspar and hornblende, together with appreciable amounts of clay minerals. Considerable amounts of micro-manganese nodules were also present and these account for the relatively high manganese content; the empirical formula of the manganese oxides is $MnO_{1.56}$. The volcanic minerals in this sample are considerably more altered than those in samples 30 and 31 and, as a consequence, ferrous iron is absent and the water content is greater. Calcium and magnesium have been lost and potassium replaces sodium. The analysis closely resembles that of pelagic palagonite formed from volcanic glass (Murray and Renard 1891, pp. 297–307).

Composition of calcareous–manganiferous mud (no. 15)

Sample 15 originated on the Easter Island Rise in the Pacific and is of unusual composition. Under the microscope it was seen to consist largely of the skeletons of foraminifera, which were heavily coated both inside and outside with iron and manganese minerals; there was some evidence of replacement of carbonate by these minerals. Some micro-manganese nodules, a little quartz and a very small amount of volcanic glass were also present. The X-ray diffraction pattern of the sample showed the presence of much calcite, together with a small amount of quartz; no lines assignable to crystalline oxides and hydroxides of iron or manganese or to clay minerals were observed.

If the Al_2O_3 content of the sample is used to calculate the approximate content of clay minerals, then the original sample must contain: ca. 3·6 per cent clay minerals, 1·6 per cent free quartz, 72·2 per cent calcium and magnesium carbonates and 19·1 per cent of manganese–iron minerals, with an Fe:Mn ratio of 2·57:1 and an average manganese valency of 3·32. The high $Na_2O:K_2O$ ratio is noteworthy and is in line with the high ratios found for other highly calcareous sediments (e.g. samples nos. 6, 11 and 1).

Comparison of sediments using Niggli values

The system devised by Niggli enables the atomic proportions of the principal cations in silicates to be compared graphically. When this procedure is applied to marine sediments, a number of interesting relationships can be seen, which are obscured by the presence of quartz and organically derived silica and carbonates, using the ordinary analyses on a weight percentage basis.

Niggli values (Niggli, 1954; Niggli and Burri, 1945), for the original sediments are shown in Table 2, (Figs. 4 and 5). As would be expected, since the effect is one of dilution with carbonate, al, fm and alk vary almost linearly with si, but there is a considerable scatter at high si values; c varies inversely with si (Fig. 4). When the values of al-alk are plotted against c, the calcareous sediments lie very close to the line found by Niggli for mixtures of terrestrial clay and lime-stone. The argillaceous sediments on the other hand are grouped fairly closely together with al-alk more or less independent of c. The samples of volcanic origin (24, 30, 31) fall within the area where both igneous and sedimentary rocks overlap, and coincidentally almost fit the line of Niggli's clay–dolomite series.

When the samples are considered on a carbonate and organic carbon-free basis (Table 3 and Fig. 6) it can be seen that al, fm, c and alk are fairly constant and

independent of si. The argillaceous samples and the residues of the calcareous samples mostly fall within the range 200–250 si, which coincides with the pelite–semipelite field (Leake, 1958).

The sediments from the Atlantic Ocean have al values of over 39·5 and fm values of under 42·0; the sediments from the Pacific have al less than 39·5 and fm greater than 42·0. The only exceptions among the data are the argillaceous sediment no. 3 from the Pacific and the samples of volcanic origin.

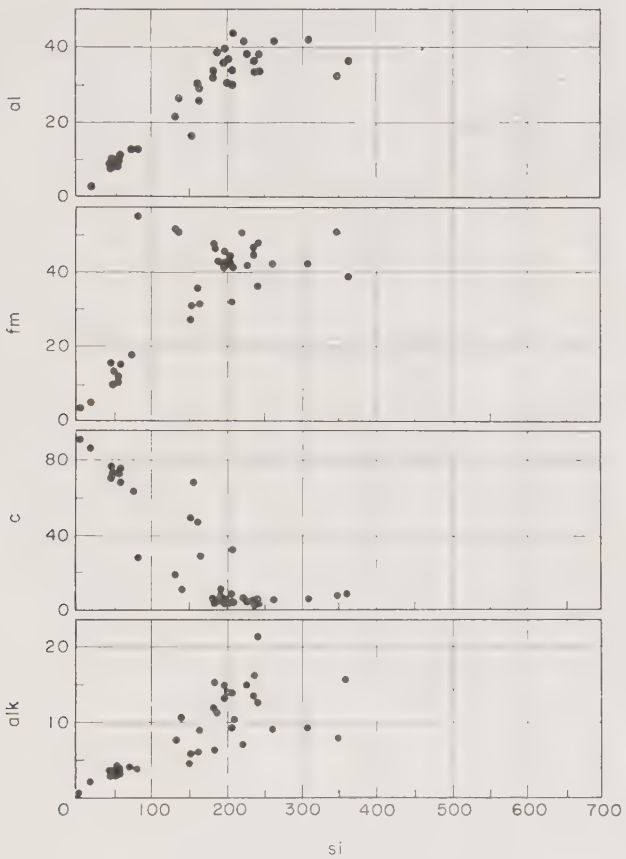

Fig. 4. Interrelationship between al, fm, c and fm and alk of sediments. (Carbonate and organic carbon not deducted.)

Comparison of results with earlier published work

Niggli values for the averages of the three principal types of deep-sea sediments (Tables 4 and 5) are plotted in Figs. 7 and 8, together with those from some of the more reliable average analyses from the literature. The latter show in general the same relationships as have been found in the present work. The very high al and low fm of the red clay from the Atlantic (E) seems highly unusual and must almost certainly be due to analytical error. The average values of al and si in the globigerina oozes (G) (on a carbonate and water-free basis) are anomalously low and the value of

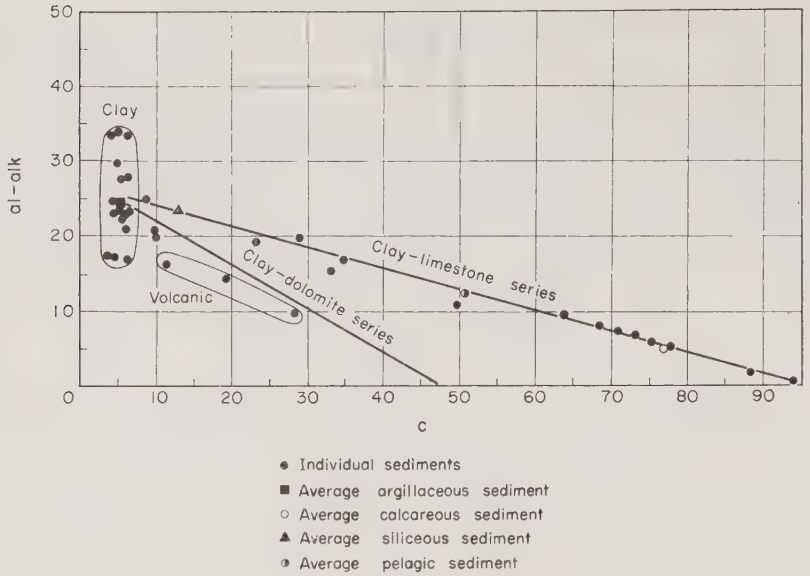

Fig. 5. Relationship between al–alk and c of sediments (carbonate and organic carbon not deducted).

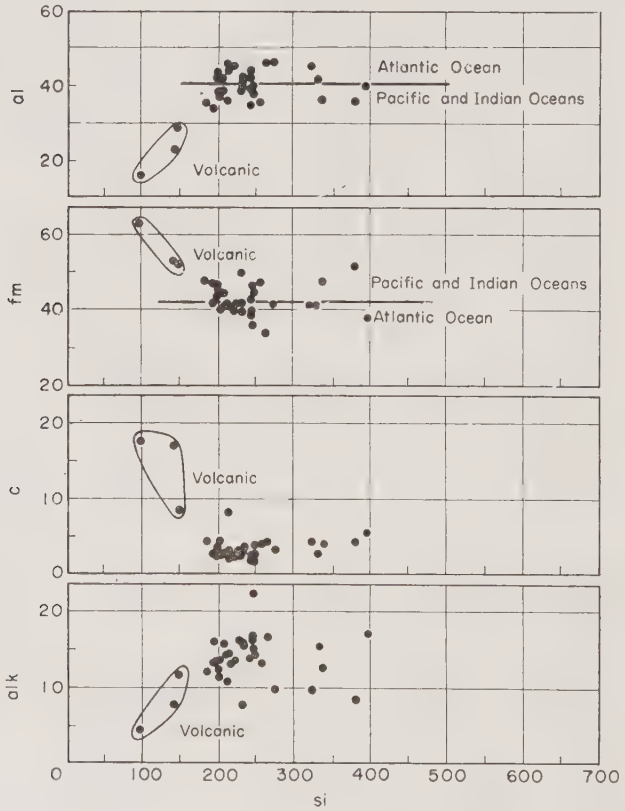

Fig. 6. Interrelationships between al, fm, c and alk and si of sediments (on a carbonate free basis).

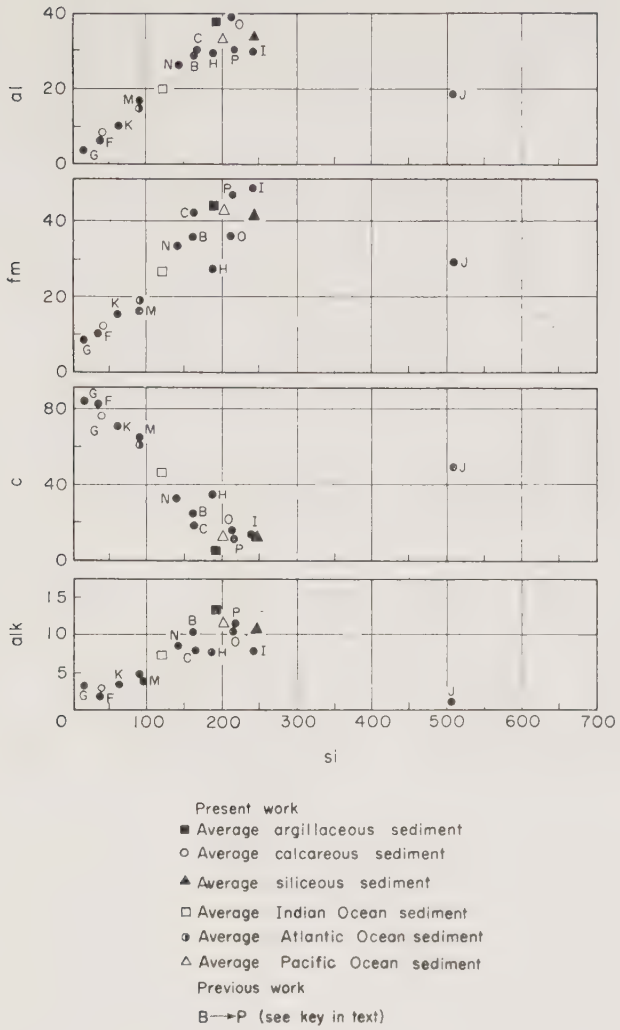

Fig. 7. Comparison of average Niggli values found in this work with those calculated from analyses in the literature (carbonate and organic carbon not deducted).

KEY TO FIG. 7

A. Composite of fifty one samples of red clay. Analyst G. STEIGER (CLARKE, 1924).
B. Average composition of red clay (water-free) recalculated from averages by RUBEY (POLDERVAART, 1955).
C. Average composition of red clay (water-free) recalculated from SUJKOWSKI (1952) (POLDERVAART, 1955).
D. Average composition of ten Pacific red clays (carbonate and organic matter deducted) (REVELLE, cited by SVERDRUP *et al.* (1942), p. 992.)
E. Atlantic red clay (carbonate and organic matter-free) (CORRENS, cited by SVERDRUP *et al.* (1942) p. 992.)
F. Average composition of calcareous oozes, (water-free) recalculated from averages by RUBEY (POLDERVAART, 1955).
G. Average composition of globigerina ooze (water-free) modified from SUJKOWSKI (1952) (POLDERVAART, 1955).
H. Average composition of siliceous ooze (water-free) recalculated from averages by RUBEY (POLDERVAART, 1955).
I. Average composition of radiolarian ooze (water-free) as modified from SUJKOWSKI (1952) (POLDERVAART, 1955).
J. Average composition of diatom ooze (water-free) as modified from SUJKOWSKI (1952) (POLDERVAART, 1955).
K. Average composition of pelagic sediments (water-free), recalculated from averages by RUBEY (POLDERVAART, 1955).
L. Composite of fifty-two samples of terrigenous clay (green and blue muds) (CLARKE, 1924).
M. Average composition of hemipelagic sediments (POLDERVAART, 1955).
N. Average composition of forty-seven samples from two Indian Ocean cores. S. LANDERGREN (private communication).
O. Average composition of 102 samples from three Atlantic cores. S. LANDERGREN (private communication).
P. Average composition of 295 samples from eight Pacific cores. S. LANDERGREN (private communication).
Q. Average of N. O. and P. S. LANDERGREN (private communication).

c (71·6) is correspondingly much too high; they are not at all comparable with those which we have found for this type of sediment. It is noteworthy that on this basis the average al, fm, c and alk values for the three classes of sediment from our work are similar; particularly if the two highly calcareous specimens (nos. 6 and 11) are excluded from the average for calcareous sediments. This suggests that these constituents have a common non-biological origin, and that it is only in samples containing more than 80 per cent of total carbonates that the amounts of iron, aluminium,

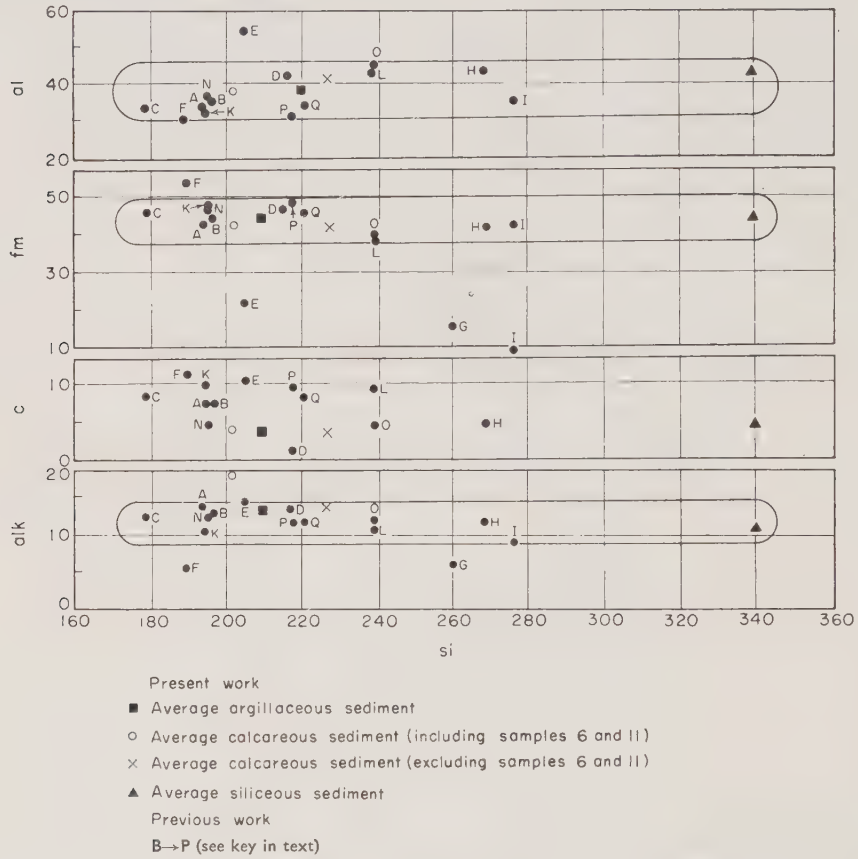

Fig. 8. Comparison of average Niggli values found in this work with those calculated from earlier published analyses (on a carbonate and organic carbon-free basis). For key, see Fig. 7.

magnesium etc., contributed by the organisms constituting the globigerina ooze become appreciable.

Trace elements in deep-sea sediments

The results of spectrographic and chemical determination of trace elements in the sediments are shown in Table 7. In general the average values agree well with the average values found for Pacific pelagic sediments by Goldberg and Arrhenius (1958), and for twenty red clays of unspecified origin reported by Young (1954).

The highest contents of strontium are found in the calcareous sediments and there is a correlation between the strontium and total carbonate contents. The value of 2100 p.p.m. Sr of sample 6 (92 per cent carbonate) closely parallels the average of 2080 p.p.m. Sr found by TUREKIAN and KULP (1956) for calcareous deep-sea sediments averaging 88 per cent total carbonates. Most of the strontium in calcareous sediments is of biological origin, and some of the variations encountered must reflect variations in the calcium to strontium ratios of the organisms from which they were formed (BOWEN, 1956; SWAN, 1956). In the argillaceous sediments, strontium is associated with the clay minerals and also with apatite derived from fish debris (ARRHENIUS *et al.*, 1957).

The correlation of the high content of barium in sediments with organic productivity was first pointed out by REVELLE (1944, pp. 66, 68). GOLDBERG and ARRHENIUS (1958) have assumed that the BaO/TiO_2 ratio of sediments is a measure of organic productivity in the euphotic layer above them. They have plotted this ratio against latitude for the surface sediments on a meridian approximating to long. 125°W, and have found a sharp maximum in the ratio at the equator decreasing rapidly to the north and south. This maximum coincides with a zone of high productivity caused by the Cromwell current (KNAUSS, 1959). None of the samples which we examined were from this region, but the BaO/TiO_2 ratios found for Pacific Ocean sediments from stations lying between 144°W and 172°W (Table 8) were only about one-fifth of the values found by GOLDBERG and ARRHENIUS at more easterly longitudes. Unfortunately no samples were available from latitudes closer to the equator than ca. 4° N and 4° S, so that it was not possible to tell whether the productive region extended to these longitudes.

Nickel, cobalt, lead, copper and molybdenum are all strongly concentrated in the marine sediments compared with igneous rocks. Approximately half to one-third of these elements are bound in the ferromanganese minerals, probably replacing manganese or iron in the disordered layers of the manganous and ferric manganites as postulated by BUSER and GRÜTTER (1956). Most of the remainder is insoluble in chelating agents, and according to GOLDBERG and ARRHENIUS (1958), is incorporated in the colloidal fraction of the sediment. It is probable that this fraction of the trace elements is held in the clay minerals either by adsorption or ion exchange mechanisms.

A proportion of the copper in marine sediments is of biogenous origin and is derived from organic-copper complexes, such as the respiratory pigment haemocyanin, derived from fish and planktonic debris. REVELLE *et al.* (1955) have found a close correlation between the barium and biogenous copper contents of Pacific sediments. Frequently, but not always, in the present work high barium contents are associated with high copper contents.

The concentrations of gallium and germanium in the argillaceous sediments are fairly constant. Since both elements only occur in the argillaceous phase of the sediments, their concentrations in the siliceous and calcareous sediments are in inverse proportion to the contents of free silica and carbonate (BURTON *et al.*, 1959). Germanium is slightly higher in the argillaceous sediments (ave. 2·4 p.p.m. Ge) compared with igneous rocks (ave. 1·7 p.p.m. Ge). The average gallium:aluminium ratio of the pelagic sediments ($2{\cdot}4 \times 10^{-4}$) is very similar to that of the granitic rocks ($2{\cdot}35 \times 10^{-4}$); this shows that very little differentiation of the two elements

Table 7. Trace elements in pelagic sediments (in p.p.m.)

	Be	Sr	Ba	Cu	Pb	Co	Ni	Ga	La	Sn	Ce	Ge	Zr	Hf	Th	V	Cr	Mo
Calcareous																		
6	–	2100	1900	160	60	36	250	3·7	20	15	63	0·0	34	<1	2·2	450	28	15
2	–	1200	680	440	180	120	250	3	36	10	—	—	250	5	—	380	130	20
1	2	1200	580	300	150	56	180	—	—	—	—	—	200	—	—	120	30	8
8	–	1050	1600	120	75	95	130	6·5	210	15	—	1·0	130	—	—	450	47	8
5	3	860	900	420	100	120	290	16	30	15	—	1·8	120	—	—	200	32	10
10	–	2400	4000	470	50	70	150	5·7	30	18	—	0·9	180	—	—	180	40	6
21	–	200	760	400	120	40	180	10	—	—	—	—	70	—	—	100	30	12
12	–	390	1200	500	320	53	180	19	—	40	—	—	10	—	—	450	60	4
4	–	1000	680	450	160	240	380	20	120	10	—	—	210	—	—	480	50	95
13	–	700	1300	120	280	80	330	20	230	—	—	—	200	—	—	180	60	23
Argillaceous																		
14	–	290	1300	320	45	60	290	18	200	—	—	—	180	—	—	250	40	15
17*	–	190	600	210	220	120	310	23	130	20	140	2·3	170	—	11	300	60	25
25	–	500	6000	430	160	170	350	20	—	—	—	—	155	4	26	380	70	10
23	–	320	700	330	200	120	330	18	100	—	197	—	120	4	48	380	50	22
16	4	350	550	400	180	87	320	21	120	25	—	2·8	140	—	—	390	60	—
28	–	410	4000	450	300	90	370	17	—	24	135	—	130	2	14	530	50	12
3	3	740	1400	370	200	86	290	28	80	10	—	2·7	20	—	—	700	60	11
32	–	160	740	410	210	70	190	22	15	20	138	—	140	2	18	200	40	5
27	–	700	600	330	120	100	320	19	—	30	—	—	120	—	—	440	60	22
19	–	810	1800	300	200	60	180	18	140	10	—	—	100	2	—	300	30	30
33	–	410	500	720	60	120	290	20	—	10	—	—	80	—	—	450	50	—
29	–	500	8000	500	200	87	380	14	180	30	26	—	156	5	10	600	100	15

* Composite sample from core.

Table 7 (*contd.*)

Siliceous	Be	Sr	Ba	Cu	Pb	Co	Ni	Ga	La	Sn	Ce	Ge	Zr	Hf	Th	V	Cr	Mo
22	–	120	760	180	200	56	310	18	120	—	—	—	140	—	—	180	62	12
20	–	390	2100	610	220	220	290	20	70	10	—	—	160	—	—	300	30	80
18	4	170	300	340	120	320	400	15	55	15	144	—	200	—	5	450	200	20
Volcanic																		
30	–	450	640	400	230	100	330	12	50	—	—	—	160	—	—	480	390	—
31	–	390	1400	1100	170	170	300	19	—	5	—	—	150	—	—	480	370	15
24	–	270	790	300	230	—	400	15	100	25	—	—	260	—	—	230	12	5
Green Mud																		
26	–	490	1900	290	260	200	380	15	200	—	—	—	250	—	—	50	8	22
Calcareous Manganiferous Mud																		
15	–	1300	800	280	200	170	470	7	65	20	—	—	130	—	—	30	8	70
Near Shore Mud (less than 2 μ fraction)																		
34	–	550	960	460	230	0	27	17	—	20	—	—	80	—	—	480	220	—
35	–	920	1300	420	230	0	31	15	—	23	—	—	210	—	—	680	300	—
Averages for sediments																		
Calcareous	–	1110	1360	338	150	91	232	12	100	18	—	1·2	140	3	—	300	51	20
Argillaceous	–	450	2000	400	175	100	300	20	90	20	130	2·5	126	6	19	390	55	17
Siliceous	–	230	1050	370	180	200	330	18	80	12	—	—	170	—	—	460	97	38
Pacific pelagic (Goldberg and Arrhenius 1958)	–	710	3900	740	150	160	320	19	140	—	—	—	180	—	—	450	93	45
Pelagic Young (1954)	–	600	8100	—	—	90	260	—	220	—	—	—	170	—	—	145	82	—

has occurred during the weathering and degradation of igneous rocks and the deposition of their decomposition products on the ocean bed.

The zirconium content of the pelagic sediments is rather variable but the averages for the three principal types of sediment and for the volcanic samples (24, 30, 31) are similar and approximate to the average value of 150 p.p.m. Zr quoted by Young (1954) for igneous rocks. A number of the argillaceous samples were analysed for hafnium, the Hf:Zr ratios, which ranged from 0·015 to 0·03, were very similar to those found for igneous rocks (Fleischer, 1955; Kosterin *et al.*, 1958).

Like zirconium, thorium is rapidly hydrolysed at the pH of sea water to a colloidal-hydrated oxide, this is readily co-precipitated during the formation of ferromanganese minerals, which may contain as much as 80 p.p.m. of thorium for 22·3 per cent Mn (Riley and Sinhaseni, 1958). Only a comparatively small amount of the

Table 8. BaO/TiO_2: ratios for Pacific Ocean sediments

Sample no.	Lat.	Long.	BaO (p.p.m.)	TiO_2 (p.p.m.)	BaO/TiO_2
18	04°04′ S	152°53′ W	759	4400	0·06
4	03°48′ S	152°56′ W	335	5700	0·17
19	04°02′ N	172°19′ W	2010	6100	0·33
29	09°09′ N	144°26′ W	8930	7300	1·22
32	29°24′ N	153°06′ W	826	9700	0·09
3	30°22′ N	154°56′ W	1340	8700	0·14
33	42°29′ N	162°08′ W	560	8400	0·06

thorium in the pelagic sediments is associated with these minerals, since the average thorium and manganese contents of the argillaceous sediments examined in the present work were 19 p.p.m. and 0·37 per cent, respectively. Most of the thorium is presumably bound in the clay fraction or biogenous apatite (Arrhenius *et al.*, 1957) of the sediment. Thorium is apparently slightly concentrated in the sediments compared with igneous rocks (average 11·5 p.p.m., Rankama and Sahama, 1950).

Compared with igneous rocks the rare earth elements are concentrated in marine sediments approximately tenfold. According to Goldberg and Arrhenius (1958) they occur mainly in the biogenous apatite or in the ferro-manganese minerals. The 500–100 μ fraction which they separated from a dark brown clay rich in micro-manganese nodules with a moderate amount of fish debris (Cap 33 B.G.) consisted mainly of apatite and phillipsite, and contained ca. 12·5 per cent P_2O_5 and 0·21 per cent La_2O_3. Riley and Sinhaseni (1958) have found concentrations of 0·021 per cent Ce_2O_3, 0·03 per cent La_2O_3 and 28·8 per cent MnO in the ferromanganese minerals of Pacific ocean manganese nodules. Assuming these values it is evident that the argillaceous sediments only contain sufficient apatite and manganese minerals to account for about one-fifth of their observed content of rare earth elements, the remainder is probably associated with the clay minerals.

Vanadium determinations were carried out on the sediments using both spectrographic and spectrophotometric methods (Sandell, 1959) and gave results somewhat higher than those obtained by other workers (Clarke (1924) and Young (1954)

found 240 p.p.m. and 145 p.p.m. of vanadium, respectively, in red clays). The element does not appear to be appreciably concentrated relative to igneous rocks. Much of the vanadium in the marine sediments is probably contained in the clay minerals (Rankama and Sahama, 1950). The element is quite strongly concentrated in the ferromanganese nodules, which may contain up to 900 p.p.m. V in their acid soluble fraction (Riley and Sinhaseni, 1958), but their contribution to the total amount of vanadium in pelagic sediments must be only quite small. Goldberg and Arrhenius (1958) have found high Ti/Al, V/Al and Cr/Al ratios in sediments from the neighbourhood of the Hawaiian Islands, they attribute these to the presence of minerals such as magnetite and ilmenite which are of volcanic origin. High V/Al ratios were not found for the samples of volcanic origin from the Pacific Ocean (samples nos. 31 and 32).

The average content of chromium found in the marine sediments is rather lower than the average value for igneous rocks accepted by Young (1954), but considerably lower than Goldschmidt's (1954) average of 200 p.p.m. for the upper lithosphere. It is probable that the oxidizing conditions prevailing in many pelagic sediments, particularly those containing appreciable quantities of ferromanganese minerals, causes oxidation of chromium to the hexavalent state and its partial loss from the sediment. In this connexion it may be noted that Sinhaseni and Riley (1960) could not detect chromium in manganese nodules using methods sensitive to 5 p.p.m. Cr.

Goldberg and Arrhenius (1958) have suggested that an excess of chromium over 100 p.p.m. in sediments, is a useful indication of the presence of altered or unaltered basaltic pyroclasts. The presence of large amounts of chromium found in the volcanic samples nos. 31 and 32 are in agreement with this hypothesis.

Conclusions

The striking similarity in composition of the terrestrial clays, the $<2\ \mu$ fraction of nearshore clays (except for their high content of ferrous iron and organic carbon) and the deep-sea argillaceous sediments suggests a mainly terrigenous origin for the latter, rather than one involving submarine weathering of volcanic rock. Young (1954) has drawn the same conclusion from the fact that the amounts of zirconium, titanium, vanadium and chromium in red clays, and near shore clays are almost identical with their average concentrations in igneous rocks. The figures presented in Table 7 in general support Young's hypothesis.

The presence in pelagic sediments of certain elements such as copper, lead, nickel and cobalt in amounts greatly exceeding their concentration in igneous rocks is difficult to explain. It is possible that some of their nickel and cobalt is derived from cosmic sources (Öpik, 1951) but according to Smales and Wiseman (1955) the amount coming from these sources is not significant. Neither lead nor copper is present in meteorites in more than trace amounts. It is likely that the sediments acquire their content of lead and transition elements from sea water by adsorption or scavenging.

Mineralogical Investigation of Samples

With the exception of two of the volcanic samples (nos. 30 and 31) all the sediments were submitted to qualitative mineralogical examination by X-ray diffraction

and differential thermal analysis. In order to avoid alteration of the clay minerals, the washed samples were dried in air at room temperature; carbonates were removed from the calcareous sediments with 0·5 N acetic acid before drying.

Major amounts of α-quartz (up to ca. 40 per cent) and feldspar (up to ca. 15 per cent) were present in all samples. Traces of apatite were detected in samples 23 and 19. The most abundant clay mineral in the samples was illite, but considerable amounts of montmorillonite and chlorite were also present. The globigerina oozes and the clays from the Atlantic Ocean also contained detectable amounts of kaolinite. The degree of crystallinity of the clay minerals, as shown by the sharpness of their X-ray diffraction lines, varied considerably. Samples 4 and 24 showed particularly diffuse lines, the latter sample which was rich in much altered volcanic material, had montmorillonite in preponderance over illite, showing that the process of illitization of montmorillonite had not proceeded far. Neither differential thermal analysis nor X-ray diffraction showed any appreciable difference in the clay mineral composition down the length of the 5 m core from the Atlantic (sample 17). Kaolinite was the predominant clay mineral in the <2 μ fractions of the two near shore clays (samples 34 and 35), but appreciable amounts of montmorillonite and illite were also present.

In general, there is a very striking qualitative similarity between the component clay minerals of the sediments of the Atlantic, Pacific and Indian Oceans. This is borne out by a more detailed, semiquantitative study of a typified argillaceous sediment from each of the three oceans carried out in the Geochemical Laboratory of the U.S. Geological Survey. Each sample was dispersed in water and sand-sized particles (>62 μ) were removed by wet sieving using a 230-mesh U.S. standard size sieve. Silt (2–6 μ) and clay (<2 μ) fractions were separated by centrifugation. The small amount of each sample available precluded accurate mechanical analysis, but all three had roughly similar compositions within the range of 2–5 per cent sand size, 25–40 per cent silt size, 55–70 per cent clay size. Sand-sized particles were examined using the optical microscope and powder X-ray diffraction camera. Silt and clay sized fractions were examined by X-ray diffraction methods only. Semiquantitative estimates were made of the minerals in the silt and clay size fractions and are given as parts in ten (Table 9).

Sand size

Sample 17* (*Atlantic*). Some black flakes of combined iron and manganese oxides; many dark brown aggregates which when ultrasonized broke up into clay, quartz and feldspar, some of them had black flakes as cores. Some calcitic shells, siliceous spicules and fragments of apatite shells were found. Grains of analcite, barite and biotite were also present.

Sample 3 (*Pacific*). Many black flakes of combined iron and manganese oxides. A few siliceous spicules were also found, together with grains of barite, amphibole, quartz, feldspar and analcite.

Sample 16 (*Indian Ocean*). Some black flakes of combined manganese and iron oxide were found, together with grains of quartz, feldspar, apatite (shells), barite, amphibole and iron oxide.

* Composite sample prepared from core.

The results of these mineralogical studies confirm the findings of earlier workers. Large amounts of illite and lesser amounts of montmorillonite were found in all the deep-sea sediments. Kaolinite, which according to MILLOT (1942) is not formed in a marine environment, and originates from the land, was present in low concentrations in samples from the Atlantic, and was the principal clay mineral in the near shore clays (samples 34 and 35). Grim *et al.* (1949) have postulated that kaolinite undergoes slow alteration to illite, or chloritic mica, in the sea. It is expected therefore

Table 9. Semiquantitative estimates of composition of silt and clay fraction (expressed as parts in 10)

	Ocean		
	Atlantic	Pacific	Indian
	Sample No.		
	17*	3	16
Silt size			
quartz	5+	5+	5
chlorite	2	1	2
mica (illite)	1+	1	2
feldspar	1+	2	1
Clay size			
chlorite	2	2	2
montmorillonite	1+	1	1
mixed layer montmorillonite and chlorite	1	tr.	tr.
mica (illite)	2+	3+	2+
mixed layer mica and chlorite	tr.	tr.	1
quartz	2	2	2
feldspar	1	1	1
Total sample			
quartz	4	4	4
feldspar	1+	1+	1+
chlorite	2	2	2
mica (illite)	1+	2+	2
others	tr.	tr.	tr.

* Composite sample prepared from core.

that only low concentrations of kaolinite will occur in deep-sea sediments far from land, and they have found that its concentration decreases markedly with increasing distance from land.

Only comparatively minor amounts of montmorillonite were found in the deep-sea sediments, confirming the deductions of previous workers that it is generally only abundant in samples of near shore origin. Exceptionally it has been found as the principal clay mineral of sediments from the Sigbee Deep in the Gulf of Mexico (MURRAY and HARRISON, 1956).

Grim *et al.* (1949) found that certain sediments from the Pacific contained a chloritic clay mineral, together with some complex mixed layer clay minerals. Chlorite was found in the routine examination of our sediments, and was detected in major proportions in both the silt and clay-size fractions of the samples 3, 17 and 16, which were submitted to a more detailed examination (Table 9). Traces of mixed layer minerals were also detected in the clay size fraction of these samples. There is good qualitative agreement between the mineralogical compositions of the individual silt and clay fractions of these sediments, which originated from different oceans. Chemically the three sediments are similar in silica content but sample 16 is relatively poor in Al_2O_3 and K_2O, but rich in MgO and Na_2O. Sample 17 is characterized by its rather higher content of Fe_2O_3 (Table 3).

Acknowledgements—The authors offer their sincere thanks to the following for gifts of sediments: The Trustees of the British Museum (samples 1, 3, 4, 5, 8–14, 16). Dr. S. Landergren and Professor Hans Pettersson for six samples from the Swedish Deep Sea Expedition; Dr. D. Ericson of the Lamont Geological Observatory for the argillaccous red clay core (sample 17); and Dr. Gustav Arrhenius of the Scripps Institute of Oceanography for eleven samples collected on Capricorn, Mid-Pacific, Cusp, Chinook and Downwind Expeditions. They are particularly indebted to Dr. Preston E. Cloud for X-ray diffraction analyses, and to Professor Hollingworth of University College, London, for making available facilities for differential thermal analysis. Thanks are also due to Dr. N. Rast for advice and assistance and to Drs. B. Leake and M. Atherton for helpful criticism.

References

Ahrens L. H. (1954) *Quantitative Spectrochemical Analysis of Silicates.* Pergamon Press, London.

Arrhenius G. O. S., Bramlette M. N. and Picciotto E. (1957) *Nature, Lond.* **180,** 85–86.

Arrhenius G. O. S. (1952) Sediment cores from the East Pacific. *Repts. Swed. Deep Sea Exped.* **3,** No. 5.

Berritt G. R. and Rotschi H. (1956) *Repts. Swed. Deep Sea Exped.* **3,** No. 2.

Bowen H. J. M. (1956) *J. Mar. Biol. Ass., U.K.* **35,** 451–60.

Bradley W. H. and Bramlette M. (1942) U.S. Geol. Survey Prof. Paper 196.

Burton J. D., Culkin F. and Riley J. P. (1959). The abundances of gallium and germanium in terrestrial materials. *Geochim. et Cosmochim Acta* **16,** 151–180.

Buser W. and Grütter A. (1956) *Schweiz. Min. Petrogr. Mitt.* **36,** 49–62.

Clarke F. W. (1924) *The Data of Geochemistry.* U.S. Geol. Survey Bull. No. 770.

Clarke F. W. and Wheeler W. C. (1922) *The Inorganic Constituents of Marine Invertebrates.* U.S. Geol. Survey Prof. Paper 124.

Conway E. J. (1950) *Microdiffusion Analysis and Volumetric Error.* Crosby Lockwood, London.

Correns C. W. (1937) *Deutsche atlantische Exped. Meteor,* 1925–1927, *Wiss. Ergeb.* **3,** Teil 3.

Correns C. W. (1954) *Deep-Sea Res.* **1,** 78–85.

Dietz R. S. (1942) *Amer. Mineral.* **27.** 219–220.

Fleischer M. (1955) U.S. Geol. Survey Bull. No. 1021A.

Goldberg E. D. and Arrhenius G. O. S. (1958) Chemistry of Pacific pelagic sediments. *Geochim. et Cosmochim. Acta* **13,** 153–212.

Goldschmidt V. M. (1954) *Geochemistry* p. 546. Oxford University Press.

Goldschmidt V. M. and Hefter O. (1933) *Nachr. Ges. Wiss. Göttingen, Math. Phys. Kl.* III, **4,** 245.

Goldschmidt V. M. and Peters C. (1931) *Nachr. Ges. Wiss. Göttingen, Math. Phys. Kl.* III, **4,** 177.

Goldschmidt V. M. and Peters C. (1932a) *Nachr. Ges. Wiss. Göttingen, Math. Phys. Kl.* III, **4,** 367.

Goldschmidt V. M. and Peters C. (1932b) *Nachr. Ges. Wiss. Göttingen, Math. Phys, Kl.* III, **4,** 404.

Goldschmidt V. M. and Peters C. (1933) *Nachr. Ges. Wiss. Göttingen, Math. Phys. Kl.* III, **4,** 155.
Grim R. E., Bradley W. G. and Brown G. (1951) *X-ray Identification and Structure of the Clay Minerals* pp. 138–172. Mineralogical Society of Great Britain.
Grim R. E., Dietz R. S. and Bradley W. F. (1949) *Bull. Geol. Soc. Amer.* **60,** 1785–1808.
Groves A. W. (1951) *Silicate Analysis* (2nd Ed.). George Allen and Unwin, London.
Hamaguchi H., Tatsumoto M. and Itaya J. (1954) *J. Chem. Soc. Japan* **75,** 119–21.
Hillier R. K. (1955) M.Sc. thesis. University College, London.
Knauss J. A. (1959) *International Oceanographic Congress, New York.* Preprints, p. 515.
Kosterin A. V., Zuev V. N. and Shevaleevski I. D. (1958) *Geokhimiya* 86–88.
Kuenen P. (1950) *Marine Geology.* John Wiley, New York.
Kullenberg B. (1947) *Sv. Hydr. Biol. Komm. Skr. (Göteborg)* 3, **1,** Hafte 2.
Landergren S. (1945) *Ark. Kemi. Min. Geol.* **19A,** No. 26, 8–14.
Landergren S. (1954) *Repts. Swed. Deep Sea Exped.* **7,** Fasc. 2, 125–148.
Leake B. (1958) *Geol. Mag.* 281–296.
Leinz V. (1937) *Deutsche atlantische Exped. Meteor.*, 1925–1927, *Wiss. Ergeb.* **3,** Teil 3, 245–262.
Millot G. (1942) Rélations entre la constitution et la genèse des roches sedimentaires argilleuses. *Geol. Appliq. et Prosp. Min. Nancy* **2.**
Murray H. H. and Harrison J. L. (1956) *J. Sed. Petrol.* **26,** 363–8.
Murray H. H. and Sayyab S. (1955) Natl. Acad. Sci.—Natl. Research Council, Publ. No. 394, 430.
Murray J. and Chumley J. (1924) *Trans. Roy. Soc. Edinb.* **54,** 217.
Murray J. and Renard A. F. (1891) *Repts. Challenger Exped.* **3.**
Neaverson E. (1934) Sea floor deposits. *Discovery Repts.* **9,** 314.
Neeb I. G. A. and Kuenen P. (1943) *Snellius Expedition in the Eastern Part of the Netherlands East Indies* **5,** pt. 3.
Niggli P. (1954) *Rocks and Mineral Deposits.* Freeman, San Francisco.
Niggli P. and Burri C. (1945) *Die jungen Eruptivgesteine des Mediterranean Orogens Zurich* **3,** 625–654.
Öpik E. J. (1951) *Irish Astron. J.* **1,** 145–158.
Pettersson H. (1949) *Nature, Lond.* **164,** 468–470.
Pettersson H. (1959) Manganese and nickel on the ocean floor. *Geochim. et Cosmochim. Acta* **17,** 209–213.
Poldervaart A. (1955) *Chemistry of the Earth's Crust.* Geol. Soc. Amer. Special Paper 62, pp. 119–144.
Rankama K. and Sahama T. G. (1950) *Geochemistry.* University of Chicago Press, 39–40.
Revelle R. R. (1935) *J. Sed. Petrol.* **5,** 37–39.
Revelle R. R. (1944) Carnegie Inst., Washington, Pub. 556.
Revelle R. R., Bramlette M., Arrhenius G. O. S. and Goldberg E. D. (1955) Geol. Soc. Amer. Special Paper 62, pp. 221–236.
Riley J. P. (1958a) *Anal. Chim. Acta* **19,** 413–428.
Riley J. P. (1958b) *Analyst.* **83,** 42–49.
Riley J. P. and Sinhaseni P. (1958) *J. Mar. Res.*
Sandell E. B. (1959) *Colorimetric Determination of Traces of Metals* (3rd Ed.) p. 934. Interscience, New York.
Schott W. (1955) Deep-sea sediments of the Indian Ocean. *Recent Marine Sediments* (Edited by Trask) pp. 396–408. Soc. Econ. Pal. Mineral, Tulsa, Oklahoma.
Shepard F. P. (1948) *Submarine Geology.* Harper, New York.
Smales A. A. and Wiseman J. D. H. (1955) *Nature, Lond.* **175,** 464.
Stubbings H. G. (1937) *John Murray Expedition* 1933–4, *Sci. Repts.* **3,** 133.
Sujkowski Z. L. (1952) *Amer. J. Sci.* **250,** 360–370.
Suzuki K. and Kitazaki U. (1954) *Japan J. Geol. Geog. Trans.* **24,** 171.
Sverdrup H. U., Johnson M. W. and Fleming R. H. (1942) *The Oceans* pp. 946–1044. Prentice Hall, New York.
Swan E. F. (1956) *Deep-Sea Res.* **4,** 71.

Trask P. D. (1955) *Recent Marine Sediments.* Soc. Econ. Pal. Mineral. Special Pub. No. 4. Tulsa, Oklahoma.

Turekian K. K. and Kulp J. L. (1956) The geochemistry of strontium. *Geochim. et Cosmochim. Acta*, **10,** 245.

Vinogradov A. P. (1953) *The Elementary Composition of Marine Organisms.* Sears Foundation Memoir II, New Haven.

Wakeel S. K. El and Riley J. P. (1957) *J. Conseil Int. Exp. Mer.* **22,** 180–3.

Wardani S. A. El (1958) Marine geochemistry of germanium and the origin of Pacific pelagic clay minerals. *Geochim. et Cosmochim. Acta* **15,** 237–243.

Young E. J. (1954) *Bull. Geol. Soc. Amer.* **65,** 1329.

Geochimica et Cosmochimica Acta, 1961, Vol. 25, pp. 147 to 157. Pergamon Press Ltd. Printed in Northern Ireland

The leakage of radiogenic argon from sanidine

H. Baadsgaard,* J. Lipson,† R. E. Folinsbee*

(*Received* 10 *November* 1960)

Abstract—The presence of unaltered sanidine in stratigraphically well-defined bentonite clay horizons offers an opportunity to date a sedimentary horizon by the Ar^{40}/K^{40} method. It has been demonstrated that radiogenic argon losses of from 15–40 per cent may take place from microcline and orthoclase, and an evaluation of the argon retentivity of sanidine is necessary. The effects of variable temperature and grain-size in short-term (days) tests of argon leakage from pure sanidines were investigated. The results indicate that the radiogenic argon is quantitatively retained at temperatures below 400°C except, possibly, for the finest grain-sizes (−325 mesh) and for sanidines with lattice irregularities. Argon loss above 400°C and below the melting temperature appears to involve the loss of at least two separate argon components for structurally inhomogeneous sanidine. Bentonitic sanidine (of homogeneous structure) showed only simple diffusion loss of argon. Argon loss from feldspars is discussed in terms of diffusion and lattice discontinuities. To test possible long term (millions of years) low-temperature losses of radiogenic argon from bentonitic sanidine, seven biotite–sanidine pairs, taken from bentonite clay horizons and ranging in age from ~65 to ~450 million years, were sampled and analysed. The sets of Ar^{40}/K^{40} values obtained are the same within analytical error (±5 per cent) over the entire range of ages and show that bentonitic sanidine retains radiogenic argon as well as comparable biotite. The data appear to indicate that fresh sanidine obtained from volcanic bentonite horizons retains radiogenic argon sufficiently well to yield reliable Ar^{40}/K^{40} ages.

Introduction

The presence of unaltered sanidine in stratigraphically well-defined bentonite clay horizons offers an opportunity to date a sedimentary horizon by the Ar^{40}/K^{40} method. It has been demonstrated, however, that variable radiogenic argon losses of from 15–40 per cent may take place from other potassium feldspars, such as microcline and orthoclase (Wetherill *et al.*, 1955; Gerling *et al.*, 1955; Wasserburg *et al.*, 1956; Folinsbee *et al.*, 1956; Jeffery, 1956; Gentner and Kley, 1957; Goldich *et al.*, 1957). These losses are indicated by data obtained from cogenetic minerals, and it is possible in the case of volcanic sanidine to find coexisting biotite in the bentonite clays. The initial data obtained on coexisting biotite and sanidine from bentonites revealed that sanidine yielded the same date as the biotite. Several bentonites containing biotite and sanidine were then investigated, and preliminary experimental work on argon leakage from sanidine carried out.

Biotite–Sanidine Pairs

A preponderant number of bentonite clay horizons contain little or no biotite and often only rare sanidine. Seven bentonite clay horizons were found in which biotite and sanidine were present in sufficient quantity for adequate sampling. Various samples and separates were prepared from each bentonite, and a number of Ar^{40}/K^{40} dates obtained for each horizon by means of conventional flux-fusion isotope dilution techniques (Baadsgaard *et al.*, 1957). Potassium was determined gravimetrically by J. L. Smith fusion and tetraphenyl borate precipitation.

The data in Table 1 indicate that the coexisting biotite and sanidine in the

*Department of Geology, University of Alberta.
†Department of Physics, University of Alberta.

sampled bentonite horizons give the same age, and that the sanidine retains radiogenic argon as well as comparable biotite. The range in dates of the samples is from 60 to 450 million years, and the agreement is surprising when the purity of the separated minerals is considered. Mixed-layer clay–quartz aggregates, quartzo-feldspathic aggregates, and what appears to be altered volcanic glass are major contaminants of the sanidine separates. These impurities contain appreciable K_2O,

Table 1. Biotite and sanidine from bentonite horizons

No.	Description	K^{40} (ppm)	Ar^{40}/K^{40}
	Whitecourt Bentonite–Upper Cretaceous (Maestrichtian)		
AK–127	Biotite, 100–170 mesh	3·85	0·00376
AK–128	Sanidine, 100–170 mesh	10·76	0·00386
	Kneehills Bentonite–Upper Cretaceous–(Maestrichtian)		
AK–19	Sanidine, 60–100 mesh	7·79	0·00396
KA–154	Sanidine, 60–100 mesh	8·50	0·00396
AK–102	Sanidine, 60–100 mesh	9·63	0·00408
AK–102P	Sanidine, 60–100 mesh	10·47	0·00397
KA–155	Biotite, altered, 60–100 mesh	1·29	0·00400
KA–155	Biotite, altered, 60–100 mesh	1·29	0·00392
AK–20	Biotite, very altered, 60–100 mesh	$0·45_8$	0·00391
	Bearpaw Bentonite, Upper Cretaceous–(Campanian)		
AK–1	Biotite, 60–100 mesh	6·03	0·00408
AK–1	Biotite, 60–100 mesh	6·03	0·00464
AK–92	Biotite, 60–100 mesh	7·05	0·00440
AK–132	Biotite, 60–100 mesh	7·02	0·00440
AK–131	Biotite, 100–170 mesh	6·67	0·00439
AK–130	Biotite, 170–270 mesh	6·28	0·00450
AK–22	Sanidine, 100–140 mesh	5·48	0·00457
AK–93	Sanidine, 100–170 mesh	10·56	0·00462
AK–129	Sanidine, 100–270 mesh	9·02	0·00461
	Belly River Bentonite–Correlative with Bearpaw		
AK–43	Biotite, 60–100 mesh	3·82	0·00461
AK–42	Sanidine, 80–170 mesh	9·80	0·00446
	Crowsnest Volcanics, Mid-Cretaceous (Cenomanian) Trachyte Flow		
AK–2	Sanidine, lower, 35–60 mesh	12·76	0·00567
AK–147 (2)	Sanidine, upper, 60–80 mesh	12·77	0·00569
AK–147 (5)	Sanidine, upper, 120–140 mesh	12·77	0·00571
AK–147 (9)	Sanidine, upper, 270–325 mesh	12·77	0·00570
AK–147 (11)	Sanidine, upper, silt size	12·77	0·00549
AK–147 (13)	Sanidine, upper, less than silt size,	12·77	0·00565
	Average Ar^{40}/K^{40}	—	0·00565

Table 1—(*contd.*)

No.	Description	K^{40}, (ppm)	Ar^{40}/K^{40}
	Crowsnest Volcanics–(cont.) Mill Creek Bentonite		
AK–97	Biotite, 60–100 mesh	6·89	0·00602
AK–97	Biotite, 60–100 mesh	6·89	0·00590
AK–98	Sanidine, 60–100 mesh	10·69	0·00615
AK–98	Sanidine, 60–100 mesh	10·69	0·00609
AK–98	Sanidine, 60–100 mesh	10·69	0·00603
	Average Ar^{40}/K^{40}		0·00604
	Gaspe Bentonite, Lower Devonian (Coblenzian)		
AK–113	Biotite, 270–325 mesh	4·01	0·0245
AK–138	Biotite, <325 mesh, silt size	3·9	0·0253
AK–120	Sanidine, 120–270 mesh	9·18	0·0259
AK–136	Sanidine, 270–325 mesh	6·98	0·0251
AK–137	Sanidine, <325 mesh, silt size	5·43	0·0253
AK–52	"Glass" aggregates, 60–120 mesh	4·90	0·0221
AK–106	Mixed layer clay mineral, 35–120 mesh	4·74	0·0209
	Kinnekulle Bentonites, Middle Ordovician (Caradocian)		
AK–59	Biotite, altered, 100–200 mesh	3·49	0·0292
AK–59	Biotite, altered, 100–200 mesh	3·49	0·0288
AK–77	Biotite, A_2-layer, fairly fresh, 60–200 mesh	4·44	0·0303
AK–82	Biotite, A_1-layer, fresh, 60–200 mesh	5·38	0·0288
AK–61	Sanidine, 100–270 mesh	10·98	0·0304
AK–90	Sanidine, 100–270 mesh	11·18	0·0296
AK–146	Sanidine, monomineralic, 170–230 mesh	12·10	0·0292
AK–69	Clay matrix of "upper bed", 45–60 mesh aggregates	4·95	0·0213

and in a few cases it was possible to separate out relatively pure fractions of these contaminants. As seen in Table 1, these materials retain a considerable portion of their radiogenic argon and give rise, apparently, to errors less than 5 per cent when their concentration in a sanidine separate is even as high as 10–15 per cent. This is a fortunate circumstance, since these impurities often are very difficult to eliminate entirely because of the range in their magnetic properties and specific gravity.

Almost without exception the sanidine in the samples examined was present as fresh anhedral grains showing few inclusions and no marked cleavage. The optic angle in every case was very small and X-ray data indicated the minerals were monoclinic. The biotite, on the other hand, ranged from fresh, unaltered biotite to badly altered material going over to vermiculite. This alteration apparently took place very soon after the volcanic material was deposited since the dates obtained on fresh biotite vs. altered biotite or altered biotite vs. very altered biotite were the same. It is difficult to believe in a diagenetic process leaching out potassium and argon equally well over a long period of time, though this might be possible.

In view of the large losses of radiogenic argon from microcline and microcline–perthites, it is interesting to find that bentonitic sanidine retains its argon as well as comparable biotite. Firm confirmation of quantitative argon retention awaits the determination of Rb–Sr dates on the biotites and possible U–Pb dates on associated zircon. For the present, preliminary laboratory tests on the effects of temperature and sample grain size on diffusion of Ar^{40} were carried out on selected samples to compare the behaviour of sanidine with that of other feldspars and to ascertain how well argon is held in the sanidine lattice.

Table 2. Optical and X-ray data on minerals used in diffusion studies

Specimen no.	$\Delta 2\theta°$*	Or (%)*	Optic plane $2V_x°$ and orientation
A. *Sanidine, Crowsnest trachyte flow (large crystals)*			
AK–147, crystal 1	0·972	76·8	19·9⊥(010) to 20·9‖(010)
AK–147, crystal 2	0·926	81·1	17·1⊥(010) to 24·4‖(010)
AK–147, crystal 3	0·887	84·5	13·5⊥(010) to 21·0‖(010)
Composite heated at 900°C, 25 hr	0·965	77·5	—
B. *Sanidine, Kinnekulle bentonite* (170–230 mesh)			
AK–146	0·990	75·2	0, 5, 4 (3 readings)
AK–146, heated at 900°C, 24 hr	0·990	75·0	—
C. *Microcline, biotite–muscovite granite, N.W. Territories* (60–80 *mesh*)†			
AK–145	0·835	90·0	81·5⊥(010)
AK–145 heated 5 days at 1000°C	0·895	83·8	38·0‖(010)

* $\Delta 2\theta$ is the difference between $\bar{2}01$ for alkali feldspar and 101 for $KBrO_3$ (Orville, 1958).

† Unheated sample has $\Delta = 12{\cdot}5(d_{131} - d_{1\bar{3}1}) = 0{\cdot}88$ (highly triclinic; see Goldsmith and Laves, 1954, p. 100).

Experimental

Three feldspars were chosen for comparative purposes in the diffusion studies (see Table 2 and Fig. 1).

(1) *Sanidine.* Source material: Crowsnest Volcanics; trachyte taken from a fresh road cut $\frac{1}{2}$ mile west of Coleman, Alberta. The sanidine is yellowish-brown (10YR 5/2), translucent in bulk, colourless in thin section, and occurs as large, strongly-zoned phenocrysts up to 3 in. × 2 in. The zoning is apparently a response to temperature of crystallization, not composition, as each crystal seems to be chemically homogeneous (X-ray powder patterns show the $\bar{2}01$ peak is not multiple; see Table 2). Crystals vary in composition between individuals, in the observed range $Or_{76·8}$–$Or_{84·5}$. Zoning covers wide range of $2V$, and optic orientations with optic plane parallel to (010) and perpendicular to (010) may be found. The range in $2V$ is from 19·9° approximately perpendicular to (010) to 24·4° parallel to (010) (see Fig. 1). Crystals are occasionally twinned, always on the Baveno law. No metamorphic alteration seen but Fe-oxide has been partially exsolved from the phenocrysts. Large single phenocrysts were crushed, and $<60 > 80$ mesh fraction used. Ar^{40}/K^{40} date on mineral is 94 million years (see Table 3). Crowsnest volcanic sanidine and biotite from a correlated bentonite give an average date of 100 million years. Possible argon loss for sanidine from this flow is ~6 per cent.

(2) *Microcline.* Source material: Yellowknife muscovite–biotite granite from Yellowknife Geologic Province, Walmsley Lake map-area, N.W.T. (Folinsbee, 1955). The mineral is white in bulk and colourless in thin section, and occurs as anhedra in granite, poikilitically enclosing quartz. Polysynthetic twinning is very prominent. No perthitic lamellae are apparent, nor was an albite phase detected by the X-ray, but the shift in $\bar{2}01$ peak on heating (Or_{90} to Or_{84}) suggests

there was some exsolution. $2V(-) = 83°$; near maximum microcline. Very slight clouding is apparent in thin section. Grain size of mineral particles used was 60–80 mesh. Ar^{40}/K^{40} date on mineral is 2000 million years, while cogenetic muscovite gives a date of 2600 million years. Calculated argon deficiency in the microcline is about 36 per cent.

(3) *Sanidine.* Source material: bentonite from Ordovician bentonite beds, Kinnekulle, Sweden. The particles are fresh anhedral fragments, less than 120 mesh, colourless in section,

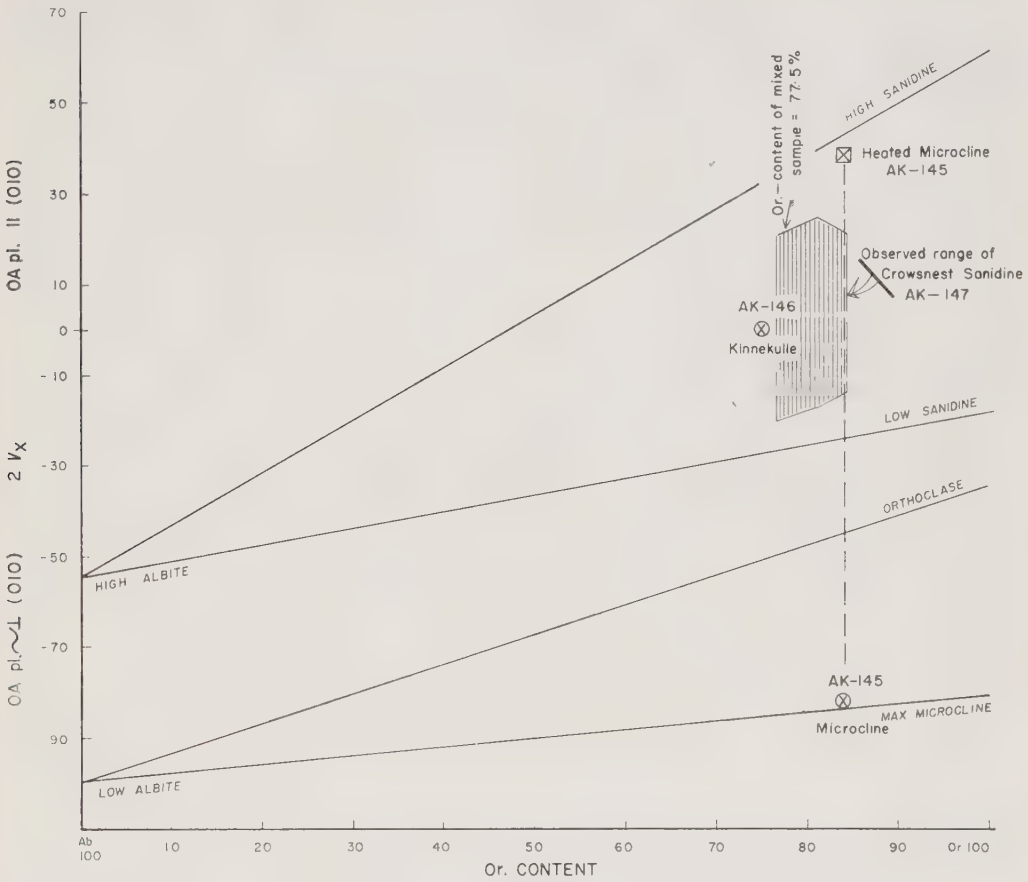

Fig. 1. Structural state of feldspars used in diffusion experiments (Diagram after Tuttle (1952) p. 557, revised by MacKenzie and Smith (1956) p. 406).

white in bulk, and generally untwinned. The $2V$ is $\sim 0°(<5°)$. It was possible to obtain a 99·8+ per cent pure sanidine separate of particle size 170–230 mesh. Ar^{40}/K^{40} date on mineral is 440 million years, and cogenetic biotite gives the same date within experimental error (see Table 1).

The method employed to determine the diffusion of radiogenic argon from the minerals was similar to that of Reynolds (1957). The minerals were outgassed at 200°C in an all-glass vacuum system containing purification materials, charcoal traps to collect evolved gases, and a number of A^{38} "spikes". After sealing the system, the mineral was kept at a specific temperature for 24 hr (Capacitrol temperature regulator) in the presence of a spike, and the gases evolved were purified and trapped out. The temperature was then increased to the next higher value selected, a new "spike" introduced, and the process repeated. A series of samples of gas was thus obtained from the same mineral sample, the diffusion time being 24 $\pm \frac{1}{2}$ hr at each temperature. The amount of Ar^{40} was determined mass spectrometrically, and corrected for small amounts of air argon.

All three of the samples were treated in the same manner and with the same apparatus except for the first Crowsnest sanidine series which went to over 1100°C. In this case the sample fused, the Ni-crucible cracked, and a new crucible was used for a rerun to 900°C as well as the subsequent runs on the other two minerals.

Results

The results of the diffusion experiments are shown in Fig. 2, where the percentage argon expelled (cumulative) is plotted against temperature. The rerun on the Crowsnest sample gave excellent reproducibility with the first series except for a

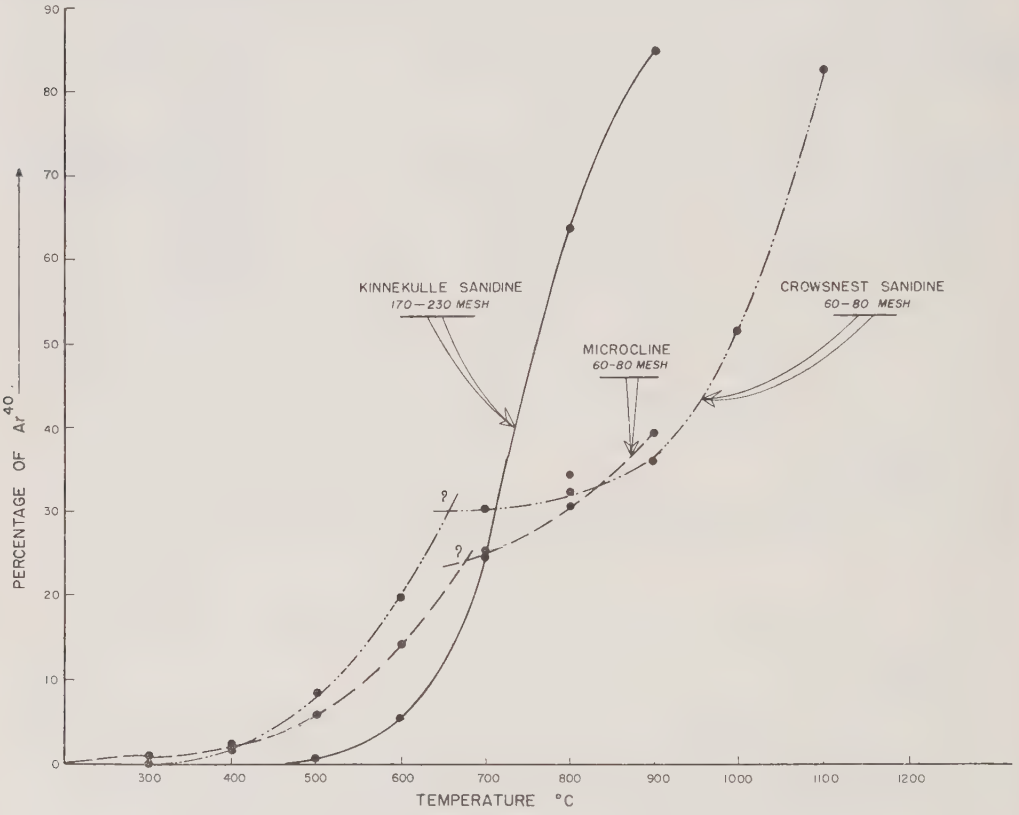

Fig. 2. Percentage of radiogenic argon expelled by 24-hr heating as a function of the temperature.

single point at 800°C. It is readily seen from Fig. 2 that the Crowsnest sanidine does not lose its Ar^{40} in a manner similar to the Kinnekulle bentonite sanidine, but evolves argon in what appears to be at least two stages. In the region 600–800°C a decrease in the rate of evolution of argon occurs, indicating that the mode of diffusion or release of the argon is changing markedly. On the other hand, the Kinnekulle sanidine shows no such change in the rate of evolution except for the highest temperature. The microcline evolves argon in a manner somewhat similar to the Crowsnest sanidine, but with a less definite break in a possible smooth curve.

To calculate the diffusion coefficient, D, the same model and procedure as used

by Reynolds (1957) was employed (isotropic volume diffusion from a sphere). The approximate relation (Carslow and Jaeger, 1947),

$$f = \frac{6}{\pi^{1/2}} \left(\frac{Dt}{a^2}\right)^{1/2} - \frac{3Dt}{a^2}$$

(where f = fraction of argon released, D = diffusion coefficient, t = time of diffusion, and a = spherical radius), is valid for the present experiments. The diffusion coefficients were calculated using $a = 1{\cdot}07 \times 10^{-2}$ cm. for the microcline and Crowsnest sanidine, $a = 3{\cdot}75 \times 10^{-3}$ for the Kinnekulle sanidine and $t = 86{,}400$ sec. A plot of the logarithm of the diffusion coefficients for each of the feldspars vs. the reciprocal of the absolute temperature is given in Fig. 3. Fig. 3 indicates that the diffusion of radiogenic argon from the Crowsnest sanidine is far from a simple process. It would appear to be explained by the scheme proposed by Reynolds (1957). That is, diffusion of the argon in the lattice occurs through vacancies in the crystals and depends upon the rate of advance of the argon into the vacancies and the volume density of the vacancies. Since both of these factors are temperature dependent there should be three regions on a ln D vs. $1/T$ plot corresponding to a high-temperature region in which both factors are temperature-activated, a transitional region and a low-temperature region. The Crowsnest sanidine plot of ln D vs. $1/T$ may then be interpreted by allowing only simple diffusion of argon in the temperature range 400°C to about 700°C, invoking a beginning of rearrangement or temperature variation of the volume density of vacancies in the range 700°C to about 900°C and assuming that above 900°C to the melting point both diffusion of the argon and the volume density of vacancies are temperature dependent to give a composite activation energy to the diffusion process. The Crowsnest sanidine is zoned and the high-temperature variation of the volume density of vacancies may be related to rearrangement of the lattice above ~900°C. However, no difference in the powder X-ray patterns between heated (~1000°C) and unheated samples was detectable.

The microcline plot of ln D vs. $1/T$ (Fig. 3) yields an approximate straight line, and it would seem that the diffusion process over the given temperature interval is controlled mainly by a single factor. More points at higher temperatures are needed for confirmation. A likely factor (assuming the above model is correct) is simple diffusion, since the changing of the volume density of vacancies or structural rearrangement of the microcline above from 700° C to 900 is a relatively slow process (5 days at 1000°C was necessary to convert the microcline to a sanidine lattice, see Fig. 1) compared to the diffusion time.

The plot of ln D vs. $1/T$ (Fig. 3) for the Kinnekulle sanidine is an excellent straight line for the point at 900°C. Had all the argon been driven off at 900°C, all the points would fall on a straight line (as indicated on Fig. 3). The sanidine is already structurally stable above 700°C and pseudostable below 700°C (Laves, 1952). Essentially no internal rearrangements have taken place on heating (see Table 2), and simple diffusion through the lattice appears to explain Fig. 3. Even if there is no structural rearrangement for the Kinnekulle sanidine, the high-temperature region should show a temperature effect on the volume density of vacancies by

Reynolds model. There does not appear to be such a factor, and another model is necessary.

The presence of various groups of argon atoms needing several activation energies for their diffusion could explain the argon diffusion in the Crowsnest sanidine (Gerling and Morozova, 1958). The different activation energies necessary for diffusion of the argon atoms may be pictured as being dependent upon the proximity of the atoms to defects or discontinuities in a regular structure. A variable

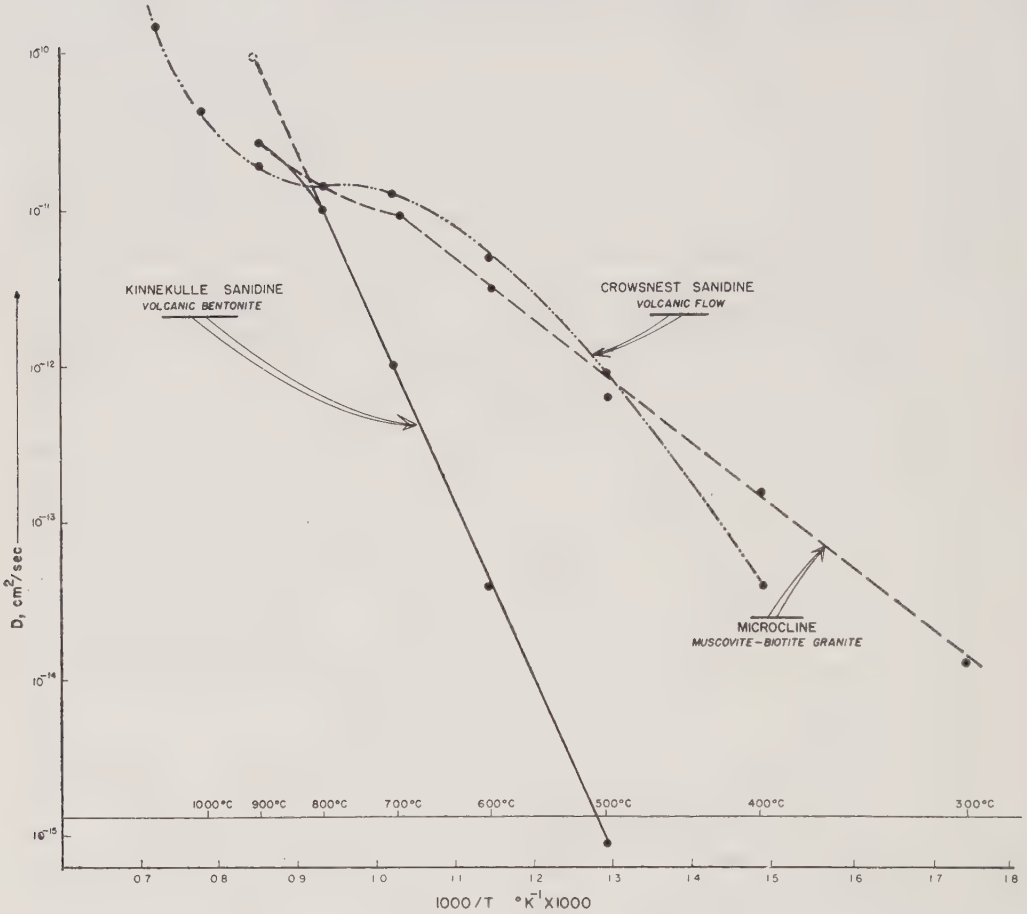

Fig. 3. The logarithm of the diffusion coefficient as a function of the reciprocal absolute temperature.

structure in the Crowsnest sanidine would permit a variety of argon positions while the regular structure of Kinnekulle sanidine would allow essentially one type of location and thus one type of diffusion. The microcline structure shows extensive polysynthetic twinning, and may be cryptoperthitic. These structural features could facilitate different types of argon diffusion, but since the ln D vs. $1/T$ plot is approximately a straight line, it is possible that essentially all the argon in positions with easy access to twin planes or exsolution lamellae has already been lost and is represented

by the 36 per cent Ar^{40}-deficiency vs. the cogenetic muscovite. The twin planes and exsolution lamellae may not basically give rise to substantial argon loss, but could partially control argon loss from the lattice by furnishing relatively "open" paths for argon from several lattice positions with regard to these planes.

It may be calculated that the diffusion coefficient at 500°C for the microcline and the Kinnekulle sanidine differ by a factor of 10^3, the bentonitic sanidine allowing much less diffusion of argon through the lattice than the microcline. Extrapolation of the lines in Fig. 3 to room temperature (~300°K) gives the following values for the diffusion coefficient at room temperature:

$$\text{microcline} \qquad D_{25°C} = 10^{-20}\ \text{cm}^2/\text{sec}$$
$$\text{Kinnekulle sanidine} \qquad D_{25°C} = 10^{-38}\ \text{cm}^2/\text{sec}$$

The work of Fechtig *et al.* (1960) has shown that at and near room temperature the diffusion of argon in the lattice of certain calcium minerals is further influenced by van der Waals absorption on surfaces, and the extrapolation of a ln D vs. $1/T$ plot is of doubtful validity. Nevertheless, the great difference between the slopes of the high-temperature lines in the ln D vs. $1/T$ plot for the microcline and sanidine indicates that the bentonitic sanidine loses its argon a great deal less readily than the microcline.

The activation energy for the argon diffusion from the microcline and sanidine may be calculated using the relation

$$D = D_0 e^{-Q/RT}$$

where D_0 = a constant (cm²/sec)
Q = activation energy (cal/mole);
R = $1{\cdot}98_7$ (cal/mole per °K), the gas constant;
T = absolute temperature.

At two temperatures with D_1 at T_1 and D_2 at T_2,

$$Q = \frac{R \ln (D_1/D_2)}{(1/T_2 - 1/T_1)}$$

For the microcline an activation energy of ~18,000 cal/mole was found, and for the Kinnekulle sanidine, ~52,000 cal/mole. The activation energy for the sanidine is comparable to that found for biotite (57,000 cal/mole) by Gerling and Morozova (1957), and substantiates the retention of radiogenic argon in bentonitic sanidines vs. cogenetic biotite.

In view of the unusual diffusion behaviour of the Crowsnest sanidine it is interesting to see whether or not there is a grain size effect in the loss of argon. Various size fractions of the Crowsnest sanidine were prepared from a single mineral aliquot by sedimentation and sieving, and the samples outgassed *in vacuo* for 24 hr at 200°C. The remaining argon was then determined. The results (Table 3) show that except for the finest size fraction, 15–1 μ, little if any argon is lost *in vacuo* at 200°C for 24 hr due to any causes other than the increase of the surface area over the volume to furnish more argon locations at the surface of the grains. In particular, no size-effect loss such as that found by Gentner and Kley (1957) was observed. The Crowsnest sanidine, though zoned (possessing optical variability), is not altered or weathered. Thus, it appears that the observed argon diffusion behaviour at higher

temperature is due to structural irregularity of the lattice. Crushing of mineral grains is not thought to be a contributing factor to argon loss since the grain-size tests showed no marked loss-pattern. The Ancient microcline tested has lost 36 per cent of its argon as measured against cogenetic muscovite. Though the microcline may be cryptoperthitic, the greater rate of argon leakage of this mineral compared to the rather retentive Kinnekulle bentonitic sanidine is likely due to the triclinic

Table 3. Argon retention for various grain sizes in sanidine from a Crowsnest trachyte flow
(K^{40} = 12·77 ppm, outgassed 24 hr at 200°C)

Particle size (μ)	Ar^{40}/K^{40}	$\frac{Ar^{40}/K^{40}}{0{\cdot}00569}$
500–250	0·00567	1·00
250–177	0·00569	1·00
125–105	0·00571	1·00
53–44	0·00570	1·00
44–8	0·00549	$0{\cdot}96_5$
30–4	0·00565	0·99
15–1	0·00536	0·94

twinned structure. Crushing during preparation of the sample may be an additional factor because of the marked cleavage of the microcline. The retention and simple diffusion behaviour of the Kinnekulle sanidine is thus attributed to the lattice regularity (random Al–Si distribution which does not change upon short-term heating) and the absence of any internal variations due to metamorphic effects.

The argon lost from feldspars to give the feldspar-mica discrepancy is believed to escape at rather low temperatures ($<200°$ C), and it is this argon loss which must be explained. Regular diffusion from the feldspar lattice has failed to give a satisfactory explanation since the argon discrepancy does not appear to be time dependent in any simple way. Escape of very loosely contained argon from a certain position(s) in the lattice could be the reason, and a small amount of loosely-held "'zero' phase" argon has been reported for experiments on a Pre-Cambrian feldspar (Amirkhanov *et al.*, 1959).

More detailed kinetic studies of the diffusion of argon are necessary, since the present treatment does not allow one to follow the rate of argon loss at any specific temperature. In addition, the effect on the argon diffusion of the lattice rearrangement in triclinic microcline at elevated temperatures must be clarified.

Summary

It would appear that fresh bentonitic sanidine is an excellent material for Ar^{40}/K^{40} age dating. The data here presented on its retentivity and argon leakage indicate it retains its radiogenic argon very well. In addition, reasons for the argon loss from other feldspars such as microcline and orthoclase are suggested by the comparison between structurally inhomogeneous and homogeneous sanidine. The controlling factor seems to be the nature of the lattice, with discontinuities such as twinning, exsolution lamellae, and metamorphic alteration probably contributing to

diffusion characteristics as well. More exhaustive studies on the Crowsnest sanidine from volcanic flows vs. the Crowsnest material from bentonite beds have been initiated and should reveal additional information concerning the diffusion of argon from feldspars.

Acknowledgements—The present investigation was made possible by grants from the Geological Survey of Canada, the National Research Council of Canada, the Geological Society of America and the Research Fund of the University of Alberta. The authors are indebted to Dr. K. A. W. Crook for helpful discussions and for the X-ray and optical data for the description of the argon diffusion samples. Mr. A. Stelmach made the potassium determinations. Dr. A. M. Byström-Asklund of the Swedish Geological Survey kindly furnished various separates and samples from the Kinnekulle bentonite beds.

References

Amirkhanov Kh. I., Brandt S. O. and Bartnitskii E. N. (1959) The diffusion of radiogenic argon in feldspars. *Dokl. Akad. Nauk. SSSR* **125**, 1345–7.

Baadsgaard H., Goldich S. S., Nier A. O. and Hoffman J. H. (1957) The reproducibility of A^{40}/K^{40} age determinations. *Trans. Amer. Geophys. Un.* **38**, 539–42.

Carslow H. S. and Jaeger J. C. (1947) *Conduction of Heat in Solids.* Oxford University Press.

Fechtig H., Gentner W. and Zähringer J. (1960) Argonbestimmungen in Kalium-mineralien —VII. Diffusionverluste von Argon in Mineralien und ihre Auswirkung auf die Kalium-Argon-Altersbestimmung. *Geochim. et Cosmochim. Acta* **19**, 70–9.

Folinsbee R. E., Lipson J. and Reynolds J. H. (1956) Potassium argon dating. *Geochim. et Cosmochim. Acta* **10**, 60–8.

Folinsbee R. E. (1955) Archean monazite in beach concentrates, Yellowknife geologic province, Northwest Territories, Canada. *Trans. Royal Soc. Canad.* 3rd ser. sect. IV, **49**, 7–24.

Gentner W. and Kley W. (1957) Argonbestimmungen an Kaliummineralien—IV. Die frage der Argonverluste in Kalifeldspaten und Glimmermineralien. *Geochim. et Cosmochim. Acta* **12**, 323–9.

Gerling E. K., Yashchenko M. L., Ermolin G. M. and Barkan V. G. (1955) *Proc. 3rd session, Commission on the Determination of Absolute Age in Geological Formations.* Izd. Akad. Nauk SSSR.

Gerling E. K. and Morozova I. M. (1957) Determination of the energy of activation of the liberation of argon from mica. *Geokhimiya* No. 4, 304–10.

Gerling E. K. and Morozova I. M. (1958) The kinetics of argon liberation from microcline–perthite. *Geokhimiya* No. 7, 775–81.

Goldich S. S., Baadsgaard H. and Nier A. O. (1957) Investigations in A^{40}/K^{40} dating. *Trans. Amer. Geophys. Un.* **38**, 547–51.

Goldsmith J. R. and Laves F. (1954) Potassium feldspars structurally intermediate between microcline and sanidine. *Geochim. et Cosmochim. Acta* **6**, 100–18.

Jeffery P. M. (1956) The radioactive age of four Western Australian pegmatites by the potassium and rubidium methods. *Geochim. et Cosmochim. Acta* **10**, 191.

Laves F. (1952) Phase relations of the alkali feldspars—II. The stable and pseudostable phase relationships in the alkali feldspar system. *J. Geol.* **60**, 549–74.

MacKenzie W. S. and Smith J. V. (1956) The alkali feldspars—III. An optical and X-ray study of high temperature feldspars. *Amer. Min.* **41**, 405–27.

Orville P. M. (1958) *Feldspar Investigations.* Ann. Rept. Geophys. Lab., Carnegie Inst. Washington for 1957–1958, pp. 206–9.

Reynolds J. H. (1957) Comparative study of argon content and argon diffusion in mica and feldspars. *Geochim. et Cosmochim. Acta* **12**, 177–84.

Tuttle O. F. (1952) Optical studies on alkali feldspars. *Amer. J. Sci.* Bowen vol. 553–67.

Wasserburg G. J., Hayden R. J. and Jensen K. T. (1956) A^{40}/K^{40} dating of igneous rocks and sediments. *Geochim. et Cosmochim. Acta* **10**, 153–65.

Wetherill G. W., Aldrich L. T. and Davis G. L. (1955) A^{40}/K^{40} ratios of feldspars and micas from the same rock. *Geochim. et Cosmochim. Acta* **8**, 171–2.

Geochimica et Cosmochimica Acta, 1961, Vol. 25, p. 158. Pergamon Press Ltd. Printed in Northern Ireland

GEOCHEMICAL NOTE

New investigations of the Igast "meteorite"

(*Received* 17 *April* 1961)

THE meteorite which allegedly fell at Igast, Estonia, in 1855 may be the only known example of a meteorite with the chemical composition of a tektite. Accordingly, the authors reinvestigated the history and possible nature of this object, which has been considered artificial since the work of MICHEL (1913).

The hand specimen and five thin sections examined by MICHEL were lent by Dr. A. SCHIENER of the Vienna Museum, who considers them artificial. The hand specimen and one thin section are melted brick; the remaining four thin sections were found by Rosiwal analysis to be from a quartz basalt porphyry with the following mineral composition: plagioclase (An_{50}–An_{70}), 40 per cent; quartz, 8·5 per cent; magnetite, 2·9 per cent, glass, 1·6 per cent, vesicles, 16·1 per cent, corresponding to a chemical composition of 50–60 per cent SiO_2. None of this material is that originally described as meteoritic by GREWINGK and SCHMIDT (1864).

The reason for this substitution was found to be the distribution to several European museums of spurious Igast specimens by J. V. SIEMASCHKO, a Russian dealer. The generally quoted opinions of the artificial nature of the Igast object are apparently based on this spurious material. Genuine specimens are probably in collections at the Paris Museum, the British Museum, and the University of Dorpat. In view of the reliability of GREWINGK and SCHMIDT'S account and the unusual composition of this meteorite, it is suggested that further investigation of surviving specimens be carried out. Attention is called to the possible existence of other highly siliceous meteorites.

A full account of this investigation will be published as an NASA Technical Report.

Acknowledgement—We are indebted to Dr. A. SCHIENER of the Vienna Museum and Mr. E. P. HENDERSON of the Smithsonian Institution for their assistance in obtaining this material.

Theoretical Division, Goddard Space Flight Center
National Aeronautics and Space Administration
Washington D.C.

JOHN A. O'KEEFE
PAUL D. LOWMAN, JR.

REFERENCES

GREWINGK C. and SCHMIDT C. (1864) Uber die Meteoritenfälle von Phillistfer, Buschhof und Igast, in Livonia und Kurland. *Arch. Naturk. Estlands Ser* 1, **3,** 421–501.

GREWINGK C. (1882) Verzeichniss der Meteoriten-Sammlung der U. Dorpat in Dezember. *Arch. Naturk. Estlands Ser* 1, **9,** 152–160.

GOEBEL A. (1867) Ubersicht der in den Museen und Sammlungen von St. Petersburg vorhandenen Aerolithen. *Bull. Imp. Acad. Sci. St. Petersb. Ser* 3, **11,** 284–291.

MICHEL H. (1913) Zur Tektitfrage. *Ann. K. K. Naturhist. Hofmus Wien* **27,** 1–12.

INFORMATION FOR CONTRIBUTORS

I. GENERAL

1. Papers on *geochemistry* should be submitted to the appropriate Executive Editor—Prof. L. R. WAGER for papers from the United Kingdom and British Commonwealth and for papers in English from Europe; PROF. C. W. CORRENS for papers in German or French; Prof. J. A. S. ADAMS for papers from the American continents. Papers submitted for publication will naturally be judged from the standpoint of scientific originality and novelty. Technical details of apparatus used in scientific investigation can, however, be presented in brief notes. Critical comments or preliminary results requiring early publication should be submitted as letters to the editors. Where possible, letters should be confined to 500 words. The preparation of progress reports and review articles will be invited by the editors from time to time. The journal appears as independent and complete numbers, which are combined into volumes of about 300 pages.

2. Only papers which have not been previously published can be accepted. Authors must agree not to publish elsewhere a paper submitted to and accepted by *Geochimica et Cosmochimica Acta*.

3. Fifty reprints of each paper are provided free. Additional copies can be purchased if ordered at the time the first proofs are returned. A reprint order form will accompany first proofs.

II. SCRIPT REQUIREMENTS

1. Scripts must be written in one of the three official languages—English, French or German.

2. The script should be typed (not a carbon copy). The text must be ready for printing and should be carefully checked for errors. Authors will receive proofs for correction. The original script plus two copies will assist in expediting publication.

3. Illustrations should accompany the script mounted on separate sheets. Line diagrams that require to be redrawn should include all relevant details. Half-tone illustrations should be restricted to the minimum necessary. Photographs should be enlarged sufficiently to permit their clear reproduction and if words or numbers appear on them, two copies should be sent, one clearly printed and the other without inscription. All illustrations should be provided with descriptive legends, which should be given on a separate sheet. Any lettering on diagrams—other than Greek letters, symbols, etc.—should be stencilled and should be sufficiently large and bold to permit reproduction when the diagram has been reduced to a size suitable for inclusion in the journal.

4. References in the text should be given by quoting the author's name and year of publication, i.e. AHRENS (1952). *Full references should be listed at the end of each paper, in alphabetical order, in the following manner*

AHRENS, L. H. (1952). The use of ionization potentials—I. Ionic radii of the elements. *Geochim. et Cosmochim. Acta* **2**, 155–169.

and should include the full title of the article, standard abbreviated title of the journal, year, volume number and inclusive page numbers.

5. The text of articles submitted should be concise and in a readily understandable style. The technical description of the methods used should only be given in detail when such methods are new. The essential contents of each paper should be briefly recapitulated in an abstract in English. Such an abstract may, however, be submitted by the author in the language of the original typescript for translation into English by the editorial staff.

6. To conserve space, authors are requested to mark less important portions of the paper (such as description of methods, record of experimental results, etc.) for printing in smaller type.

7. Indices of refraction should be denoted by the symbols α, β, γ, ω, ε, n, and vibration directions by X, Y, Z, O and E.

Pergamon Press are also publishers of the following Journals.

JOURNAL OF NUCLEAR ENERGY:
PARTS A/B: REACTOR SCIENCE AND TECHNOLOGY;
PART C: PLASMA PHYSICS—ACCELERATORS—THERMONUCLEAR RESEARCH
HEALTH PHYSICS (*The Official Journal of the Health Physics Society*)
JOURNAL OF INORGANIC AND NUCLEAR CHEMISTRY
TETRAHEDRON (*The International Journal of Organic Chemistry*)
TALANTA (*An International Journal of Analytical Chemistry*)
INTERNATIONAL JOURNAL OF APPLIED RADIATION AND ISOTOPES
BIOCHEMICAL PHARMACOLOGY
ARCHIVES OF ORAL BIOLOGY
* BIOPHYSICS
* JOURNAL OF MICROBIOLOGY, EPIDEMIOLOGY AND IMMUNO-BIOLOGY
* PROBLEMS OF HEMATOLOGY AND BLOOD TRANSFUSION
* PROBLEMS OF VIROLOGY
* PROBLEMS OF ONCOLOGY
* SECHENOV PHYSIOLOGICAL JOURNAL OF THE U.S.S.R.
* PAVLOV JOURNAL OF HIGHER NERVOUS ACTIVITY
* ELECTRIC TECHNOLOGY, U.S.S.R.
* RADIO ENGINEERING
* RADIO ENGINEERING AND ELECTRONICS
* TELECOMMUNICATIONS
* PHYSICS OF METALS AND METALLOGRAPHY
* THE ABSTRACTS JOURNAL OF METALLURGY
* APPLIED MATHEMATICS AND MECHANICS
CHEMICAL ENGINEERING SCIENCE
JOURNAL OF ATMOSPHERIC AND TERRESTRIAL PHYSICS
PLANETARY AND SPACE SCIENCE
ANNALS OF THE INTERNATIONAL GEOPHYSICAL YEAR
SPECTROCHIMICA ACTA
JOURNAL OF THE MECHANICS AND PHYSICS OF SOLIDS
ACTA METALLURGICA (*for the Board of Governors of Acta Metallurgica*)
INTERNATIONAL JOURNAL OF THE PHYSICS AND CHEMISTRY OF SOLIDS
DEEP-SEA RESEARCH
JOURNAL OF NEUROCHEMISTRY
JOURNAL OF PSYCHOSOMATIC RESEARCH
JOURNAL OF INSECT PHYSIOLOGY
INTERNATIONAL JOURNAL OF AIR AND WATER POLLUTION
INTERNATIONAL ABSTRACTS OF BIOLOGICAL SCIENCES (*for Biological and Medical Abstracts Ltd.*)
RHEOLOGY ABSTRACTS
VACUUM
OPERATIONAL RESEARCH QUARTERLY
ANNALS OF OCCUPATIONAL HYGIENE
ELECTROCHIMICA ACTA
JOURNAL OF CHILD PSYCHOLOGY AND PSYCHIATRY
JOURNAL OF SMALL ANIMAL PRACTICE
SOLID-STATE ELECTRONICS
INTERNATIONAL JOURNAL OF MECHANICAL SCIENCES

* *Translations of Russian journals published on behalf of the Pergamon Institute, a division of Pergamon International Corporation*

Leaflets giving further details and subscription rates of each of these journals are available on request

27 Nov + R

ED IN STACK
22May 64 H

THE GEOCHEMICAL SOCIETY

OFFICERS

HAROLD C. UREY, President
ROBERT M. GARRELS Vice-President
FRANCIS R. BOYD, JR., Secretary
GEORGE T. FAUST, Treasurer

COUNCILLORS

FRANS E. WICKMAN, 1961–1963
O. FRANK TUTTLE, 1961–1963
ALBERT E. J. ENGEL, 1959–1961
FRIEDRICH G. HOUTERMANS, 1959–1961
RALPH CANNON, 1960–1962
TH. G. SAHAMA, 1960–1962

REGIONAL VICE-PRESIDENTS

LOUIS H. AHRENS
RUI RIBEIRO FRANCO
ING. GEORGES ORDOÑEZ
C. W. CORRENS
J. F. LOVERING
KEN SUGAWARA

COMMITTEES

Auditing Committee

WILLIAM L. HILL, Chairman
JOSEPH J. TREGONING
C. R. NASSER

Constitution and By-Laws

BRIAN J. SKINNER, Chairman
BRIAN H. MASON
WILLIAM S. FYFE

Education Committee

KURT E. LOWE, Chairman
JOHN G. WOODRUFF
PAUL L. CLOKE
J. LAWRENCE KULP
D. M. HENDERSON

Membership Committee

RICHARD H. JAHNS, Chairman
HARVEY C. DIEHL
CHESTER B. SLAWSON
JAMES E. SLOSSON
WALLACE A. BROECKER

Nominating Committee

RUSTUM ROY, Chairman
HAROLD M. SMITH
PAUL B. BARTON, JR.
ROBERT M. GROGAN
GEORGE W. WETHERILL

Programme Committee

REYNOLDS DENNING, Chairman
HAROLD M. SMITH

Publications Committee

E. WM. HEINRICH

Research Committee

CLIFFORD A. HOPSON, Chairman
EWART A. VINCENT
KEN SUGAWARA
KARL H. WEDEPOHL
KALERVO RANKAMA

Russian Translations Committee

EARL INGERSON, Chairman
JOHN M. HUNT
THURE G. SAHAMA
CHARLES F. DAVIDSON
ZDENEK PÁCAL
RAYMOND SIEVER
SOL R. SILVERMAN

Standards Committee

ALVIN VAN VALKENBURG, Chairman
FELIX CHAYES
GEORGE S. SWITZER
JOHN A. MAXWELL
LORIN R. STIEFF
MICHAEL FLEISCHER
GUNNAR KULLERUD
J. FRANK SCHAIRER
THOMAS C. HOERING

Tellers Committee

JOSEPH J. FAHEY, Chairman
CHARLES R. NASSER
HUGH GREENWOOD